Energy Bands Of Copper-chloride: The Mixed-basis Method.

ENERGY BANDS OF COPPER CHLORIDE: THE MIXED-BASIS METHOD

by

Eduardo Calabrese

A Dissertation

Presented to the Graduate Committee

of Lehigh University

in candidacy for the Degree of

Doctor of Philosophy

in

Physics

Lehigh University

1970

Approved and recommended for acceptance as a dissertation in partial fulfillment of the requirements for the degree of Doctor of Philosophy.

January 4, 1971
(date)

W. Beall Fowler
Professor in Charge

Accepted January 4, 1971
(date)

Special committee directing the doctoral work of Mr. Eduardo Calabrese

W. Beall Fowler
Chairman

Robert T. Folk

James J. McLennan

William Silvia

Roland W. Lovejoy

ACKNOWLEDGMENTS

The author would like to express his deepest gratitude to Professor W. Beall Fowler, his thesis advisor, who suggested this problem and constantly guided him during the course of this work. He also would like to thank Dr. A. Barry Kunz, who introduced the author to the adventure of the mixed-basis and gave him a copy of his computer program. Many helpful discussions with Dr. Nunzio O. Lipari, during his graduate studies at Lehigh University, are gratefully acknowledged. The author wishes to thank Mr. Kenneth Klenk for his suggestions concerning the English text.

The cooperation and patience of the staff of the computing centers of Lehigh University and of New York University, where the numerical calculations were performed, are acknowledged. The financial support of the U. S. Air Force Office of Scientific Research during part of this work is also acknowledged.

The author is indebted to Professor Franco Bassani, who helped him to come to this country and showed constant interest to his scholastic career.

Finally, the author wishes to thank his mother, who gave up so much to make all this possible.

TABLE OF CONTENTS

LIST OF FIGURES

LIST OF TABLES

ABSTRACT

The one-electron energy bands of copper chloride have been calculated by using two different approaches: the tight-binding approximation for the valence bands and the mixed-basis method for the valence and conduction bands. The crystal potential was written as a sum of ionic-like potentials, whose exchange part is the sum of two terms: a Slater exchange for the core electrons, and a screened free-electron exchange for the valence electrons. In the mixed-basis calculation, both this exchange potential and an unscreened Slater exchange potential were used.

The tight-binding calculation was done in a traditional manner, mainly for comparison with a previous theoretical study of CuCl by Song. The mixed-basis method was applied in the form recently developed by Kunz. The characteristics of this method are discussed and it is shown how it is a quite rigorous and general method, which essentially involves no other approximations besides the use of a model crystal potential.

The spin-orbit splitting at the top of the valence bands (Γ_{15}) has been computed in the tight-binding approximation and it is found to be 0.14 eV. No spin-orbit effects

have been included in the mixed-basis calculation, but a way to incorporate them in the method is shown. The effective mass has been computed at the bottom of the conduction bands (Γ_1) for both types of exchange potentials. The result is 0.23 m_o for the Slater exchange, and 0.17 m_o for the screened exchange. The energy gap is 1.0eV and 0.3eV, respectively, for the two types of potentials.

Our results show that the contribution of the 3p orbital of $C\ell^-$ to the top valence band is larger than that of the 3d orbital of Cu^+, in disagreement with Song's result and with the common interpretation of the experimental data. Apart from this discrepancy, there is a general qualitative agreement with Song's result and with the experiment. An argument is given why the quantitative agreement is sometimes poor.

INTRODUCTION

The purpose of the present work is two-fold: to investigate the energy bands of copper chloride and to review a new method of calculating energy bands in solids.

The copper halides have been the object of extensive experimental investigation in recent years.* A theoretical study of the energy bands of copper chloride has been made by Song [Son 67, 67a], who used the tight-binding method for the valence bands and the orthogonalized-plane-wave method for the conduction bands. We will apply the tight-binding approximation to the calculation of the valence bands of copper chloride and compare our results with Song's results.

The tight-binding method involves several approximations which may affect the results in such a way that any agreement with the experiment may be completely fortuitous. From the theoretical point of view, it is desirable to have a method which involves only few approximations, whose validity can be ascertained by comparison with experiment. For example, if we are able to solve a one-particle Schrödinger equation for the crystal with reasonable accuracy, the result will tell us how closely the effective potential used describes the one-electron properties of the system. The

---

*We will not attempt to give a complete list of references on the experimental work. A good amount of information on this topic can be found in Song's thesis [Son 67].

mixed-basis method appears a quite general and rigorous method of solution of the equation. By the use of this method, various model crystal potentials can be tested and more insight in the one-electron theory can be obtained.

In Chapter I we review the energy band theory and discuss some models of the effective crystal potential. In Chapter II we analyze the symmetry of the zinc blende structure, which is the structure of the CuCℓ crystal below 680°K. In that chapter, we also do the group-theoretical analysis and obtain basis functions of the appropriate symmetry for the expansion of the crystal wave function. In Chapter III the basic equations of the tight-binding approximation are derived for the case of an ionic crystal and applied to the calculation of the valence bands of copper chloride. In Chapter IV we describe and discuss the mixed-basis method and its application to the calculation of the energy bands of an ionic crystal. We then discuss in detail the application of this method to CuCℓ. In Chapter V we present and discuss the results of both the tight-binding and the mixed-basis calculations. The results are then compared with previous theoretical and experimental studies.

Chapter I

REVIEW OF ENERGY BAND THEORY

I-1. The one-electron approximation.

A crystal is a very complicated quantum-mechanical system. Some aspects of the structure of materials, however, are amenable to approximate analysis. For instance, by a description of the energy levels of electrons in solids it can be determined whether a material should be a metal or an insulator, optical spectra can be analyzed and interpreted, calculations of binding energies are possible.

The first step in such approximate analysis [cf. Fow 63] is to use a non-relativistically covariant Schrödinger equation for the system:

$$H \Psi_M(\underset{\sim}{r}, \underset{\sim}{R}) = E_M \Psi_M(\underset{\sim}{r}, \underset{\sim}{R}), \tag{I-1}$$

where H, the crystal Hamiltonian, is

$$H = -\sum_{i}^{n} \frac{\hbar^2}{2m} \nabla_i^2 - \sum_{I}^{N} \frac{\hbar^2}{2M_I} \nabla_I^2 + \sum_{i<j} \frac{e^2}{r_{ij}} - \sum_{i,I} \frac{Z_I e^2}{|\underset{\sim}{r}_i - \underset{\sim}{R}_I|} + \sum_{I<J} \frac{Z_I Z_J e^2}{R_{IJ}} + H_{rel} + H_{ext}. \tag{I-2}$$

In Eq. (I-1), $\Psi_M(\underset{\sim}{r},\underset{\sim}{R})$ is a particular eigenfunction of H, and E_M the corresponding eigenvalue. $\underset{\sim}{r}$ and $\underset{\sim}{R}$ represent the space and spin coordinates of electrons and nuclei, respectively. In Eq. (I-2), $\underset{\sim}{r}_i$ and $\underset{\sim}{R}_I$ are the position vectors of

the i^{th} electron and of the I^{th} nucleus, respectively; $r_{ij}=|\underset{\sim}{r}_j-\underset{\sim}{r}_i|$ and $R_{IJ}=|\underset{\sim}{R}_J-\underset{\sim}{R}_I|$; $Z_I e$ is the charge of the I^{th} nucleus. H_{rel} includes all the relativistic terms, and H_{ext} includes any interaction with external fields.

We shall consider an isolated system, for which $H_{ext}=0$, and shall neglect, for the present, any relativistic effects, i.e. $H_{rel}=0$. The inclusion of the spin-orbit interaction is discussed in Sec. I-4.

The next step in simplifying our problem is the use of the so-called adiabatic or Born-Oppenheimer approximation [Bor 27]. Since the nuclei are much heavier than the electrons, they move much slower. We then assume that the electrons follow only adiabatically the motion of the nuclei and that we can separate the equation for the electronic motion from the one for the nuclear motion. We write the total wave function in the form

$$\Psi_M(\underset{\sim}{r},\underset{\sim}{R}) = \Phi_{n,\underset{\sim}{R}}(\underset{\sim}{r})\, X_{n,\eta}(\underset{\sim}{R}), \qquad \text{(I-3)}$$

where $\Phi_{n,\underset{\sim}{R}}(\underset{\sim}{r})$ is an electronic wave function which depends parametrically on the nuclear position $\underset{\sim}{R}$, and $X_{n,\eta}(\underset{\sim}{R})$ is a nuclear wave function depending on the electronic state n. By applying the operator H to this wave function, and ignoring the non-adiabatic terms, we obtain the following equations [see Sei 40; Zim 64]:

$$\left\{-\sum_i \frac{\hbar^2}{2m}\nabla_i^2 + \sum_{i<j}\frac{e^2}{r_{ij}} - \sum_{i,I}\frac{Z_I e^2}{|\underset{\sim}{r}_i-\underset{\sim}{R}_I|}\right\}\Phi_{n,\underset{\sim}{R}}(\underset{\sim}{r}) = \mathcal{E}_n(\underset{\sim}{R})\,\Phi_{n,\underset{\sim}{R}}(\underset{\sim}{r}); \qquad \text{(I-4)}$$

$$\left\{-\sum_I \frac{\hbar^2}{2M_I}\nabla_I^2 + \sum_{I<J}\frac{Z_I Z_J e^2}{R_{IJ}} + \varepsilon_n(\underset{\sim}{R})\right\}\chi_{n,\eta}(\underset{\sim}{R}) = E_M \chi_{n,\eta}(\underset{\sim}{R}). \quad \text{(I-5)}$$

As long as we are not interested in the electron-lattice dynamics, we can assume that the nuclei are fixed in their equilibrium positions and study only the electronic motion, described by Eq. (I-4). This is still a many-body problem, involving a number of particles of the order of 10^{23}.

The third step toward the solution of the problem is the one-electron approximation [Sei 40; Rei 55]. We look for a set of one-electron equations that are somehow equivalent to Eq. (I-4). One-electron processes are very important in solid state physics and one may expect to describe them quite accurately by the use of one-electron equations. Such equations might also give a qualitative account of some many-electron processes.

In the one-electron approximation the wave function of the system is approximated by a determinant of orthonormal one-electron functions of the form

$$\phi_i(\underset{\sim}{r}_j) = \psi_i(x_j, y_j, z_j)\,\gamma_i(\zeta_j), \quad \text{(I-6)}$$

that is, a product of space and spin parts. A determinant of these one-electron functions obeys the Pauli exclusion principle, that is, it is antisymmetric under electronic permutations. The best determinantal wave function which can be constructed is the one which minimizes the expectation

value of the operator

$$H_{es} = -\sum_i \frac{\hbar^2}{2m} \nabla_i^2 + \sum_{i<j} \frac{e^2}{r_{ij}} - \sum_{i,I} \frac{Z_I e^2}{|\underset{\sim}{r}_i - \underset{\sim}{R}_I|} , \qquad \text{(I-7)}$$

which is the Hamiltonian for the electronic system (cf. Eq. I-4). The application of the variational principle, subject to the constraint that the one-electron functions be orthonormal, yields a set of equations which must be satisfied by the one-electron functions. These are the Hartree-Fock equations [Sei 40; Sla 63].

We can write the Hartree-Fock equations in the following form

$$\left\{ -\frac{\hbar^2}{2m} \nabla^2 + W(\underset{\sim}{r}) + U(\underset{\sim}{r}) + A_i(\underset{\sim}{r}) \right\} \phi_i(\underset{\sim}{r}) = \varepsilon_i \phi_i(\underset{\sim}{r}) , \qquad \text{(I-8)}$$

in which $W(\underset{\sim}{r})$ is the potential energy of an electron in the field of the nuclei of the system; $U(\underset{\sim}{r})$ is the ordinary average electrostatic potential energy of an electron in the field of all the electrons of the system; $A_i(\underset{\sim}{r})$ is the so-called "exchange" potential: it is essentially a correlation term between electrons of the same spin, which arises from the antisymmetry of the wave function. The explicit form of the exchange potential is

$$A_i(\underset{\sim}{r}) = -\sum_j e^2 \frac{\phi_j(\underset{\sim}{r})}{\phi_i(\underset{\sim}{r})} \int \frac{\phi_j^*(\underset{\sim}{r}') \phi_i(\underset{\sim}{r}')}{|\underset{\sim}{r}' - \underset{\sim}{r}|} d^3\underset{\sim}{r}' . \qquad \text{(I-9)}$$

The sum over j includes only states with the same spin as ϕ_i. A_i depends on the state i whose wave function is being

calculated.*

The one-electron energy parameter ε_i in Eq. (I-8) gives the energy required to remove an electron from state i; or, more precisely, $\varepsilon_j - \varepsilon_i$ is the energy which has to be added to the system in order to remove an electron from state i and place it in an unoccupied state j. This interpretation comes from Koopmans' theorem [Koo 33; see also Sei 40], which shows that, if we consider the difference in energy between two systems, containing N and N-1 particles, respectively, but otherwise identical, and we suppose that the one-electron wave functions ϕ_j are the same in each case, except that in one the state ϕ_i is unoccupied, then we have $\Delta E \equiv \varepsilon_i$.

Particular solutions of Eq. (I-8) may be found by the method of self-consistent fields [Har 57]. In this method, the Coulomb and exchange potentials are calculated with an assumed set of wave functions; the resulting linear equations are then solved; the potentials are recalculated with the new functions, and the process is repeated until the successive iterations agree within some assigned limit. The process has been carried through with precision for some relatively simple atomic systems, but application to solids is rendered very difficult by the necessity of evaluating sums over a very large number of states. What is generally

---

*For a more detailed discussion of these terms, see, e.g., Har 58, Sla 51.

done is to assume a potential and reduce the problem to the solution of a one-particle Schrödinger equation.

We define an "effective one-particle Hamiltonian" for the crystal as

$$H_o = -\frac{\hbar^2}{2m}\nabla^2 + V(\underset{\sim}{r}), \qquad \text{(I-10)}$$

where $V(\underset{\sim}{r})$ is an "effective one-electron crystal potential." In the Hartree-Fock case, $V \equiv W + \mathcal{U} + A_i$. We will discuss the choice of the crystal potential in Sec. I-5. For the moment let us assume that $V(\underset{\sim}{r})$ is known. Thus our problem is reduced to the solution of the equation

$$H_o \phi_i(\underset{\sim}{r}) = \varepsilon_i \phi_i(\underset{\sim}{r}), \qquad \text{(I-11)}$$

where H_o is given in Eq. (I-10).

It is convenient to use <u>atomic units</u> (a.u.) in energy band calculations [see Cal 64]. We set $\hbar$ equal to unity. The Bohr radius $a_o = \hbar^2/me^2$ is taken as unit of length, and the rydberg $(= e^2/2a_o)$ as unit of energy (1 Ry=13.6058 eV [Tay 69]). In a.u. Eq. (I-10) becomes

$$H_o = -\nabla^2 + V(\underset{\sim}{r}), \qquad \text{(I-12)}$$

where the potential $V(\underset{\sim}{r})$, as well as the eigenvalue ε_i, is now in rydbergs.

I-2. The use of group theory.

By the use of group theory*, we can determine some properties of the eigenfunctions $\phi_i(\underset{\sim}{r})$ before attempting to solve Eq. (I-11). We assume that we have an infinite, perfect crystal, i.e., a crystal whose nuclei occupy equivalent positions with respect to the sites of a lattice. For computational convenience, we impose periodic boundary conditions over a sufficiently large region of the crystal (Born-von Kármán B.C.) [see, e.g., Zim 64, Sec. 1.6].

All the operations (combinations of translations, rotations and reflections) which carry a crystal into itself form a group G, called the "space group" of the crystal. The general element of a space group is a combination of a (proper or improper) rotation and a translation. The operator corresponding to such element is denoted by $\{R|\underset{\sim}{t}\}$, which acts on functions of position and corresponds to the coordinate transformation $\{\alpha|\underset{\sim}{t}\}$ according to the following definitions:

$$\{R|\underset{\sim}{t}\}\,f(\underset{\sim}{r}) = f(\{\alpha|\underset{\sim}{t}\}^{-1}\underset{\sim}{r})\ ;$$

$$\{\alpha|\underset{\sim}{t}\}\,\underset{\sim}{r} = \alpha\,\underset{\sim}{r} + \underset{\sim}{t}\ . \qquad \text{(I-13)}$$

In Eq. (I-13), α is the 3 x 3 rotation matrix corresponding to the rotation operator R; $\underset{\sim}{t}$ is a translation vector. The

*See, e.g., Tin 64 for a general account of group theory.

matrices α are real orthogonal matrices [cf. Wig 59, Tin 64]. These are unitary matrices with real elements. Thus,

$$\alpha^{-1} = \alpha^{+} = \tilde{\alpha}, \tag{I-14}$$

and $(\alpha^{-1})_{ij} = \alpha_{ji}$. The rows (or columns) of α form a set of orthonormal vectors:

$$\begin{aligned} \sum_{k=1}^{3} \alpha_{ik}\,\alpha_{jk} &= \delta_{ij} \ ; \\ \sum_{k=1}^{3} \alpha_{ki}\,\alpha_{kj} &= \delta_{ij} \ . \end{aligned} \tag{I-15}$$

The determinant of α is 1, if α corresponds to a proper rotation; -1, if it corresponds to an improper rotation.

The fact that the crystal is invariant under the operations of the space group G implies that the operators $\{R|\underset{\sim}{t}\}$ of G leave the crystal potential $V(\underset{\sim}{r})$ invariant; therefore, they commute with the Hamiltonian H_o. Operators commuting with the Hamiltonian are very important because of the following general principle of quantum theory: The wave functions of a quantum system must form bases for irreducible representations of the group of operators which commute with the Hamiltonian of the system [see Wig 59, Ch. 12]. Thus, the wave function $\phi_i(\underset{\sim}{r})$ in Eq. (I-11) must be a basis for an irreducible representation of the space group of the crystal.

A detailed analysis of the irreducible representations of space groups is given by Koster [Kos 57]. We will summarize here some of his results. We restrict our discussion to "symmorphic" groups, for which $\underset{\sim}{t}$ is always a lattice

translation $\underset{\sim}{R}_\nu$:

$$\underset{\sim}{R}_\nu = n_{\nu 1}\,\underset{\sim}{a}_1 + n_{\nu 2}\,\underset{\sim}{a}_2 + n_{\nu 3}\,\underset{\sim}{a}_3 \,. \qquad \text{(I-16)}$$

In Eq. (I-16), the $\underset{\sim}{a}_i$'s are basic translation vectors and the $n_{\nu i}$'s are integers. The pure translation operators are denoted as $\{E|\underset{\sim}{R}_\nu\}$ and form an invariant subgroup of the space group.

Before considering the representations of space groups, we consider the subgroup of lattice translations. Since this is an Abelian group (the operators commute with each other), all the irreducible representations are one-dimensional. A consequence of this and of the general principle stated above is Bloch's theorem [Blo 28], which states that any eigenfunction of the Hamiltonian (I-10 or 12) can be written in the form

$$\phi_i(\underset{\sim}{r}) = e^{i\underset{\sim}{k}\cdot\underset{\sim}{r}}\, u^i_{\underset{\sim}{k}}(\underset{\sim}{r}) \,. \qquad \text{(I-17)}$$

In Eq. (I-17), $\underset{\sim}{k}$ is a vector in the (first) Brillouin zone [Bri 31] and $u^i_{\underset{\sim}{k}}(\underset{\sim}{r})$ is a function which has the full periodicity of the crystal.

At a general point in the Brillouin zone, it is sufficient that the wave function have the form (I-17) in order that it be an acceptable basis function for an irreducible representation of the space group. At some particular points in the zone, however, we can obtain more information

about the basis functions by a study of the point group of the crystal.

The rotational parts R of the operators $\{R|\underset{\sim}{t}\}$ of G form a group G_o, called the "point group" of the crystal. For a given $\underset{\sim}{k}$ in the Brillouin zone, those operators of G_o that leave $\underset{\sim}{k}$ invariant or bring it into $\underset{\sim}{k} + \underset{\sim}{h}_\mu$, where $\underset{\sim}{h}_\mu$ is a reciprocal lattice vector (cf. Eq. II-6), also form a group, called the "point group of $\underset{\sim}{k}$", denoted by $G_o(\underset{\sim}{k})$. Any operator of G_o, not contained in $G_o(\underset{\sim}{k})$, will bring the vector $\underset{\sim}{k}$ into a different vector $\underset{\sim}{k}'$. The figure of these $\underset{\sim}{k}$ vectors is referred to as a "star." It exhibits all of the rotational and reflectional symmetry of the lattice. If the point group G_o contains n elements and $G_o(\underset{\sim}{k})$ contains g elements, the star of $\underset{\sim}{k}$ will contain q = n/g vectors. All the groups of the $\underset{\sim}{k}$ vectors belonging to the same star are isomorphic. For a given star, there will be as many distinct irreducible representations of the space group G as there are irreducible representations of the point group of a wave vector in the star. If d is the dimension of an irreducible representation of the group of $\underset{\sim}{k}$, the dimension D of the corresponding irreducible representation of G is given by D = qd.

The knowledge of the irreducible representations of $G_o(\underset{\sim}{k})$, sometimes called the "small representations of $\underset{\sim}{k}$" [cf. Bou 36], is sufficient to determine the irreducible representations of the space group G. If $\Gamma(R)$ is a

representation of the operator $\{R|0\}$ in the point group of the wave vector, the representation of the operator $\{R|\underset{\sim}{t}\}$ in the space group (K) of the wave vector $\underset{\sim}{k}$ is $e^{i\underset{\sim}{k}\cdot\underset{\sim}{t}}\Gamma(R)$. If we have d orthogonal functions $\phi^j_{\underset{\sim}{k}}$ (where j runs from 1 to d) of the Bloch form (Eq. I-17), which are basis functions for a small representation of $\underset{\sim}{k}$, these same functions are also bases for an irreducible representation of the space group of $\underset{\sim}{k}$. There will exist q = n/g operators in the space group G, $\{E|0\}$, $\{R_2|\underset{\sim}{a}_2\}$, $\{R_3|\underset{\sim}{a}_3\}$, ..., $\{R_q|\underset{\sim}{a}_q\}$, such that the full space group G may be expressed as the sum of its left cosets with respect to K:

$$G = K + \{R_2|\underset{\sim}{a}_2\}K + \cdots + \{R_q|\underset{\sim}{a}_q\}K . \qquad \text{(I-18)}$$

The D = qd functions

$$\phi^j_{\underset{\sim}{k}_\ell} = \{R_\ell|\underset{\sim}{a}_\ell\}\,\phi^j_{\underset{\sim}{k}} , \qquad \text{(I-19)}$$

where ℓ = 1,2,..., q and j = 1,2, ..., d, form bases for an irreducible representation of the space group G.

Remembering that all the partners of an irreducible representation belong to the same energy [Wig 59, loc. cit.], we can choose the wave function $\phi_i(\underset{\sim}{r})$ in Eq. (I-11) to be a basis for an irreducible representation of the space group of a wave vector $\underset{\sim}{k}$. We can relabel Eq. (I-11) in the following way:

$$H\,\phi^\sigma_i(\underset{\sim}{r}) = \varepsilon^\sigma_i\,\phi^\sigma_i(\underset{\sim}{r}) , \qquad \text{(I-20)}$$

where $\sigma \equiv (k, \alpha, \gamma)$ characterizes the symmetry of the wave function. $\underset{\sim}{k}$ is a vector in the Brillouin zone. The function ϕ_i^σ is the i^{th} function belonging to the γ^{th} row of the α^{th} irreducible representation of the group K, the space group of the wave vector $\underset{\sim}{k}$. Once ϕ_i^σ and its partners in the small representation are known, all other partners can be obtained from Eq. (I-19).

To the above results we add the following well-known theorem of group theory: Matrix elements of an operator S which is invariant under all operations of a group vanish between functions belonging to different irreducible representations or to different rows of the same unitary representation [cf. Tin 64, Sec. 4-9].

It is now evident that the first steps toward the solution of Eq. (I-20) are the following: (a) choose a value of $\underset{\sim}{k}$ in the Brillouin zone; (b) determine the point group of $\underset{\sim}{k}$, $G_o(\underset{\sim}{k})$; (c) find all the distinct irreducible representations of $G_o(\underset{\sim}{k})$. The wave function $\phi_i(\underset{\sim}{r})$ must be of the Bloch form and can be chosen to belong to the γ^{th} row of the irreducible representation Γ_α of $G_o(\underset{\sim}{k})$. We need to solve only one equation for each irreducible representation of the point group of $\underset{\sim}{k}$, since all eigenfunctions which are degenerate* with $\phi_i^\sigma(\underset{\sim}{r})$ can be determined by the use of group theory, once $\phi_i^\sigma(\underset{\sim}{r})$ is known.

---

*We refer here to degeneracies caused by symmetry. Accidental degeneracies must be considered separately [see Wig 59, loc. cit.].

I-3. Solution of the equation.

The problem of finding solutions to Eq. (I-11 or 20) is still by no means trivial. Even assuming that $V(\underset{\sim}{r})$ is known, an exact solution to this equation cannot be obtained. However, several methods have been devised to approximate such solutions. They all involve the use of a trial function, which is a linear combination of a finite number of known functions. The coefficients of this linear combination are then varied to minimize the expectation value of the Hamiltonian. The choice of the basis set of functions characterizes the various methods of calculation. We will consider this choice in Chapters III and IV.

Let $\{\chi_j\}$ (j = 1, ..., N) be a set of linearly independent, but not necessarily orthonormal, functions. Such a finite set of functions is referred to as a "truncated basis set." Let $f_i(\underset{\sim}{r})$ be a trial function given by the expansion

$$f_i(\underset{\sim}{r}) = \sum_{j}^{N} c_{ij}\,\chi_j(\underset{\sim}{r}). \qquad \text{(I-21)}$$

The function f_i is called a "linear variation function" [cf. Lev 70, Sec. 8-5]. The expectation value of H with respect to the function f_i is

$$E_i \equiv \langle H \rangle_i \equiv \frac{\langle f_i | H | f_i \rangle}{\langle f_i | f_i \rangle} = \frac{\sum_k \sum_l c_{ik}^* c_{il} H_{kl}}{\sum_k \sum_l c_{ik}^* c_{il} O_{kl}}, \qquad \text{(I-22)}$$

where

$$H_{kl} = \langle \chi_k | H | \chi_l \rangle, \quad \text{and} \quad O_{kl} = \langle \chi_k | \chi_l \rangle. \tag{I-23}$$

H_{kl} and O_{kl} are the matrix elements of the Hamiltonian and of unity, respectively, in the basis $\{\chi_j\}$.

Applying the variation theorem to Eq. (I-22), we obtain [cf., e.g., Pil 68]:

$$\delta E_i = 0 = \frac{1}{\sum_k \sum_l c_{ik}^* c_{il} O_{kl}} \left[\sum_k \sum_l \delta c_{ik}^* c_{il} H_{kl} + \sum_k \sum_l c_{ik}^* \delta c_{il} H_{kl} \right.$$
$$\left. - E_i \left(\sum_k \sum_l \delta c_{ik}^* c_{il} O_{kl} + \sum_k \sum_l c_{ik}^* \delta c_{il} O_{kl} \right) \right]$$
$$= \frac{1}{\langle f_i | f_i \rangle} \left\{ \sum_k \delta c_{ik}^* \left[\sum_l c_{il} (H_{kl} - E_i O_{kl}) \right] + \text{complex conjugate} \right\}. \tag{I-24}$$

In Eq. (I-24), we made use of the hermitian property of H ($H = H^\dagger$). Thus, the variation theorem is satisfied if

$$\sum_k \delta c_{ik}^* \left[\sum_l c_{il} (H_{kl} - E_i O_{kl}) \right] = 0. \tag{I-25}$$

In order for Eq. (I-25) to be satisfied for any artibrary variation δc_{ik}^* of the coefficients, it is necessary that the term in brackets vanish for all values of k, namely,

$$\sum_l c_{il} (H_{kl} - E_i O_{kl}) = 0; \quad k = 1, 2, \ldots, N. \tag{I-26}$$

For a given i, this is a set of N homogeneous equations in the N unknowns $c_{i1}, c_{i2}, \ldots, c_{iN}$. Nontrivial solutions can be found if, and only if,

$$\text{Det } (\underline{H} - E_i \underline{O}) = 0. \tag{I-27}$$

In Eq. (I-27), $\underset{\simeq}{H}$ and $\underset{\simeq}{O}$ are the "Hamiltonian" and "overlap" matrices, respectively. These are square matrices of dimension N, whose elements are given by Eq. (I-23). The determinant in Eq. (I-27) is called the "secular determinant," and the equation the "secular equation."

The secular equation is an algebraic equation of degree N in the unknown E_i, which from Eq. (I-22) is seen to be the expectation value of the Hamiltonian. We label the N roots of the equation by E_1, E_2, ..., E_N and order them in such way that $E_i<E_2<\ldots<E_N$. Associated with each root E_i, there is a set of coefficients $\{c_{i\ell}\}$ and a function f_i. If ε_1 is the exact energy of the lowest state of the system, whose wave function is approximated by f_1, then, by the variational principle we have

$$E_1 \geq \varepsilon_1. \qquad \text{(I-28)}$$

It has been shown [Hyl 30, Mac 33] that if one extends the truncated basis set by one more function, the roots of the NxN secular equation (I-27) will separate the roots of the (N+1) x (N+1) secular equation resulting from the extended basis. Denoting the roots of the extended basis by primes, this fact can be written

$$E_1' < E_1 < E_2' < E_2 < \cdots < E_{N-1}' < E_{N-1} < E_N' < E_N < E_{N+1}'. \qquad \text{(I-29)}$$

By extending this analysis to an infinite basis set, one can readily show that the j^{th} root E_j of the secular equation of

order NxN is an upper limit to the j^{th} exact energy, that is,

$$E_j \geq \varepsilon_j \; ; \qquad j = 1, 2, \cdots, N . \tag{I-30}$$

The roots $\{E_j\}$ are thus approximations to the energy of the ground state and the N-1 lowest excited states of the system.

There are two important features of the linear variation method. The first is that, by choosing a trial function (I-21) which is orthogonal to the first n "exact" eigenfunctions of the system, the roots E_1, E_2, ..., E_N will be approximations to the energies ε_{n+1}, ε_{n+2}, ..., ε_{n+N} of the system [see Lev 70, Sec. 8-2]. The second feature follows from Eq. (I-29). If we increase the number of basis functions in the trial function f_i (Eq. I-21) and consider one root of the secular equation, say E_i, we see from Eq. (I-29) that

$$E_i > E_i' > E_i'' > \cdots > \varepsilon_i . \tag{I-31}$$

Eq. (I-31) shows that, by increasing the number of functions in the basis set $\{\chi_j\}$, the variational energies will converge to the "exact" energy ε_i. A study of the convergence of E_i versus number of basis functions can provide us with a good estimate of the exact energy.

Once the secular equation is solved, we can obtain an approximation to the wave function corresponding to the energy E_i by substituting E_i in the set of equations (I-26) and solve them for the coefficients c_{i1}, c_{i2}, ..., c_{iN}. We

have a set of N homogeneous equations in N unknowns. To solve them, we assign an arbitrary value to any one of the unknowns, say c_{iN}, discard any one of the equations, say the last one, and solve the remaining system of N-1 linear inhomogeneous equations in N-1 unknowns. The coefficients $c_{i1}, c_{i2}, \ldots, c_{iN-1}$ will then be given in terms of c_{iN}, and the normalization condition for the wave function

$$\langle f_i | f_i \rangle = \sum_k \sum_l c^*_{ik} c_{il} \varphi_{kl} = 1 \qquad \text{(I-32)}$$

provides an additional equation to determine c_{iN}.

In consideration of the results of the previous section, we can restrict the truncated basis set $\{\chi_j\}$ to functions having the same symmetry σ of the wave function that we are trying to approximate. Thus, our trial function $f_i(\underset{\sim}{r})$ will be a linear combination of functions of the Bloch form (Eq. I-17), which belong to the γ^{th} row of the representation Γ_α of the group of $\underset{\sim}{k}$. We can put the symmetry label in Eq. (I-21) and write

$$\phi_i^\sigma(\underset{\sim}{r}) \simeq f_i^\sigma(\underset{\sim}{r}) = \sum_j^N c_{ij}^\sigma \chi_j^\sigma(\underset{\sim}{r}). \qquad \text{(I-33)}$$

The problem of calculating the energy levels of electrons in solids is now reduced to the solution of the secular equation (I-27). For a general point in the Brillouin zone, where the group $G_o(\underset{\sim}{k})$ contains only the identity, this is still a hard task, since we might need a large number of functions χ_j^σ to approximate the wave function ϕ_i^σ, due to

the general form of the latter. At some special points or lines, however, the symmetry considerably restricts the choice of basis functions and relatively few of them may give a good approximation to the wave function.

As a continuation of the last paragraph of the preceding section, the next steps toward the solution of Eq. (I-20) are the following: (d) choose a set of functions $\chi_j(\underset{\sim}{r})$; (e) from this set, construct functions $\chi_j^{\sigma}(\underset{\sim}{r})$ which belong to the γ^{th} row of Γ_α; (f) calculate all the matrix elements H_{kl} and O_{kl}; (g) solve the secular equation. For a given point in the zone, we have to solve one secular equation for each small representation of $\underset{\sim}{k}$. However, as we will see in the next chapter, some representations are "uninteresting" because they correspond to too high energies, and we shall not consider them. Steps (a), (b), (c), and (e) are performed in Chapter II. Steps (d) and (f) are considered and further discussed in Chapters III and IV. Step (g) is only a computational problem that can be left to the computer, since standard Fortran routines to diagonalize complex matrices are available (see Appendix G).

I-4. Spin-orbit interaction.

With the inclusion of the spin-orbit interaction, the effective Schrödinger equation for an electron in the crystal can be written

$$\{H_o + H_{so}\}\ \psi = \varepsilon\psi, \qquad \text{(I-34)}$$

where H_o is given by Eq. (I-10) and

$$H_{so} = \frac{\hbar}{4m^2c^2} \underset{\sim}{\sigma} \cdot \quad (\underset{\sim}{\nabla} V \times \underset{\sim}{p}). \tag{I-35}$$

The eigenfunction ψ is now a two-component Pauli spinor; $\underset{\sim}{\sigma}$ represents the 2 x 2 Pauli spin matrices [see Sch 68, p. 374]; V is the effective crystal potential, as it appears in Eq. (I-10); $\underset{\sim}{p} = -i\hbar\underset{\sim}{\nabla}$ is the linear momentum operator. The Hamiltonian operator still has the symmetry of the lattice, but, due to the transformation properties of spinors, now there are two different quantum mechanical operators which correspond to the same transformation of points in space. It is these operators, rather than the physical transformations themselves, which form the group whose irreducible respresentations are required.

The intrinsic transformation properties of spinors under rotations are given by 2 x 2 unitary matrices having determinant unity. Consider a proper rotation R, corresponding to the Euler angles α,β,γ [see Ros 57, Ch. IV]. The 2 x 2 matrix corresponding to this rotation can be written in the form $\pm D(R)$, where [cf. Tin 64, Eq. (5-34)]

$$\begin{aligned} D_{11}(R) &= D_{22}(R)^* = \cos\frac{\beta}{2} \exp\left[-i(\alpha+\gamma)/2\right]; \\ D_{21}(R) &= -D_{12}(R)^* = \sin\frac{\beta}{2} \exp\left[i(\alpha-\gamma)/2\right]. \end{aligned} \tag{I-36}$$

If we have a spinor whose two components are scalar functions of position, the total operator corresponding to this coordinate transformation is

$$\pm D(R)R. \tag{I-37}$$

Here R is the operator which acts on the two scalar components of the spinor. Thus, due to the ambiguity in sign in Eq. (I-37), there are two operators corresponding to each proper rotation of the coordinates. Given a collection of g spatial operators R which form a group, the 2g operators of the form (I-37) corresponding to them also form a group, called the "double group."

We must also be concerned with improper rotations. The operators of the double group corresponding to the inversion are $\pm D(I)I$, where D(I) is the two-dimensional unit matrix and I is the spatial inversion operator. Since any improper rotation can be considered as the product of a proper rotation R and the inversion, we obtain: $D(IR) = D(R)$.

A double point group can leave a lattice invariant only if the corresponding point group leaves it invariant. The results of Sec. I-2 still hold, except that we now consider double groups. To each transformation $\{R|\underset{\sim}{t}\}$ previously considered, there correspond two quantum operators. One must determine, as before, the group of the wave vector, which is now a double group. A wave function must be of the Bloch form $e^{i\underset{\sim}{k}\cdot\underset{\sim}{r}}u_{\underset{\sim}{k}}(\underset{\sim}{r})$ (cf. Eq. I-17), where $u_{\underset{\sim}{k}}$ is a spinor, and must transform according to one of the additional representations of this double group.

Obviously the matrices $\pm D(R)$ form a two-dimensional representation of the double point group. This representation is irreducible and is usually called $D_{\frac{1}{2}}$, because it

corresponds to the $j = \frac{1}{2}$ representation of the rotation group. A spinor, whose components belong to the representation Γ_ℓ of a point group, transforms according to the direct product representation $\Gamma_\ell \times D_{\frac{1}{2}}$. This representation may be reducible:

$$\Gamma_\ell \times D_{\frac{1}{2}} = \sum_j c_{\ell j} \Gamma_j , \qquad \text{(I-38)}$$

where the Γ_j's can only be additional irreducible representations of the double group. The physical interpretation of Eq. (I-38) is that it expresses the splitting of a degenerate state Γ_ℓ by spin-orbit coupling into states of symmetry Γ_j.

In atomic units, defined on p. , the speed of light has the numerical value $c = 274.074$, and Eq. (I-35) becomes

$$H_{so} = (274.074)^{-2} \, \underset{\sim}{\sigma} \cdot (\underset{\sim}{\nabla} V \times \underset{\sim}{p}) . \qquad \text{(I-39)}$$

The procedure for solving Eq. (I-34) is the same as that described in Section I-3, with $H = H_o + H_{so}$.

The spin-orbit interaction is further discussed in Sec. II-4, Sec. III-3, and Appendix F.

I-5. The crystal potential.

The previous considerations in this chapter were quite general and did not depend on a particular type of crystal. In discussing the crystal potential, it is

convenient to restrict ourselves to a particular type of crystal: an ionic crystal with two ions per basis. This is the type of crystal on which the present work is based. We call the two types of ions A and B, respectively. They form two identical lattices, displaced from each other by the vector $\underset{\sim}{d}$.

The crystal potential $V(\underset{\sim}{r})$ must have the translational symmetry of the lattice. Therefore, we can write, without loss of generality,

$$V(\underset{\sim}{r}) = \sum_{\nu} \left[V_A(\underset{\sim}{r} - \underset{\sim}{R}_\nu) + V_B(\underset{\sim}{r} - \underset{\sim}{R}_\nu - \underset{\sim}{d}) \right]. \qquad \text{(I-40)}$$

Here, the sum is over all lattice translation vectors $\underset{\sim}{R}_\nu$. The origin is taken on an ion of type A. V_A and V_B are "ionic-like" potentials, centered on an A and B ion, respectively. We will often refer to either of them as V_a, understanding that the subscript a can be either A or B.

We call the potential V_a an "ionic-like" potential because we do not expect it to differ very much from an ionic potential. In the limit where the lattice parameter becomes very large, the potentials V_A and V_B become the potentials of isolated ions. In a real crystal, on the other hand, the electronic charges of different ions overlap and the potential V_a will no longer be the potential of an isolated ion.

If $V(\underset{\sim}{r})$ is invariant under the operations of a point

group, performed either around A or B, the potential $V_a(\underset{\sim}{r})$ must be invariant under the same operations. We assume that the ionic-like potentials have spherical symmetry around the nucleus:

$$V_a(\underset{\sim}{r} - \underset{\sim}{R}_\nu^a) = V_a(|\underset{\sim}{r} - \underset{\sim}{R}_\nu^a|), \tag{I-41}$$

where $\underset{\sim}{R}_\nu^A = \underset{\sim}{R}_\nu$ and $\underset{\sim}{R}_\nu^B = \underset{\sim}{R}_\nu + \underset{\sim}{d}$. The potential $V_a(r)$ can be written (in rydbergs) [cf. Bas 65]

$$V_a(r) = -\frac{2z_a}{r} + U_a(r), \tag{I-42}$$

where z_a is the ionicity of ion a, and $z_A + z_B = 0$. The two terms at the right hand side of Eq. (I-42) are called the "long-range" and the "short-range" term, respectively. At large r, $U_a(r)$ is practically zero and $V_a(r)$ is equal to $-2z_a/r$. The short range part of the potential is defined through Eq. (I-42), once $V_a(r)$ is known.

By using Eq. (I-42), the crystal potential (I-40) can be written

$$V(\underset{\sim}{r}) = V_A(r) + \left[\sum_\nu{}' \frac{-2z_A}{|\underset{\sim}{r} - \underset{\sim}{R}_\nu|} + \sum_\nu \frac{-2z_B}{|\underset{\sim}{r} - \underset{\sim}{R}_\nu - \underset{\sim}{d}|}\right]$$

$$+ \left[\sum_\nu{}' U_A(|\underset{\sim}{r} - \underset{\sim}{R}_\nu|) + \sum_\nu U_B(|\underset{\sim}{r} - \underset{\sim}{R}_\nu - \underset{\sim}{d}|)\right], \tag{I-43}$$

where the prime in the summation means that the term with $\underset{\sim}{R}_\nu = 0$ is excluded. If the origin is on an ion of type B, we have to exchange A and B, and change the sign of $\underset{\sim}{d}$ in

Eq. (I-43). In general, we can write

$$V(\underset{\sim}{r}) = V_a(r) + M_a(\underset{\sim}{r}) + [\Sigma' U]_o , \tag{I-44}$$

where

$$M_a(\underset{\sim}{r}) = 2 z_a \left[\sum_{\nu}{}' \frac{-1}{|\underset{\sim}{r} - \underset{\sim}{R}_\nu|} + \sum_{\nu} \frac{1}{|\underset{\sim}{r} - \underset{\sim}{R}_\nu \mp \underset{\sim}{d}|} \right] \tag{I-45}$$

and

$$[\Sigma' U]_o = \begin{cases} \sum_{\nu}{}' U_A(|\underset{\sim}{r} - \underset{\sim}{R}_\nu|) + \sum_{\nu} U_B(|\underset{\sim}{r} - \underset{\sim}{R}_\nu - \underset{\sim}{d}|), & \text{if origin on } A ; \\ \sum_{\nu}{}' U_B(|\underset{\sim}{r} - \underset{\sim}{R}_\nu|) + \sum_{\nu} U_A(|\underset{\sim}{r} - \underset{\sim}{R}_\nu + \underset{\sim}{d}|), & \text{if origin on } B . \end{cases} \tag{I-46}$$

$M_a(\underset{\sim}{r})$ is the "Madelung potential" centered on an ion of type a. $[\Sigma' U]_o$ is the sum of all the short-range potentials, except the one at the origin.

The Madelung potential is the contribution to the crystal potential due to all the ions, except the one at the origin, as if they were point charges $z_a e$ located at the nuclear positions. This potential has the point symmetry of the crystal around the origin; therefore, it transforms according to the identical representation of the point group of the crystal. This implies that, if we expand $M_a(\underset{\sim}{r})$ in a series of spherical harmonics,

$$M_a(\underset{\sim}{r}) = \sum_{lm} a^a_{lm}(r) Y^m_l(\theta, \phi) , \tag{I-47}$$

the coefficients $a^a_{lm}(r)$ of spherical harmonics that have no components belonging to the identical representation of the point group are identically zero. By far the most important

term in the expansion (I-47) is the spherically symmetric term having $\ell=0$ [cf. Bal 62, Ch. 4]. If we retain only this term, we can write

$$M_a(\underset{\sim}{r}) \approx M_a(r) = \frac{1}{\sqrt{4\pi}} a^a_{00}(r) . \qquad \text{(I-48)}$$

We now consider the ionic-like potential $V_a(r)$. For an isolated ion this would be the Hartree-Fock potential for the free ion, which is state-dependent (cf. Eq. I-8). It is convenient to have a potential which is the same for all the electrons in the ion. One way to obtain such a potential is by the use of the Slater approximation to the exchange term in the Hartree-Fock equations [Sla 51, 60]. Slater assumes that the exchange potential in an electron system with a given charge density $\rho = \Sigma_i \phi_i^* \phi_i$ is the same as in a free electron gas of the same density:

$$A_i(\underset{\sim}{r}) = -6\left[\frac{3}{8\pi}\rho(\underset{\sim}{r})\right]^{\frac{1}{3}} . \qquad \text{(I-49)}$$

The spherically symmetric Hartree-Fock potential, with the Slater approximation for the exchange term, is [see, e.g., Her 63, p. 1-7]

$$V_a(r) = -\frac{2Z_a}{r} + \frac{2}{r}\int_0^r \sigma_a(r')\,dr' + 2\int_r^\infty \frac{\sigma_a(r')}{r'}\,dr' - 6\left[\frac{3}{8\pi}\frac{\sigma_a(r)}{4\pi r^2}\right]^{\frac{1}{3}} , \qquad \text{(I-50)}$$

in rydberg units. Z_a is the atomic number and $\sigma_a(r)$ is the total radial density of electrons:

$$\sigma_a(r) = \sum_i \left|P_i^a(r)\right|^2 = 4\pi r^2 \rho_a(r) . \qquad \text{(I-51)}$$

The potential (I-50) is referred to as the Hartree-Fock-Slater (HFS) potential.

The Slater exchange is too large in the low density tail of an atomic potential. Robinson *et al.* [Rob 62] have modified the original Slater result to include the influence of electron correlation on pair interactions. They obtain a screened exchange potential of the form

$$A_i = -6\left[\frac{3}{8\pi}\rho\right]^{\frac{1}{3}} F(\alpha), \qquad \text{(I-52)}$$

where

$$F(\alpha) = 1 - \frac{\alpha^2}{6} - \frac{4}{3}\alpha \tan^{-1}\frac{2}{\alpha} + \left(1+\frac{\alpha^2}{12}\right)\frac{\alpha^2}{2}\ln\left(1+\frac{4}{\alpha^2}\right) \qquad \text{(I-53)}$$

and

$$\alpha = 2\left(3\pi^5\rho\right)^{-\frac{1}{6}} \simeq 0.64153\,\rho^{-\frac{1}{6}}. \qquad \text{(I-54)}$$

The screening factor F(α) goes from 1, at very large densities, to 0, when the density ρ becomes very small [cf. op. cit., Fig. 1]. F(α) (Eq. I-53) is the limit for $\kappa\to\infty$ of the following expression [W. Beall Fowler, private communication; see also Rob 62]

$$F_\kappa(\alpha) = 1 - \frac{\alpha^2}{6} - \frac{2}{3}\frac{\alpha^2}{a}\tan^{-1}\frac{1}{a} + \left(1+\frac{a^2}{3}\right)\frac{\alpha^2}{2}\ln\left(1+\frac{1}{a^2}\right), \qquad \text{(I-55)}$$

where

$$a = \frac{\alpha}{2}\sqrt{\frac{\kappa}{\kappa-1}} \qquad \text{(I-56)}$$

and κ is the optical dielectric constant.

If, following Brinkman's idea [Bri 65, 66; see also Lip 70, Fig. 13], we assume that the core electrons are essentially unscreened and that the screening effect occurs mainly between the valence electrons, we can write an exchange potential which is the sum of two parts: a Slater exchange, which depends only on the density of the "core" electrons ρ_c, and a screened exchange with the factor (I-55), which depends only on the density of the "valence" electrons ρ_v. Thus,

$$A_i = -6\left[\frac{3}{8\pi}\rho_c\right]^{\frac{1}{3}} - 6\left[\frac{3}{8\pi}\rho_v\right]^{\frac{1}{3}} F_\kappa(x), \quad \rho_c + \rho_v = \rho. \qquad \text{(I-57)}$$

Our point of view is that the Slater exchange is often not a very good approximation to the exchange term in the Hartree-Fock equations, which are an approximate description of the real system. We then feel justified, from a physical and practical point of view, in trying different models of the exchange potential, feeling that a one-particle effective potential is a practical means of doing calculations, more than a true description of the physical situation.

In our calculations, we will use the expression (I-57) for the exchange potential, which has the largest number of parameters. By giving suitable values to these parameters, we can obtain all the exchange potentials described in this section. Thus, if we let $\rho_c = \rho$ and $\rho_v = 0$, we obtain

the Slater exchange (Eq. I-49); by putting $\rho_c=0$, $\rho_v=\rho$ and $\kappa\to\infty$, we get the RBKS (Robinson, Bassani, Knox and Schrieffer) exchange potential (Eq. I-52); and finally, if we let $\rho_c=0$, $\rho_v=\rho$ and κ=dielectric constant, we obtain the RBKS exchange with the screening factor (I-55). Various exchange potentials are shown in Fig. 1 for Cl^-. The total ionic-like potential, with the valence screening (I-57), is now

$$V_a(r) = -\frac{2Z_a}{r} + \frac{2}{r}\int_0^r \sigma_a(r')\,dr' + 2\int_r^\infty \frac{\sigma_a(r')}{r'}\,dr' - 6\left(\frac{3}{8\pi}\right)^{\frac{1}{3}}\left[\rho_{ac}^{\frac{1}{3}} + \rho_{av}^{\frac{1}{3}}\,F_\kappa(\kappa)\right]. \quad \text{(I-58)}$$

It must be noted that for large r the ionic potentials (I-50) and (I-58) go as -2(Z-N)/r, where N is the number of electrons in the ion. This asymptotic behavior is incorrect for atomic structure calculations. An electron in the ion sees a potential due to the nucleus and to the remaining N-1 electrons, which goes as -2(Z-N+1)/r at large distance. The error comes from the Slater approximation to the exchange potential and is not present in the original Hartree-Fock equations.

Herman and Skillman [Her 63] have used Latter's modification [Lat 55] to the HFS potential in their atomic structure calculations, so that the modified potential has the correct behavior at large r. They use

$$V_a(r) = V_o(r) \qquad \text{for } r \le r_o,$$

and $$V_a(r) = -2(Z-N+1)/r \qquad \text{for } r > r_o; \quad \text{(I-59)}$$

where V_o is the Hartree-Fock-Slater potential (I-50) and r_o

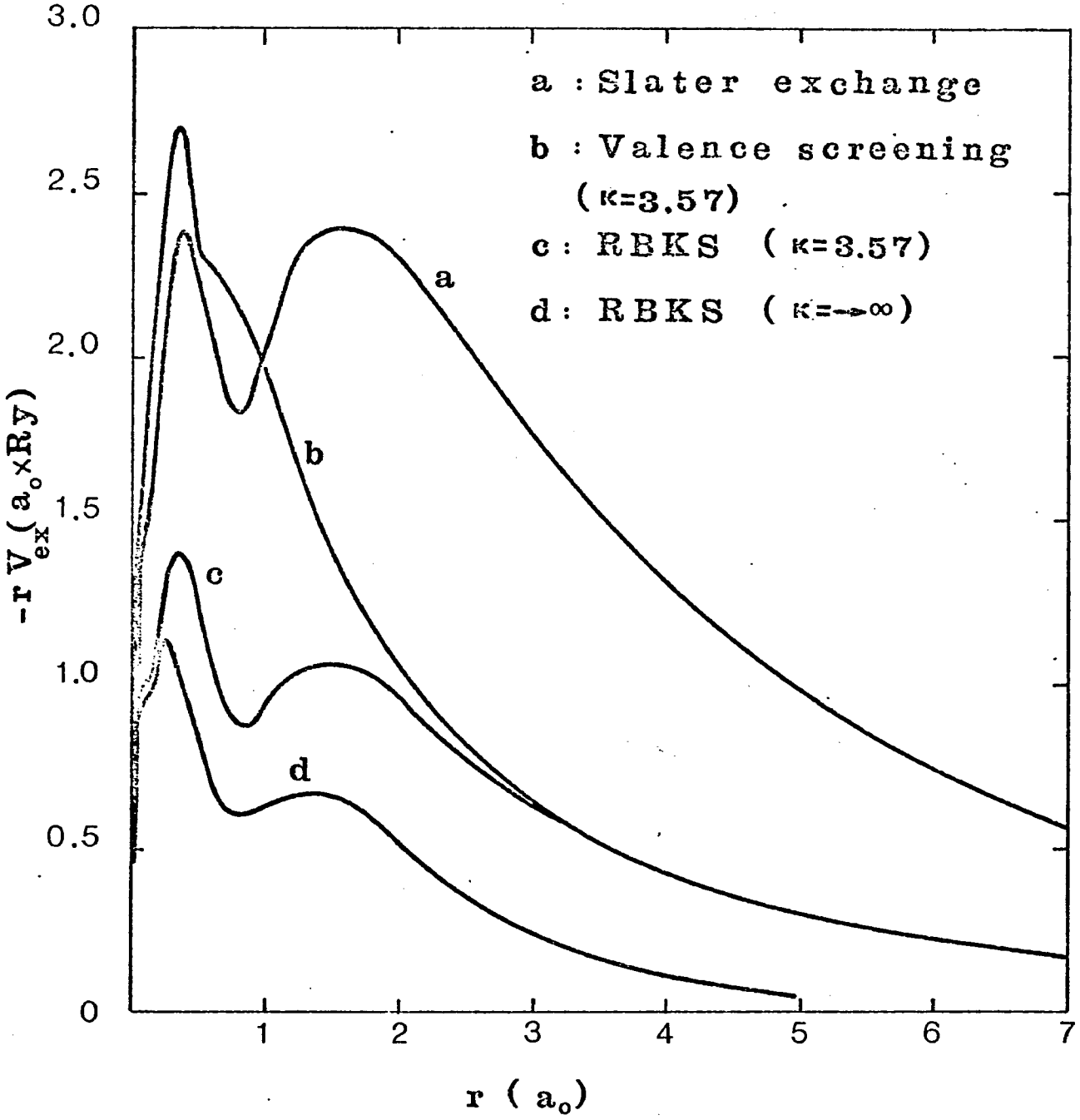

Fig. 1 - Various effective exchange potentials for CuCl. a_o is the Bohr radius.

is that value of r for which $V_o(r_o) = -2(Z-N+1)/r_o$.

In a previous work [Cal 66] we have used a Hartree-Fock potential with the RBKS exchange (Eq. I-52), where the density was that of N-1 electrons. The potential was state-dependent, since the wave function in consideration was excluded from the calculation of the density, and resembled more closely the Hartree-Fock potential. Besides, it had the correct behavior at large r.

In the crystal the situation is different. There, we may consider the electron, whose wave function is being calculated, as an external electron and construct the crystal potential as a sum of ionic potentials that go as $-2(Z-N)/r$ at large distance from the nucleus. This type of potential seems particularly suitable for calculation of conduction states. For valence states, however, a slightly different approach may be used [see, e.g., Kun 68]. Here we can assume that the electron is essentially localized around a particular ion and sees a potential of Z-N+1 charges due to that ion and a potential of Z-N charges due to the other ions in the crystal.

Since the question of what type of crystal potential to use depends mostly on the bands that are being studied and on the method used, we will postpone any further discussion of this point to Chapters III and IV, where two methods of band structure calculations are described.

The problem remains how to calculate the potential

(I-58). We will use a self-consistent-field method [Har 57; see also Her 63], in which we assume that the ion feels the presence of the crystalline environment only through the spherically averaged Madelung potential (I-48).

Chapter II

THE ZINC BLENDE STRUCTURE

II-1. The crystal lattice and the point group T_d.

The zinc blende structure is composed of two face-centered cubic (f c c) lattices displaced from each other by one quarter of a body diagonal. The first lattice is formed by atoms of type A, the second by atoms of type B (cf. Sec. I-5). The unit cube is shown in Fig. 2, where the empty circles represent atoms of type A and the shaded circles atoms of type B. There are four molecules AB per unit cube. About each atom there are four equally distant atoms of the opposite kind arranged at the corners of a regular tetrahedron. The number, position, and distance of the first few neighbors are given in Table 1.

The primitive cell can be defined by the basic translation vectors

$$\underset{\sim}{a}_1 = \frac{a}{2}(1,1,0), \quad \underset{\sim}{a}_2 = \frac{a}{2}(0,1,1), \quad \underset{\sim}{a}_3 = \frac{a}{2}(1,0,1), \tag{II-1}$$

and contains one atom of type A at the origin and one of type B at

$$\underset{\sim}{d} = \frac{a}{4}(1,1,1). \tag{II-2}$$

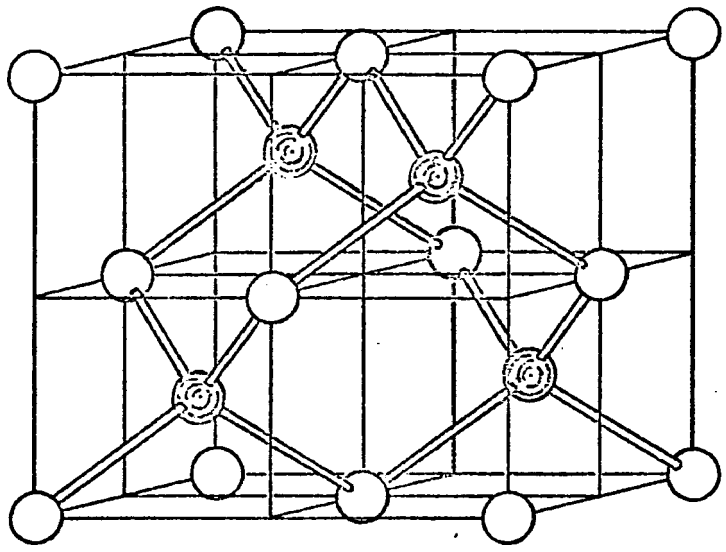

Fig. 2 - Unit cube for the zinc blende structure.

TABLE I

SOME SHELLS OF NEAREST NEIGHBORS IN THE ZINC BLENDE STRUCTURE.

Shell	Number of ions	Coordinates (in units of $\frac{a}{2}$)	Distance from the origin (in units of $\frac{a}{2}$)	Type of ions (origin +)
1	4	$(\frac{1}{2}\ \frac{1}{2}\ \frac{1}{2})$	$\frac{\sqrt{3}}{2} = 0.86603$	-
2	12	(1 1 0)	$\sqrt{2} = 1.41421$	+
3	12	$(\frac{1}{2}\ \frac{1}{2}\ \frac{3}{2})$	$\frac{\sqrt{11}}{2} = 1.65831$	-
4	6	(2 0 0)	2	+
5	12	$(\frac{1}{2}\ \frac{3}{2}\ \frac{3}{2})$	$\frac{\sqrt{19}}{2} = 2.17945$	-
6	24	(2 1 1)	$\sqrt{6} = 2.44949$	+
7	16	$(\frac{1}{2}\ \frac{1}{2}\ \frac{5}{2})$	$\frac{\sqrt{27}}{2} = 2.59808$	-

The volume of the primitive cell is $\frac{1}{4}a^3$ where a^3 is the volume of the unit cube shown in Fig. 2.

The space group of the zinc blende structure is denoted as T_d^2 ($F\bar{4}3m$), in a standard notation [Int 52]. This is a symmorphic space group, with the face-centered cubic Bravais lattice and the point group T_d. The subgroup of pure translations contains all the operators of the form $\{E|\underset{\sim}{R}_\nu\}$, where $\underset{\sim}{R}_\nu$ is given by Eq. (I-16).

We now study the point group T_d [cf. Sla 63, pp. 353-359], which is a subgroup of the space group T_d^2. This is the group of all operations, both of rotation and reflection, which transform a regular tetrahedron into itself. There are 24 operations, indicated in Fig. 3, where the four corners of the tetrahedron coincide with the corners a b c d of the cube. The first 12 operations are proper rotations, the remaining 12 are improper rotations, that is a combination of rotations and reflections. The 24 operations are: $R_1 \equiv E$, the identity; R_2, R_3, R_4, rotations of π about the x, y, and z axes, respectively; R_5, R_6, R_7, and R_8, rotations of $2\pi/3$ in a positive direction about lines joining the origin with points a, b, c, and d, respectively; R_9, R_{10}, R_{11}, and R_{12}, rotations of $4\pi/3$ about the same four axes; R_{13}, R_{14}, rotations of $\pi/2$, and $-\pi/2$, respectively, about the x axis, followed by a reflection in the plane $x = 0$; R_{15}, R_{16}, same kind of improper rotations about the y axis; R_{17}, R_{18}, about the z axis; R_{19}, R_{20}, R_{21}, R_{22}, R_{23}, and R_{24}, reflections in

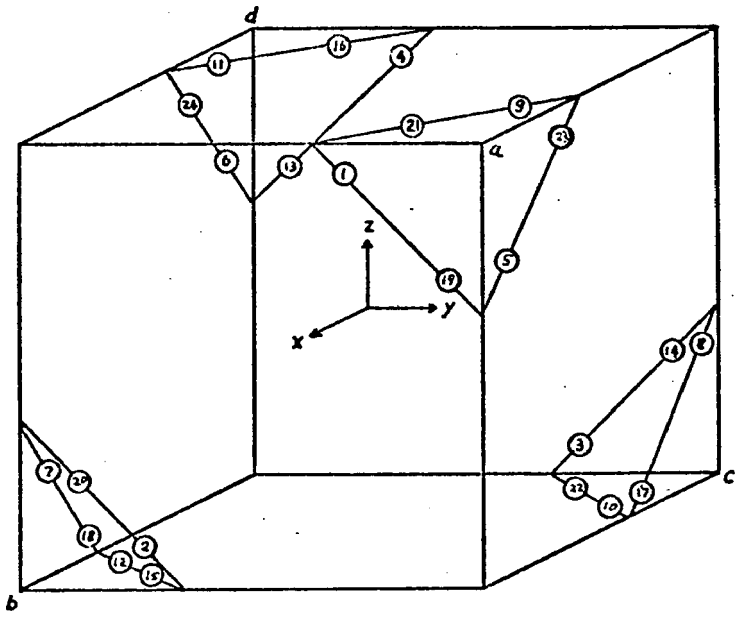

Fig. 3 - Symmetry operations of the group T_d. The point 1 is transformed into one of the points 1...24 by each of the operations of the group. Operations are numbered as in Table 2.

the six planes $y = z$, $y = -z$, $z = x$, $z = -x$, $x = y$, $x = -y$, respectively. The analytical formulation of these operations is given in Table 2. The symbol R_n is equivalent to the space group operator $\{R_n|0\}$. From Table 2 we can obtain the rotation matrices α by using Eq. (I-13), which for pure rotations can be written

$$Rf(\underset{\sim}{r}) = f\ (\alpha^{-1}\underset{\sim}{r}). \qquad \text{(II-3)}$$

The multiplication table of the group T_d is given in Slater's book, *Quantum Theory of Molecules and Solids*, Vol. 1 [Sla 63, Table A12-10] and Vol. 2 [Sla 65, Table A3-17]. By examining this table we find that there are five classes: the identity; the two-fold rotations R_2, R_3, and R_4; the three-fold rotations R_5, ..., R_{12}; the improper rotations through $\pm\pi/2$, R_{13}, ..., R_{18}; and the reflections R_{19}, ..., R_{24}. In the next section we will consider the irreducible representations of the group T_d in connection with the group of $\Gamma(\underset{\sim}{k} = 0)$.

II-2. The reciprocal lattice and the group of the wave vector.

The reciprocal lattice to the f c c crystal lattice is a body-centered cubic (b c c) lattice, whose basic translation vectors are

$$\underset{\sim}{b}_1 = \frac{2\pi}{a}(1,1,\bar{1}), \quad \underset{\sim}{b}_2 = \frac{2\pi}{a}(\bar{1},1,1), \quad \underset{\sim}{b}_3 = \frac{2\pi}{a}(1,\bar{1},1). \qquad \text{(II-4)}$$

TABLE 2

OPERATIONS OF THE GROUP T_d.

$R_1 f(x,y,z) = f(x,y,z)$	$R_{13} f(x,y,z) = f(-x,z,-y)$
$R_2 f(x,y,z) = f(x,-y,-z)$	$R_{14} f(x,y,z) = f(-x,-z,y)$
$R_3 f(x,y,z) = f(-x,y,-z)$	$R_{15} f(x,y,z) = f(-z,-y,x)$
$R_4 f(x,y,z) = f(-x,-y,z)$	$R_{16} f(x,y,z) = f(z,-y,-x)$
$R_5 f(x,y,z) = f(y,z,x)$	$R_{17} f(x,y,z) = f(y,-x,-z)$
$R_6 f(x,y,z) = f(-y,z,-x)$	$R_{18} f(x,y,z) = f(-y,x,-z)$
$R_7 f(x,y,z) = f(-y,-z,x)$	$R_{19} f(x,y,z) = f(x,z,y)$
$R_8 f(x,y,z) = f(y,-z,-x)$	$R_{20} f(x,y,z) = f(x,-z,-y)$
$R_9 f(x,y,z) = f(z,x,y)$	$R_{21} f(x,y,z) = f(z,y,x)$
$R_{10} f(x,y,z) = f(-z,-x,y)$	$R_{22} f(x,y,z) = f(-z,y,-x)$
$R_{11} f(x,y,z) = f(z,-x,-y)$	$R_{23} f(x,y,z) = f(y,x,z)$
$R_{12} f(x,y,z) = f(-z,x,-y)$	$R_{24} f(x,y,z) = f(-y,-x,z)$

The vectors $\underset{\sim}{a}_i$ (Eq. II-1) and $\underset{\sim}{b}_j$ (Eq. II-4) satisfy the well known relations

$$\underset{\sim}{a}_i \cdot \underset{\sim}{b}_j = 2\pi \delta_{ij} , \qquad (i,j = 1,2,3). \tag{II-5}$$

The Wigner-Seitz cell of the reciprocal lattice is shown in Fig. 4. This is the Brillouin zone of the f c c crystal lattice. Some symmetry points are shown in the figure, following the standard notation of Bouckaert, Smoluchowski, and Wigner [Bou 36].

As discussed in Sec. I-2, we need to know the point group of the wave vector for vectors $\underset{\sim}{k}$ in the Brillouin zone. We will select the following points: $\Gamma \equiv (0,0,0)$, $X \equiv (2\pi/a)(1,0,0)$, $L \equiv (2\pi/a)(\frac{1}{2},\frac{1}{2},\frac{1}{2})$, $\Delta \equiv (2\pi/a)(\rho,0,0)$, and $\Lambda \equiv (2\pi/a)(\rho/2,\rho/2,\rho/2)$, where $0<\rho<1$. For each of these points we want to find the subgroup of T_d that leaves the vector $\underset{\sim}{k}$ invariant, or brings it into $\underset{\sim}{k} + \underset{\sim}{h}_\mu$, where $\underset{\sim}{h}_\mu$ is a reciprocal lattice vector defined by

$$\underset{\sim}{h}_\mu = n_{\mu 1} \underset{\sim}{b}_1 + n_{\mu 2} \underset{\sim}{b}_2 + n_{\mu 3} \underset{\sim}{b}_3 . \tag{II-6}$$

The point group of Γ is the entire group T_d, described in the preceding section. This is true because Γ is at the origin of the Brillouin zone and any operation of T_d leaves the origin invariant.

The group of X is the point group D_{2d}, of order 8. As a subgroup of T_d, it contains the elements R_1, R_2, R_3, R_4, R_{13}, R_{14}, R_{19}, and R_{20}. The multiplication table of this group, as of any subgroup of T_d, can be derived from Slater's table [Sla 63, Table A12-10; or Sla 65, Table A3-

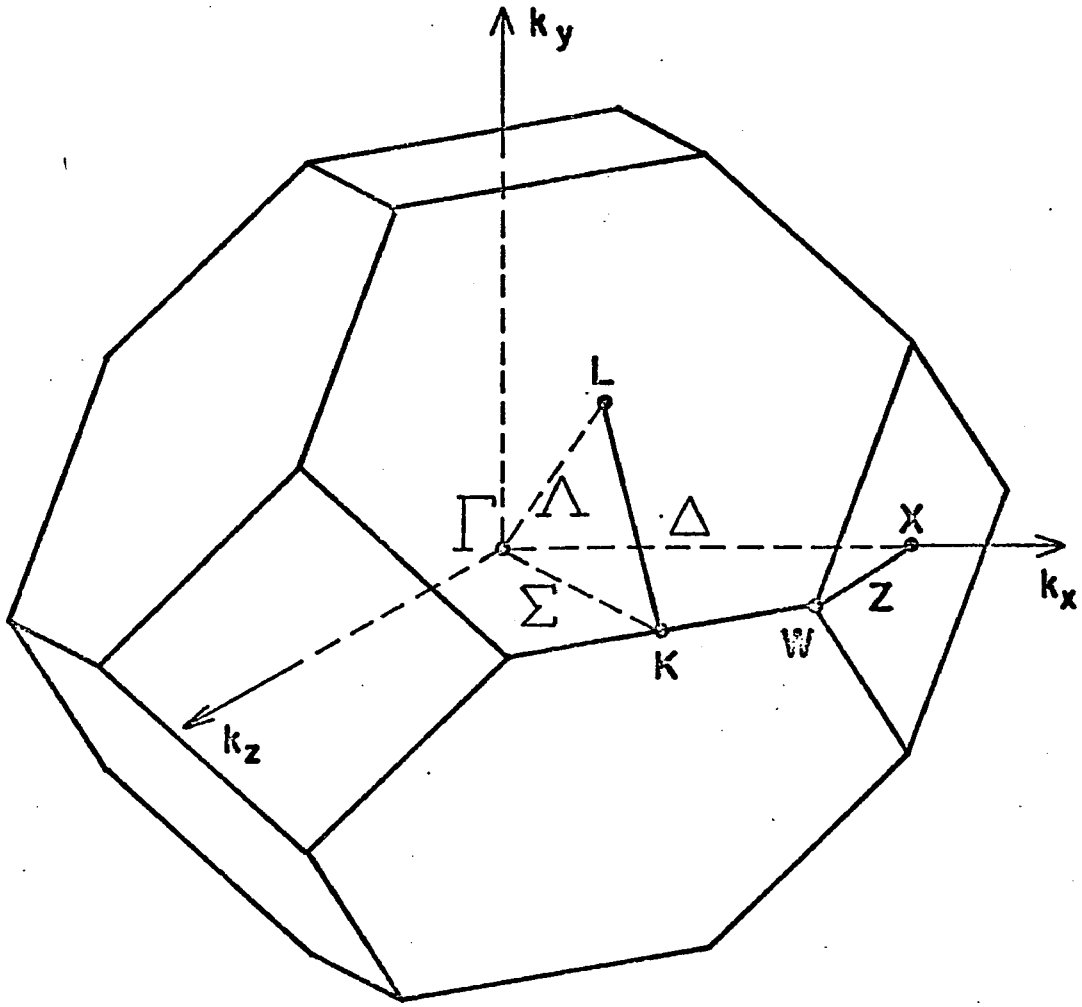

Fig. 4 - Brillouin zone of the fcc lattice.

17], by selecting the appropriate elements. We see that the group of X contains five classes: R_1; R_2; R_3, R_4; R_{13}, R_{14}; and R_{19}, R_{20}.

The group of L is C_{3v}, of order 6. It contains the elements R_1, R_5, R_9, R_{19}, R_{21}, and R_{23}. There are three classes: R_1; R_5, R_9; and R_{19}, R_{21}, R_{23}.

The group of Δ is C_{2v}, of order 4. It contains the elements R_1, R_2, R_{19}, and R_{20}. This is an Abelian group: each element is in a class by itself. Thus, there are four classes.

The group of Λ is C_{3v}, the same as the group of L, and needs not be considered separately at this point. All the groups mentioned above are described in Koster's article [Kos 57].

We now want the irreducible representations of these groups. Usually only the character tables are given in the literature [cf., e.g., Par 55], but a knowledge of the matrices of a representation is necessary to construct basis functions, as we will see in the next section. The matrices and characters of the small representations for 20 space groups are given in Appendix 3 of Slater's *Quantum Theory of Molecules and Solids*, Volume 2 [Sla 65]. We reproduce in Tables 3 to 6 the tables of interest to us. These tables give the matrix elements and characters of the small representations of Γ, X, L, and Δ for the space group T_d^2.

TABLE 3

MATRIX ELEMENTS AND CHARACTERS AT POINT Γ.

		R_1	R_2	R_3	R_4	R_5	R_6	R_7	R_8	R_9	R_{10}	R_{11}	R_{12}	R_{13}	R_{14}	R_{15}	R_{16}	R_{17}	R_{18}	R_{19}	R_{20}	R_{21}	R_{22}	R_{23}	R_{24}
	Γ_1	1	1	1	1	1	1	1	1	1	1	1	1	1	1	1	1	1	1	1	1	1	1	1	1
	Γ_2	1	1	1	1	1	1	1	1	1	1	1	1	−1	−1	−1	−1	−1	−1	−1	−1	−1	−1	−1	−1
	$(\Gamma_{12})_{11}$	1	1	1	1	$-\frac{1}{2}$	$-\frac{1}{2}$	$-\frac{1}{2}$	$-\frac{1}{2}$	$-\frac{1}{2}$	$-\frac{1}{2}$	$-\frac{1}{2}$	$-\frac{1}{2}$	1	1	$-\frac{1}{2}$	$-\frac{1}{2}$	$-\frac{1}{2}$	$-\frac{1}{2}$	1	1	$-\frac{1}{2}$	$-\frac{1}{2}$	$-\frac{1}{2}$	$-\frac{1}{2}$
	$(\Gamma_{12})_{21}$	0	0	0	0	$\frac{\sqrt{3}}{2}$	$\frac{\sqrt{3}}{2}$	$\frac{\sqrt{3}}{2}$	$\frac{\sqrt{3}}{2}$	$-\frac{\sqrt{3}}{2}$	$-\frac{\sqrt{3}}{2}$	$-\frac{\sqrt{3}}{2}$	$-\frac{\sqrt{3}}{2}$	0	0	$-\frac{\sqrt{3}}{2}$	$-\frac{\sqrt{3}}{2}$	$\frac{\sqrt{3}}{2}$	$\frac{\sqrt{3}}{2}$	0	0	$-\frac{\sqrt{3}}{2}$	$-\frac{\sqrt{3}}{2}$	$\frac{\sqrt{3}}{2}$	$\frac{\sqrt{3}}{2}$
	$(\Gamma_{12})_{12}$	0	0	0	0	$-\frac{\sqrt{3}}{2}$	$-\frac{\sqrt{3}}{2}$	$-\frac{\sqrt{3}}{2}$	$-\frac{\sqrt{3}}{2}$	$\frac{\sqrt{3}}{2}$	$\frac{\sqrt{3}}{2}$	$\frac{\sqrt{3}}{2}$	$\frac{\sqrt{3}}{2}$	0	0	$-\frac{\sqrt{3}}{2}$	$-\frac{\sqrt{3}}{2}$	$\frac{\sqrt{3}}{2}$	$\frac{\sqrt{3}}{2}$	0	0	$-\frac{\sqrt{3}}{2}$	$-\frac{\sqrt{3}}{2}$	$\frac{\sqrt{3}}{2}$	$\frac{\sqrt{3}}{2}$
	$(\Gamma_{12})_{22}$	1	1	1	1	$-\frac{1}{2}$	$-\frac{1}{2}$	$-\frac{1}{2}$	$-\frac{1}{2}$	$-\frac{1}{2}$	$-\frac{1}{2}$	$-\frac{1}{2}$	$-\frac{1}{2}$	−1	−1	$\frac{1}{2}$	$\frac{1}{2}$	$\frac{1}{2}$	$\frac{1}{2}$	−1	−1	$\frac{1}{2}$	$\frac{1}{2}$	$\frac{1}{2}$	$\frac{1}{2}$
	$\chi(\Gamma_{12})$	2	2	2	2	−1	−1	−1	−1	−1	−1	−1	−1	0	0	0	0	0	0	0	0	0	0	0	0
	$(\Gamma'_{25})_{11}$	1	1	−1	−1	0	0	0	0	0	0	0	0	−1	−1	0	0	0	0	1	1	0	0	0	0
	$(\Gamma'_{25})_{21}$	0	0	0	0	1	−1	−1	1	0	0	0	0	0	0	0	0	1	−1	0	0	0	0	1	−1
	$(\Gamma'_{25})_{31}$	0	0	0	0	0	0	0	0	1	−1	1	−1	0	0	−1	1	0	0	0	0	1	−1	0	0
	$(\Gamma'_{25})_{12}$	0	0	0	0	0	0	0	0	1	−1	−1	1	0	0	0	0	−1	1	0	0	0	0	1	−1
Γ_{15}	$(\Gamma'_{25})_{22}$	1	−1	1	−1	0	0	0	0	0	0	0	0	0	0	−1	−1	0	0	0	0	1	1	0	0
	$(\Gamma'_{25})_{32}$	0	0	0	0	1	1	−1	−1	0	0	0	0	1	−1	0	0	0	0	1	−1	0	0	0	0
	$(\Gamma'_{25})_{13}$	0	0	0	0	1	−1	1	−1	0	0	0	0	0	0	1	−1	0	0	1	−1	0	0	0	0
	$(\Gamma'_{25})_{23}$	0	0	0	0	0	0	0	0	1	1	−1	−1	−1	1	0	0	0	0	1	−1	0	0	0	0
	$(\Gamma'_{25})_{33}$	1	−1	−1	1	0	0	0	0	0	0	0	0	0	0	0	0	−1	−1	0	0	0	0	1	1
	$\chi(\Gamma'_{25})$	3	−1	−1	−1	0	0	0	0	0	0	0	0	−1	−1	−1	−1	−1	−1	1	1	1	1	1	1
	$(\Gamma'_{15})_{11}$	1	1	−1	−1	0	0	0	0	0	0	0	0	1	1	0	0	0	0	−1	−1	0	0	0	0
	$(\Gamma'_{15})_{21}$	0	0	0	0	1	−1	−1	1	0	0	0	0	0	0	0	0	−1	1	0	0	0	0	−1	1
	$(\Gamma'_{15})_{31}$	0	0	0	0	0	0	0	0	1	−1	1	−1	0	0	1	−1	0	0	0	0	−1	1	0	0
	$(\Gamma'_{15})_{12}$	0	0	0	0	0	0	0	0	1	−1	−1	1	0	0	0	0	1	−1	0	0	0	0	−1	1
Γ_{25}	$(\Gamma'_{15})_{22}$	1	−1	1	−1	0	0	0	0	0	0	0	0	0	0	1	1	0	0	−1	−1	0	0	0	0
	$(\Gamma'_{15})_{32}$	0	0	0	0	1	1	−1	−1	0	0	0	0	−1	1	0	0	0	0	−1	1	0	0	0	0
	$(\Gamma'_{15})_{13}$	0	0	0	0	1	−1	1	−1	0	0	0	0	0	0	−1	1	0	0	0	0	−1	1	0	0
	$(\Gamma'_{15})_{23}$	0	0	0	0	0	0	0	0	1	1	−1	−1	1	−1	0	0	0	0	−1	1	0	0	0	0
	$(\Gamma'_{15})_{33}$	1	−1	−1	1	0	0	0	0	0	0	0	0	0	0	0	0	1	1	0	0	0	0	−1	−1
	$\chi(\Gamma'_{15})$	3	−1	−1	−1	0	0	0	0	0	0	0	0	1	1	1	1	1	1	−1	−1	−1	−1	−1	−1

TABLE 4

MATRIX ELEMENTS AND CHARACTERS AT POINT X.

	R_1	R_2	R_3	R_4	R_{13}	R_{14}	R_{19}	R_{20}
X_1	1	1	1	1	1	1	1	1
X_2	1	1	1	1	-1	-1	-1	-1
X_3	1	1	-1	-1	-1	-1	1	1
X_4	1	1	-1	-1	1	1	-1	-1
X_5 11	1	-1	-1	1	0	0	0	0
X_5 21	0	0	0	0	-1	1	1	-1
X_5 12	0	0	0	0	1	-1	1	-1
X_5 22	1	-1	1	-1	0	0	0	0
$\chi(X_5)$	2	-2	0	0	0	0	0	0

TABLE 5

MATRIX ELEMENTS AND CHARACTERS AT POINT L AND ALONG THE DIRECTION Λ.

		R_1	R_5	R_9	R_{19}	R_{21}	R_{23}
L_1, Λ_1		1	1	1	1	1	1
L_2, Λ_2		1	1	1	-1	-1	-1
L_3, Λ_3	11	1	-1/2	-1/2	1	-1/2	-1/2
	21	0	$\sqrt{3}/2$	$-\sqrt{3}/2$	0	$-\sqrt{3}/2$	$\sqrt{3}/2$
	12	0	$-\sqrt{3}/2$	$\sqrt{3}/2$	0	$-\sqrt{3}/2$	$\sqrt{3}/2$
	22	1	-1/2	-1/2	-1	1/2	1/2
$\chi(L_3,\Lambda_3)$		2	-1	-1	0	0	0

TABLE 6

MATRIX ELEMENTS AND CHARACTERS ALONG THE DIRECTION Δ.

	R_1	R_2	R_{19}	R_{20}
Δ_1	1	1	1	1
Δ_2	1	1	-1	-1
Δ_3	1	-1	1	-1
Δ_4	1	-1	-1	1

II-3. Basis functions for the small representations.

For our calculations in the next chapters, we need basis functions of two types: Bloch functions and linear combinations of plane waves. According to the results of Sections I-2 and 3, these functions must be of the Bloch form (cf. Eq. I-17) and must be bases for small representations of $\underset{\sim}{k}$. A Bloch function has the form

$$F_n^\sigma(\underset{\sim}{r}) = \eta_n^\sigma \sum_\nu e^{i\underset{\sim}{k}\cdot\underset{\sim}{R}_\nu} v_n^\sigma(\underset{\sim}{r} - \underset{\sim}{R}_\nu - \delta_n \underset{\sim}{d}), \qquad \text{(II-7)}$$

where $\sigma \equiv (\underset{\sim}{k}, \alpha, \gamma)$ characterizes the symmetry of the function (cf. Eq. I-20). η_n^σ is a normalization factor. The function v_n^σ is a linear combination of atomic-like orbitals with the same principal quantum number n and the same orbital quantum number ℓ, centered at $\underset{\sim}{R}_\nu + \delta_n \underset{\sim}{d}$:

$$v_n^\sigma(\underset{\sim}{r} - \underset{\sim}{R}_\nu - \delta_n \underset{\sim}{d}) = R_{n\ell}(|\underset{\sim}{r} - \underset{\sim}{R}_\nu - \delta_n \underset{\sim}{d}|) \sum_m c_{nm}^\sigma Y_\ell^m(\theta,\phi)_{\underset{\sim}{r} - \underset{\sim}{R}_\nu - \delta_n \underset{\sim}{d}}. \qquad \text{(II-8)}$$

In Eq. (II-8) $R_{n\ell}$ is a radial function (for example, the solution of the radial equation for the atom in the central field approximation) and the Y_ℓ^m's are spherical harmonics with the same value of ℓ. The value of δ_n is 0 or 1, according to whether the functions v_n^σ are centered on atoms of type A or B, respectively. The coefficients c_{nm}^σ must be determined by the symmetry conditions imposed on v_n^σ. We will examine this point later in this section. A pair of atomic quantum numbers $n\ell$ is associated with the subscript

n in v_n^σ; so we will occasionally use n for nℓ.

A symmetrized combination of plane waves (S.C.P.W.) has the form

$$S_m^\sigma = \theta_m^\sigma \sum_\mu d_{m\mu}^\sigma \, e^{i(\underset{\sim}{k}+\underset{\sim}{h}_\mu)\cdot\underset{\sim}{r}}, \qquad \text{(II-9)}$$

where θ_m^σ is a normalization factor and the $\underset{\sim}{h}_\mu$'s are reciprocal lattice vectors (cf. Eq. II-6). The coefficients $d_{m\mu}^\sigma$ are determined by the symmetry of the function S_m^σ. The vectors $\underset{\sim}{h}_\mu$, as we will see later, must satisfy the condition: $|\underset{\sim}{k} + \underset{\sim}{h}_\mu|$ = constant, for all μ in the sum.

The procedure to form a set of basis functions for a particular irreducible representation has been called the "basis-function generating machine" [cf. Tin 64, p. 41]. Given an irreducible representation Γ_α of a group of operators R, we construct the operator

$$P_{ij}^\alpha = \frac{d_\alpha}{g} \sum_R \Gamma_{ij}^\alpha(R)^* \, R, \qquad \text{(II-10)}$$

where d_α is the dimensionality of the representation; g is the order of the group; $\Gamma_{ij}^\alpha(R)$ is the ij element of the matrix of the representation Γ_α corresponding to the operator R of the group; and the sum is over all the elements of the group. It is obvious that, for a representation of dimensionality d_α, we can construct d_α^2 operators of type (II-10). It is well known from group theory that application of the operator P_{ij}^α to a basis function gives zero, unless the function belongs to the j^{th} row of Γ_α. If this

condition is satisfied, then the result is the partner function belonging to the i^{th} row of Γ_α. It is also known that application of the operator P^α_{ii} to any function f, in the space operated on by R, projects out the part of f which belongs to the i^{th} row of the representation Γ_α. An operator of the form P^α_{ii} is called a "projection operator" [cf. op. cit.].

The basis-function generating machine works very simply. Starting with an arbitrary function f, we can project out the function f^α_i, which belongs to the i^{th} row of Γ_α. After normalization, this is a suitable basis function. Then use of the transfer operators P^α_{ji} yields all its partners. In practice (cf. Sec. I-2), we don't need to know all the partners of an irreducible representation, but only the functions belonging to a particular row, say the first.

We are now ready to form Bloch functions and linear combinations of plane waves which belong to the first row of the various irreducible representations of the group of $\underset{\sim}{k}$ given in the preceding section. We consider Bloch functions first. It is shown in Appendix A that, for a Bloch function $F^\sigma_n(\underset{\sim}{r})$ (Eq. II-7) to belong to the γ^{th} row of the irreducible representation Γ_α of the group of $\underset{\sim}{k}$, the function v^σ_n must belong to the γ^{th} row of the representation Γ_β of the same group, where (cf. Eq. A-12)

$$\Gamma_\beta(R) = \Gamma_\alpha(R)\, e^{-i\,\underset{\sim}{\delta}\cdot\underset{\sim}{k}\cdot(\underset{\sim}{d}-R\,\underset{\sim}{d})}. \qquad \text{(II-11)}$$

Here, α is the rotation matrix defined by Eq. (II-3). We see from Eq. (II-11) that the representation Γ_β is the same as Γ_α when the exponential factor is equal to one. This occurs when $\delta_n = 0$ (v_n^σ centered on atoms of type A); when $\underset{\sim}{k} = 0$ (point Γ); when $\underset{\sim}{d} = \alpha\underset{\sim}{d}$ (line Λ and point L); or when $\underset{\sim}{d} - \alpha\underset{\sim}{d}$ is perpendicular to $\underset{\sim}{k}$ (line Δ). In all other cases, some matrices of Γ_β will be different from the corresponding matrices of Γ_α, and the two representations may be equivalent or different. At the point X, for instance, the exponential factor in Eq. (II-11) assumes the values 1,1,-1,-1, -1,-1,1,1, in correspondence to the eight elements of the group (R_n: n=1,2,3,4,13,14,19,20). As a result, X_3,X_4,X_1, and X_2 are the representations Γ_β corresponding to X_1, X_2, X_3, and X_4, respectively (see Table 4). The representation X_5 goes into an equivalent representation, whose matrices can be obtained from those of Table 4 by exchanging the indeces 1 and 2. This corresponds to a similarity transformation SX_5S^{-1}, with the matrix $S = \left(\begin{smallmatrix}0 & 1\\ 1 & 0\end{smallmatrix}\right)$.

We would now like to determine the coefficients c_{nm}^σ in Eq. (II-8). It is convenient to start with linear combinations of spherical harmonics that are proportional to: 1, for $\ell = 0$; x,y,z, for $\ell = 1$; and xy,yz,zx, x^2-y^2, $3z^2-r^2$, for $\ell = 2$. These combinations, that we denote by Q_ℓ^m, are sometimes called "cubic harmonics" [cf. VdL 47, Sla 63]. The normalized cubic harmonics through $\ell = 2$ are given in Table 7. In Table 8 we give the linear combinations of cubic

harmonics for Bloch functions belonging to the first row of some of the irreducible representations given in Tables 3 to 6. At all points, except X, the combinations are the same, whether the Bloch function is formed from atomic-like orbitals centered on A or B. At X, as we have seen in the preceding paragraph, this is not true, and we give the combinations separately for atoms of type A and atoms of type B. Not all the irreducible representations previously tabulated are present in Table 8 because some of them correspond to energies that are too high and are, therefore, physically uninteresting, as we already mentioned in Sec. I-3.

We now consider another type of basis functions: symmetrized combinations of plane waves (cf. Eq. II-9). The way to form S.C.P.W.'s is straightforward: we start with a plane wave of the type

$$e^{i(\underset{\sim}{k}+\underset{\sim}{h}_\mu)\cdot\underset{\sim}{r}} \qquad \text{(II-12)}$$

and apply the projection operator P^{α}_{ii} to obtain a basis for the i^{th} row of the representation Γ_α of the group of $\underset{\sim}{k}$. It is obvious that the plane wave (II-12) has the Bloch form (cf. Eq. I-17). Application of the operator R, of the group of $\underset{\sim}{k}$, to the function (II-12) yields

$$R\, e^{i(\underset{\sim}{k}+\underset{\sim}{h}_\mu)\cdot\underset{\sim}{r}} = e^{i(\underset{\sim}{k}+\underset{\sim}{h}_\mu)\cdot\alpha^{-1}\underset{\sim}{r}} = e^{i\alpha(\underset{\sim}{k}+\underset{\sim}{h}_\mu)\cdot\underset{\sim}{r}}. \qquad \text{(II-13)}$$

In Eq. (II-13), we have made use of Eq. (II-3) and of the following property of the scalar product:

TABLE 7

NORMALIZED CUBIC HARMONICS THROUGH $\ell=2$.(+)

$$s = Y_0^0 = \sqrt{\frac{1}{4\pi}}$$

$$p_x = \sqrt{\frac{3}{4\pi}}\frac{x}{r} = \frac{1}{\sqrt{2}}(Y_1^{-1}-Y_1^1) = \sqrt{\frac{3}{4\pi}}\sin\theta\cos\phi$$

$$p_y = \sqrt{\frac{3}{4\pi}}\frac{y}{r} = \frac{i}{\sqrt{2}}(Y_1^{-1}+Y_1^1) = \sqrt{\frac{3}{4\pi}}\sin\theta\sin\phi$$

$$p_z = \sqrt{\frac{3}{4\pi}}\frac{z}{r} = Y_1^0 = \sqrt{\frac{3}{4\pi}}\cos\theta$$

$$d_{xy} = \sqrt{\frac{15}{4\pi}}\frac{xy}{r^2} = \frac{i}{\sqrt{2}}(Y_2^{-2}-Y_2^2) = \sqrt{\frac{15}{4\pi}}\sin^2\theta\cos\phi\sin\phi$$

$$d_{yz} = \sqrt{\frac{15}{4\pi}}\frac{yz}{r^2} = \frac{i}{\sqrt{2}}(Y_2^{-1}+Y_2^1) = \sqrt{\frac{15}{4\pi}}\sin\theta\cos\theta\sin\phi$$

$$d_{zx} = \sqrt{\frac{15}{4\pi}}\frac{zx}{r^2} = \frac{1}{\sqrt{2}}(Y_2^{-1}-Y_2^1) = \sqrt{\frac{15}{4\pi}}\sin\theta\cos\theta\cos\phi$$

$$d_{x^2-y^2} = \sqrt{\frac{15}{16\pi}}\frac{x^2-y^2}{r^2} = \frac{1}{\sqrt{2}}(Y_2^{-2}+Y_2^2) = \sqrt{\frac{15}{16\pi}}\sin^2\theta(\cos^2\phi-\sin^2\phi)$$

$$d_{3z^2-r^2} = \sqrt{\frac{5}{16\pi}}\frac{3z^2-r^2}{r^2} = Y_2^0 = \sqrt{\frac{5}{16\pi}}(3\cos^2\theta-1)$$

(+) The phase convention is that of Condon and Shortley [Con 64].

TABLE 8

BASIS FUNCTIONS FOR IRREDUCIBLE REPRESENTATIONS OF THE GROUP OF $\underset{\sim}{k}$: BLOCH FUNCTIONS.(+)

Γ_1	u_s
Γ_{15}	u_x, u_{yz}
Γ_{12}	$u_{3x^2-r^2}$
X_1	u_s^A, $u_{3x^2-r^2}^A$, u_x^B, u_{yz}^B
X_2	$u_{y^2-z^2}^A$
X_3	u_x^A, u_{yz}^A, u_s^B, $u_{3x^2-r^2}^B$
X_4	$u_{y^2-z^2}^B$
X_5	u_y^A, u_{zx}^A, u_z^B, u_{xy}^B
L_1, Λ_1	u_s, $\frac{1}{\sqrt{3}}(u_x+u_y+u_z)$, $\frac{1}{\sqrt{3}}(u_{xy}+u_{yz}+u_{zx})$
L_3, Λ_3	$\frac{1}{\sqrt{2}}(u_x-u_y)$, $\frac{1}{\sqrt{2}}(u_{yz}-u_{zx})$, $u_{x^2-y^2}$
Δ_1	u_s, u_x, u_{yz}, $u_{3x^2-r^2}$
Δ_2	$u_{y^2-z^2}$
Δ_3	$\frac{1}{\sqrt{2}}(u_y-u_z)$, $\frac{1}{\sqrt{2}}(u_{zx}-u_{xy})$
Δ_4	$\frac{1}{\sqrt{2}}(u_y+u_z)$, $\frac{1}{\sqrt{2}}(u_{zx}+u_{xy})$

(+) As an example, u_x^A represents a normalized Bloch function formed from atomic-like orbitals centered on ions of type A, whose angular part is p_x(cf. Table 7). If the superscript is missing, the basis functions are the same for A and B.

$$\underset{\sim}{a} \cdot \underset{\sim}{b} = \alpha \underset{\sim}{a} \cdot \alpha \underset{\sim}{b} , \qquad \text{(II-14)}$$

where α is any (proper or improper) rotation matrix. Eq. (II-14) is easily proved by using the orthogonality conditions (I-15) for the elements of α.

From these considerations it follows that a S.C.P.W. can be written in the form (cf. Eq. II-9)

$$S_m^\sigma = \theta_m^\sigma \sum_R \Gamma_{\gamma\gamma}^{\alpha}(R)^* e^{i\alpha(\underset{\sim}{k} + \underset{\sim}{h}_\mu)\cdot \underset{\sim}{r}} . \qquad \text{(II-15)}$$

The reciprocal lattice vector $\underset{\sim}{h}_\mu$ in Eq. (II-15) can be called the "generator" of the S.C.P.W. S_m^σ. We see from Eq. (II-15) that a plane wave of wave vector $\underset{\sim}{k} + \underset{\sim}{h}_\mu$ combines only with plane waves of wave vector $\alpha(\underset{\sim}{k} + \underset{\sim}{h}_\mu)$. Thus all the plane waves in a S.C.P.W. have the same kinetic energy, since $|\underset{\sim}{k} + \underset{\sim}{h}_\mu|^2 = |\alpha\ (\underset{\sim}{k} + \underset{\sim}{h}_\mu)|^2$. We already stated this condition in connection with Eq. (II-9).

The effect of operators of T_d on a plane wave (see Eq. II-13) is given in Table 9. We use a standard notation, by which a plane wave of wave vector $\underset{\sim}{K} \equiv (\ell,m,n)$ is denoted by the components of $\underset{\sim}{K}$:

$$(\ell, m, n) \equiv e^{i(\ell x + m y + n z)} = e^{i \underset{\sim}{K}\cdot \underset{\sim}{r}} . \qquad \text{(II-16)}$$

Some generators of S.C.P.W.'s for the representations of interest are given in Tables 10 to 16. They are listed in order of increasing $|\underset{\sim}{k} + \underset{\sim}{h}_\mu|$.

TABLE 9

EFFECT OF OPERATORS OF T_d ON A PLANE WAVE.

$R_1(1\ m\ n) = (1\ m\ n)$	$R_{13}(1\ m\ n) = (\bar{1}\ \bar{n}\ m)$
$R_2(1\ m\ n) = (1\ \bar{m}\ \bar{n})$	$R_{14}(1\ m\ n) = (\bar{1}\ n\ \bar{m})$
$R_3(1\ m\ n) = (\bar{1}\ m\ \bar{n})$	$R_{15}(1\ m\ n) = (n\ \bar{m}\ \bar{1})$
$R_4(1\ m\ n) = (\bar{1}\ \bar{m}\ n)$	$R_{16}(1\ m\ n) = (\bar{n}\ \bar{m}\ 1)$
$R_5(1\ m\ n) = (n\ 1\ m)$	$R_{17}(1\ m\ n) = (\bar{m}\ 1\ \bar{n})$
$R_6(1\ m\ n) = (\bar{n}\ \bar{1}\ m)$	$R_{18}(1\ m\ n) = (m\ \bar{1}\ \bar{n})$
$R_7(1\ m\ n) = (n\ \bar{1}\ \bar{m})$	$R_{19}(1\ m\ n) = (1\ n\ m)$
$R_8(1\ m\ n) = (\bar{n}\ 1\ \bar{m})$	$R_{20}(1\ m\ n) = (1\ \bar{n}\ \bar{m})$
$R_9(1\ m\ n) = (m\ n\ 1)$	$R_{21}(1\ m\ n) = (n\ m\ 1)$
$R_{10}(1\ m\ n) = (\bar{m}\ n\ \bar{1})$	$R_{22}(1\ m\ n) = (\bar{n}\ m\ \bar{1})$
$R_{11}(1\ m\ n) = (\bar{m}\ \bar{n}\ 1)$	$R_{23}(1\ m\ n) = (m\ 1\ n)$
$R_{12}(1\ m\ n) = (m\ \bar{n}\ \bar{1})$	$R_{24}(1\ m\ n) = (\bar{m}\ \bar{1}\ n)$

TABLE 10

GENERATORS OF S.C.P.W.'S IN UNITS OF $\frac{2\pi}{a}$.

POINT Γ : (0 0 0)

Γ_1	Γ_{15}	Γ_{12}
(0 0 0)	(1 1 1)	(2 0 0)
(1 1 1)	($\bar{1}$ $\bar{1}$ $\bar{1}$)	(2 2 0)
($\bar{1}$ $\bar{1}$ $\bar{1}$)	(2 0 0)	(3 1 1)
(2 0 0)	(2 2 0)	($\bar{3}$ $\bar{1}$ $\bar{1}$)
(2 2 0)	(0 2 2)	(4 0 0)
(3 1 1)	(3 1 1)	(3 3 1)
($\bar{3}$ $\bar{1}$ $\bar{1}$)	($\bar{3}$ $\bar{1}$ $\bar{1}$)	($\bar{3}$ $\bar{3}$ $\bar{1}$)
(2 2 2)	(1 3 1)	(4 2 0)
($\bar{2}$ $\bar{2}$ $\bar{2}$)	($\bar{1}$ $\bar{3}$ $\bar{1}$)	(2 4 0)
(4 0 0)	(2 2 2)	(4 2 2)
(3 3 1)	($\bar{2}$ $\bar{2}$ $\bar{2}$)	($\bar{4}$ $\bar{2}$ $\bar{2}$)
($\bar{3}$ $\bar{3}$ $\bar{1}$)	(4 0 0)	(5 1 1)
(4 2 0)	(3 3 1)	($\bar{5}$ $\bar{1}$ $\bar{1}$)
(4 2 2)	($\bar{3}$ $\bar{3}$ $\bar{1}$)	
($\bar{4}$ $\bar{2}$ $\bar{2}$)	(1 3 3)	
(3 3 3)	($\bar{1}$ $\bar{3}$ $\bar{3}$)	
($\bar{3}$ $\bar{3}$ $\bar{3}$)	(4 2 0)	
(5 1 1)	(2 4 0)	
($\bar{5}$ $\bar{1}$ $\bar{1}$)	(0 4 2)	
	(4 2 2)	
	($\bar{4}$ $\bar{2}$ $\bar{2}$)	
	(2 4 2)	
	($\bar{2}$ $\bar{4}$ $\bar{2}$)	
	(3 3 3)	
	($\bar{3}$ $\bar{3}$ $\bar{3}$)	
	(5 1 1)	
	($\bar{5}$ $\bar{1}$ $\bar{1}$)	
	(1 5 1)	
	($\bar{1}$ $\bar{5}$ $\bar{1}$)	

TABLE 11

GENERATORS OF S.C.P.W.'S IN UNITS OF $\frac{2\pi}{a}$.

POINT X : $\frac{2\pi}{a}$ (100).

X_1	X_3	X_4	X_5
(0 0 0)	(0 0 0)	(0 2 0)	($\bar{1}$ 1 1)
($\bar{1}$ 1 1)	($\bar{1}$ 1 1)	($\bar{1}$ 3 1)	(0 2 0)
(0 2 0)	(0 2 0)	(2 2 0)	(0 0 2)
(1 1 1)	(1 1 1)	(1 3 1)	(1 1 1)
($\bar{3}$ 1 1)	($\bar{3}$ 1 1)	(1 3 $\bar{1}$)	($\bar{3}$ 1 1)
(0 2 2)	(0 2 2)	(0 4 0)	(0 2 2)
(0 2 $\bar{2}$)	(0 2 $\bar{2}$)	($\bar{1}$ 3 3)	(0 2 $\bar{2}$)
(2 0 0)	(2 0 0)	(3 1 1)	($\bar{1}$ 3 1)
($\bar{1}$ 3 1)	($\bar{1}$ 3 1)	(3 1 $\bar{1}$)	($\bar{1}$ 1 3)
(2 2 0)	(2 2 0)	(0 4 2)	(2 2 0)
(1 3 1)	(1 3 1)	(0 4 $\bar{2}$)	(2 0 2)
(1 3 $\bar{1}$)	(1 3 $\bar{1}$)	(1 3 3)	(1 3 1)
(2 2 2)	(2 2 2)	(1 3 $\bar{3}$)	(1 1 3)
(2 2 $\bar{2}$)	(2 2 $\bar{2}$)		(1 3 $\bar{1}$)
(0 4 0)	(0 4 0)		(1 1 $\bar{3}$)
($\bar{1}$ 3 3)	($\bar{1}$ 3 3)		(2 2 2)
(3 1 1)	(3 1 1)		(2 2 $\bar{2}$)
(3 1 $\bar{1}$)	(3 1 $\bar{1}$)		(0 4 0)
(0 4 2)	(0 4 2)		(0 0 4)
(0 4 $\bar{2}$)	(0 4 $\bar{2}$)		($\bar{1}$ 3 3)
(1 3 3)	(1 3 3)		(3 1 1)
(1 3 $\bar{3}$)	(1 3 $\bar{3}$)		(3 1 $\bar{1}$)
			(0 4 2)
			(0 2 4)
			(0 4 $\bar{2}$)
			(0 2 $\bar{4}$)
			(1 3 3)
			(1 3 $\bar{3}$)

TABLE 12

GENERATORS OF S.C.P.W.'S IN UNITS OF $\frac{2\pi}{a}$.

POINT L : $\frac{2\pi}{a}(\frac{1}{2}\ \frac{1}{2}\ \frac{1}{2})$.

L_1		L_3	
(0 0 0)	(3 1 $\bar{1}$)	(1 $\bar{1}$ $\bar{1}$)	(3 1 1)
($\bar{1}$ $\bar{1}$ $\bar{1}$)	($\bar{4}$ $\bar{2}$ 0)	($\bar{2}$ 0 0)	($\bar{4}$ $\bar{2}$ $\bar{2}$)
(1 $\bar{1}$ $\bar{1}$)	(3 1 1)	(0 $\bar{2}$ $\bar{2}$)	(3 $\bar{3}$ $\bar{1}$)
($\bar{2}$ 0 0)	($\bar{4}$ $\bar{2}$ $\bar{2}$)	($\bar{1}$ 1 1)	($\bar{1}$ 3 $\bar{3}$)
(0 $\bar{2}$ $\bar{2}$)	(2 2 2)	(2 0 0)	($\bar{4}$ 2 0)
($\bar{1}$ 1 1)	($\bar{3}$ $\bar{3}$ $\bar{3}$)	($\bar{3}$ $\bar{1}$ $\bar{1}$)	(0 $\bar{4}$ 2)
(1 1 1)	(3 $\bar{3}$ $\bar{1}$)	(2 $\bar{2}$ 0)	(3 $\bar{3}$ 1)
($\bar{2}$ $\bar{2}$ $\bar{2}$)	($\bar{4}$ 2 0)	(0 2 $\bar{2}$)	(1 3 $\bar{3}$)
(2 0 0)	(3 $\bar{3}$ 1)	($\bar{3}$ 1 $\bar{1}$)	($\bar{4}$ 2 $\bar{2}$)
($\bar{3}$ $\bar{1}$ $\bar{1}$)	($\bar{4}$ 2 $\bar{2}$)	($\bar{1}$ $\bar{3}$ 1)	($\bar{2}$ $\bar{4}$ 2)
(2 $\bar{2}$ 0)	(4 0 0)	(2 $\bar{2}$ $\bar{2}$)	(4 0 0)
($\bar{3}$ 1 $\bar{1}$)	($\bar{5}$ $\bar{1}$ $\bar{1}$)	($\bar{3}$ 1 1)	($\bar{5}$ $\bar{1}$ $\bar{1}$)
(2 $\bar{2}$ $\bar{2}$)	(4 $\bar{2}$ 0)	(0 2 2)	(4 $\bar{2}$ 0)
($\bar{3}$ 1 1)	($\bar{5}$ 1 $\bar{1}$)	($\bar{1}$ $\bar{3}$ $\bar{3}$)	(0 4 $\bar{2}$)
(0 2 2)	(3 $\bar{3}$ $\bar{3}$)	(3 $\bar{1}$ $\bar{1}$)	($\bar{5}$ 1 $\bar{1}$)
($\bar{1}$ $\bar{3}$ $\bar{3}$)	($\bar{4}$ 2 2)	($\bar{4}$ 0 0)	($\bar{1}$ $\bar{5}$ 1)
(3 $\bar{1}$ $\bar{1}$)	($\bar{1}$ 3 3)	(1 $\bar{3}$ $\bar{3}$)	(3 $\bar{3}$ $\bar{3}$)
($\bar{4}$ 0 0)	(0 $\bar{4}$ $\bar{4}$)	($\bar{2}$ 2 2)	($\bar{4}$ 2 2)
(1 $\bar{3}$ $\bar{3}$)	(4 $\bar{2}$ $\bar{2}$)	(3 1 $\bar{1}$)	($\bar{1}$ 3 3)
($\bar{2}$ 2 2)	($\bar{5}$ 1 1)	($\bar{1}$ 3 1)	(0 $\bar{4}$ $\bar{4}$)
		($\bar{4}$ $\bar{2}$ 0)	(4 $\bar{2}$ $\bar{2}$)
		(0 $\bar{4}$ $\bar{2}$)	($\bar{5}$ 1 1)

TABLE 13

GENERATORS OF S.C.P.W.'S IN UNITS OF $\frac{2\pi}{a}$.

POINT Δ^2 : $\frac{1}{2}\frac{2\pi}{a}$ (1 0 0).

Δ_1^2		Δ_2^2	Δ_3^2		Δ_4^2	
(0 0 0)	($\bar{1}$ 3 3)	(0 2 0)	($\bar{1}$ 1 $\bar{1}$)	(1 3 $\bar{3}$)	($\bar{1}$ 1 1)	(1 3 3)
($\bar{2}$ 0 0)	($\bar{1}$ 3 $\bar{3}$)	($\bar{2}$ 2 0)	(1 1 $\bar{1}$)	(0 2 4)	(1 1 1)	(0 2 4)
($\bar{1}$ 1 1)	($\bar{2}$ 4 0)	(2 2 0)	(0 2 0)	(0 2 $\bar{4}$)	(0 2 0)	(0 2 $\bar{4}$)
($\bar{1}$ 1 $\bar{1}$)	(1 3 3)	($\bar{1}$ 3 1)	($\bar{2}$ 2 0)	($\bar{4}$ 2 $\bar{2}$)	($\bar{2}$ 2 0)	($\bar{4}$ 2 2)
(1 1 1)	(1 3 $\bar{3}$)	($\bar{1}$ 3 $\bar{1}$)	(0 2 $\bar{2}$)	(3 3 1)	(0 2 2)	(3 3 1)
(1 1 $\bar{1}$)	(0 2 4)	(1 3 1)	($\bar{3}$ 1 $\bar{1}$)	(3 3 $\bar{1}$)	($\bar{3}$ 1 1)	(3 3 $\bar{1}$)
(0 2 0)	(0 2 $\bar{4}$)	(1 3 $\bar{1}$)	(2 2 0)	($\bar{2}$ 2 4)	(2 2 0)	($\bar{2}$ 2 4)
($\bar{2}$ 2 0)	($\bar{4}$ 2 2)	($\bar{4}$ 2 0)	($\bar{2}$ 2 $\bar{2}$)	($\bar{2}$ 2 $\bar{4}$)	($\bar{2}$ 2 2)	($\bar{2}$ 2 $\bar{4}$)
(2 0 0)	($\bar{4}$ 2 $\bar{2}$)	(0 4 0)	($\bar{1}$ 3 1)	(2 4 0)	($\bar{1}$ 3 1)	(2 4 0)
(0 2 2)	(4 0 0)	($\bar{3}$ 3 1)	($\bar{1}$ 3 $\bar{1}$)	($\bar{5}$ 1 $\bar{1}$)	($\bar{1}$ 3 $\bar{1}$)	($\bar{5}$ 1 1)
(0 2 $\bar{2}$)	(3 3 1)	($\bar{3}$ 3 $\bar{1}$)	(1 3 1)	($\bar{3}$ 3 $\bar{3}$)	(1 3 1)	($\bar{3}$ 3 3)
($\bar{3}$ 1 1)	(3 3 $\bar{1}$)	($\bar{2}$ 4 0)	(1 3 $\bar{1}$)	(4 2 0)	(1 3 $\bar{1}$)	(4 2 0)
($\bar{3}$ 1 $\bar{1}$)	($\bar{2}$ 2 4)	(0 2 4)	(3 1 $\bar{1}$)	(2 4 2)	(3 1 1)	(2 4 2)
(2 2 0)	($\bar{2}$ 2 $\bar{4}$)	(0 2 $\bar{4}$)	(2 2 $\bar{2}$)	(2 4 $\bar{2}$)	(2 2 2)	(2 4 $\bar{2}$)
($\bar{2}$ 2 2)	(2 4 0)	(3 3 1)	($\bar{4}$ 2 0)	($\bar{1}$ 1 5)	($\bar{4}$ 2 0)	($\bar{1}$ 1 5)
($\bar{2}$ 2 $\bar{2}$)	($\bar{5}$ 1 1)	(3 3 $\bar{1}$)	(0 4 0)	($\bar{1}$ 1 $\bar{5}$)	(0 4 0)	($\bar{1}$ 1 $\bar{5}$)
($\bar{1}$ 3 1)	($\bar{5}$ 1 $\bar{1}$)	($\bar{2}$ 2 4)	($\bar{3}$ 3 1)	(4 2 $\bar{2}$)	($\bar{3}$ 3 1)	(4 2 2)
($\bar{1}$ 3 $\bar{1}$)	($\bar{3}$ 3 3)	($\bar{2}$ 2 $\bar{4}$)	($\bar{3}$ 3 $\bar{1}$)	(1 5 1)	($\bar{3}$ 3 $\bar{1}$)	(1 5 1)
(1 3 1)	($\bar{3}$ 3 $\bar{3}$)	(2 4 0)	($\bar{1}$ 3 $\bar{3}$)	(1 5 $\bar{1}$)	($\bar{1}$ 3 3)	(1 5 $\bar{1}$)
(1 3 $\bar{1}$)	(4 2 0)	(4 2 0)	($\bar{2}$ 4 0)	($\bar{4}$ 4 0)	($\bar{2}$ 4 0)	($\bar{4}$ 4 0)
($\bar{4}$ 0 0)	(2 4 2)	(2 4 2)				
(3 1 1)	(2 4 $\bar{2}$)	(2 4 $\bar{2}$)				
(3 1 $\bar{1}$)	($\bar{1}$ 1 5)	($\bar{1}$ 1 5)				
(2 2 2)	($\bar{1}$ 1 $\bar{5}$)	($\bar{1}$ 1 $\bar{5}$)				
(2 2 $\bar{2}$)	(4 2 2)	(1 5 1)				
($\bar{4}$ 2 0)	(4 2 $\bar{2}$)	(1 5 $\bar{1}$)				
(0 4 0)	(1 5 1)	($\bar{4}$ 4 0)				
($\bar{3}$ 3 1)	(1 5 $\bar{1}$)					
($\bar{3}$ 3 $\bar{1}$)	($\bar{4}$ 4 0)					

TABLE 14

GENERATORS OF S.C.P.W.'S IN UNITS OF $\frac{2\pi}{a}$.

POINT Λ^2 : $\frac{1}{2}\frac{2\pi}{a}$ $(\frac{1}{2}\ \frac{1}{2}\ \frac{1}{2})$.

Λ_1^2		Λ_3^2	
(0 0 0)	(2 2 2)	(1 $\bar{1}$ $\bar{1}$)	(0 $\bar{4}$ $\bar{2}$)
($\bar{1}$ $\bar{1}$ $\bar{1}$)	($\bar{1}$ $\bar{3}$ $\bar{3}$)	($\bar{2}$ 0 0)	(4 0 0)
(1 $\bar{1}$ $\bar{1}$)	(1 $\bar{3}$ $\bar{3}$)	($\bar{1}$ 1 1)	(3 $\bar{3}$ $\bar{1}$)
($\bar{2}$ 0 0)	($\bar{4}$ $\bar{2}$ 0)	(2 0 0)	($\bar{1}$ 3 $\bar{3}$)
($\bar{1}$ 1 1)	(4 0 0)	(0 $\bar{2}$ $\bar{2}$)	($\bar{4}$ 2 0)
(1 1 1)	(3 $\bar{3}$ $\bar{1}$)	(2 $\bar{2}$ 0)	(0 $\bar{4}$ 2)
(2 0 0)	($\bar{4}$ 2 0)	(0 2 $\bar{2}$)	(3 $\bar{3}$ 1)
(0 $\bar{2}$ $\bar{2}$)	(3 $\bar{3}$ 1)	($\bar{3}$ $\bar{1}$ $\bar{1}$)	(1 3 $\bar{3}$)
(2 $\bar{2}$ 0)	($\bar{4}$ $\bar{2}$ $\bar{2}$)	($\bar{3}$ 1 $\bar{1}$)	($\bar{4}$ $\bar{2}$ $\bar{2}$)
($\bar{3}$ $\bar{1}$ $\bar{1}$)	(4 $\bar{2}$ 0)	($\bar{1}$ $\bar{3}$ 1)	(4 $\bar{2}$ 0)
($\bar{2}$ $\bar{2}$ $\bar{2}$)	($\bar{1}$ 3 3)	(0 2 2)	(0 4 $\bar{2}$)
($\bar{3}$ 1 $\bar{1}$)	($\bar{4}$ 2 $\bar{2}$)	($\bar{3}$ 1 1)	($\bar{1}$ 3 3)
(0 2 2)	($\bar{3}$ $\bar{3}$ $\bar{3}$)	(2 $\bar{2}$ $\bar{2}$)	($\bar{4}$ 2 $\bar{2}$)
($\bar{3}$ 1 1)	(1 3 3)	(3 $\bar{1}$ $\bar{1}$)	($\bar{2}$ $\bar{4}$ 2)
(2 $\bar{2}$ $\bar{2}$)	(4 2 0)	(3 1 $\bar{1}$)	(1 3 3)
(3 $\bar{1}$ $\bar{1}$)	($\bar{5}$ $\bar{1}$ $\bar{1}$)	($\bar{1}$ 3 1)	(4 2 0)
(3 1 $\bar{1}$)	($\bar{4}$ 2 2)	($\bar{2}$ 2 2)	(0 4 2)
($\bar{2}$ 2 2)	(4 $\bar{2}$ $\bar{2}$)	(3 1 1)	($\bar{5}$ $\bar{1}$ $\bar{1}$)
(3 1 1)	($\bar{5}$ 1 $\bar{1}$)	($\bar{4}$ 0 0)	($\bar{4}$ 2 2)
($\bar{4}$ 0 0)		($\bar{1}$ $\bar{3}$ $\bar{3}$)	(4 $\bar{2}$ $\bar{2}$)
		(1 $\bar{3}$ $\bar{3}$)	($\bar{5}$ 1 $\bar{1}$)
		($\bar{4}$ $\bar{2}$ 0)	($\bar{1}$ $\bar{5}$ 1)

TABLE 15

GENERATORS OF S.C.P.W.'S IN UNITS OF $\frac{2\pi}{a}$.

POINT Δ^4 : $\frac{1}{4}\frac{2\pi}{a}$ (1 0 0).

Δ_1^4		Δ_2^4	Δ_3^4		Δ_4^4	
(0 0 0)	(0 4 0)	(0 2 0)	($\bar{1}$ 1 $\bar{1}$)	($\bar{4}$ 2 0)	($\bar{1}$ 1 1)	($\bar{4}$ 2 0)
($\bar{1}$ 1 1)	($\bar{3}$ 3 1)	($\bar{2}$ 2 0)	(1 1 $\bar{1}$)	($\bar{1}$ 3 $\bar{3}$)	(1 1 1)	($\bar{1}$ 3 3)
($\bar{1}$ 1 $\bar{1}$)	($\bar{3}$ 3 $\bar{1}$)	(2 2 0)	(0 2 0)	($\bar{2}$ 4 0)	(0 2 0)	($\bar{2}$ 4 0)
($\bar{2}$ 0 0)	($\bar{4}$ 2 0)	($\bar{1}$ 3 1)	($\bar{2}$ 2 0)	(1 3 $\bar{3}$)	($\bar{2}$ 2 0)	(1 3 3)
(1 1 1)	(4 0 0)	($\bar{1}$ 3 $\bar{1}$)	(0 2 $\bar{2}$)	(0 4 2)	(0 2 2)	(0 4 2)
(1 1 $\bar{1}$)	($\bar{1}$ 3 3)	(1 3 1)	(2 2 0)	(0 4 $\bar{2}$)	(2 2 0)	(0 4 $\bar{2}$)
(0 2 0)	($\bar{1}$ 3 $\bar{3}$)	(1 3 $\bar{1}$)	($\bar{3}$ 1 $\bar{1}$)	(3 3 1)	($\bar{3}$ 1 1)	(3 3 1)
(2 0 0)	($\bar{2}$ 4 0)	(0 4 0)	($\bar{1}$ 3 1)	(3 3 $\bar{1}$)	($\bar{1}$ 3 1)	(3 3 $\bar{1}$)
($\bar{2}$ 2 0)	(1 3 3)	($\bar{3}$ 3 1)	($\bar{1}$ 3 $\bar{1}$)	(2 4 0)	($\bar{1}$ 3 $\bar{1}$)	(2 4 0)
(0 2 2)	(1 3 $\bar{3}$)	($\bar{3}$ 3 $\bar{1}$)	($\bar{2}$ 2 $\bar{2}$)	(4 2 0)	($\bar{2}$ 2 2)	(4 2 0)
(0 2 $\bar{2}$)	(0 4 2)	($\bar{4}$ 2 0)	(1 3 1)	($\bar{4}$ 2 $\bar{2}$)	(1 3 1)	($\bar{4}$ 2 2)
(2 2 0)	(0 4 $\bar{2}$)	($\bar{2}$ 4 0)	(1 3 $\bar{1}$)	($\bar{2}$ 4 2)	(1 3 $\bar{1}$)	($\bar{2}$ 4 2)
($\bar{3}$ 1 1)	(3 3 1)	(0 4 2)	(3 1 $\bar{1}$)	($\bar{2}$ 4 $\bar{2}$)	(3 1 1)	($\bar{2}$ 4 $\bar{2}$)
($\bar{3}$ 1 $\bar{1}$)	(3 3 $\bar{1}$)	(0 4 $\bar{2}$)	(2 2 $\bar{2}$)	(2 4 2)	(2 2 2)	(2 4 2)
($\bar{1}$ 3 1)	(2 4 0)	(3 3 1)	(0 4 0)	(2 4 $\bar{2}$)	(0 4 0)	(2 4 $\bar{2}$)
($\bar{1}$ 3 $\bar{1}$)	(4 2 0)	(3 3 $\bar{1}$)	($\bar{3}$ 3 1)	(4 2 $\bar{2}$)	($\bar{3}$ 3 1)	(4 2 2)
($\bar{2}$ 2 2)	($\bar{4}$ 2 2)	(2 4 0)	($\bar{3}$ 3 $\bar{1}$)		($\bar{3}$ 3 $\bar{1}$)	
($\bar{2}$ 2 $\bar{2}$)	($\bar{4}$ 2 $\bar{2}$)	(4 2 0)				
(1 3 1)	($\bar{2}$ 4 2)	($\bar{2}$ 4 2)				
(1 3 $\bar{1}$)	($\bar{2}$ 4 $\bar{2}$)	($\bar{2}$ 4 $\bar{2}$)				
(3 1 1)	(2 4 2)	(2 4 2)				
(3 1 $\bar{1}$)	(2 4 $\bar{2}$)	(2 4 $\bar{2}$)				
(2 2 2)	(4 2 2)					
(2 2 $\bar{2}$)	(4 2 $\bar{2}$)					
($\bar{4}$ 0 0)						

TABLE 16

GENERATORS OF S.C.P.W.'S IN UNITS OF $\frac{2\pi}{a}$.

POINT Λ^4 : $\frac{1}{4}\ \frac{2\pi}{a}\ (\frac{1}{2}\ \frac{1}{2}\ \frac{1}{2})$.

Λ_1^4		Λ_3^4	
(0 0 0)	($\bar{4}$ 0 0)	(1 $\bar{1}$ $\bar{1}$)	($\bar{4}$ $\bar{2}$ 0)
($\bar{1}$ $\bar{1}$ $\bar{1}$)	(4 0 0)	($\bar{1}$ 1 1)	(0 $\bar{4}$ $\bar{2}$)
(1 $\bar{1}$ $\bar{1}$)	($\bar{1}$ $\bar{3}$ $\bar{3}$)	($\bar{2}$ 0 0)	(3 $\bar{3}$ $\bar{1}$)
($\bar{1}$ 1 1)	(1 $\bar{3}$ $\bar{3}$)	(2 0 0)	($\bar{1}$ 3 $\bar{3}$)
($\bar{2}$ 0 0)	($\bar{4}$ $\bar{2}$ 0)	(0 $\bar{2}$ $\bar{2}$)	(3 $\bar{3}$ 1)
(1 1 1)	(3 $\bar{3}$ $\bar{1}$)	(2 $\bar{2}$ 0)	(1 3 $\bar{3}$)
(2 0 0)	(3 $\bar{3}$ 1)	(0 2 $\bar{2}$)	($\bar{4}$ 2 0)
(0 $\bar{2}$ $\bar{2}$)	($\bar{4}$ 2 0)	(0 2 2)	(0 $\bar{4}$ 2)
(2 $\bar{2}$ 0)	($\bar{1}$ 3 3)	($\bar{3}$ $\bar{1}$ $\bar{1}$)	($\bar{1}$ 3 3)
(0 2 2)	(4 $\bar{2}$ 0)	($\bar{3}$ 1 $\bar{1}$)	(4 $\bar{2}$ 0)
($\bar{3}$ $\bar{1}$ $\bar{1}$)	(1 3 3)	($\bar{1}$ $\bar{3}$ 1)	(0 4 $\bar{2}$)
($\bar{3}$ 1 $\bar{1}$)	(4 2 0)	($\bar{3}$ 1 1)	(1 3 3)
($\bar{2}$ $\bar{2}$ $\bar{2}$)	($\bar{4}$ $\bar{2}$ $\bar{2}$)	(3 $\bar{1}$ $\bar{1}$)	(4 2 0)
($\bar{3}$ 1 1)	($\bar{4}$ 2 $\bar{2}$)	(2 $\bar{2}$ $\bar{2}$)	(0 4 2)
(3 $\bar{1}$ $\bar{1}$)	($\bar{4}$ 2 2)	(3 1 $\bar{1}$)	($\bar{4}$ $\bar{2}$ $\bar{2}$)
(2 $\bar{2}$ $\bar{2}$)	(4 $\bar{2}$ $\bar{2}$)	($\bar{1}$ 3 1)	($\bar{4}$ 2 $\bar{2}$)
(3 1 $\bar{1}$)	($\bar{3}$ $\bar{3}$ $\bar{3}$)	(3 1 1)	($\bar{2}$ $\bar{4}$ 2)
(3 1 1)	(4 2 $\bar{2}$)	($\bar{2}$ 2 2)	($\bar{4}$ 2 2)
($\bar{2}$ 2 2)	($\bar{5}$ $\bar{1}$ $\bar{1}$)	($\bar{4}$ 0 0)	(4 $\bar{2}$ $\bar{2}$)
(2 2 2)		(4 0 0)	(4 2 $\bar{2}$)
		($\bar{1}$ $\bar{3}$ $\bar{3}$)	($\bar{2}$ 4 2)
		(1 $\bar{3}$ $\bar{3}$)	($\bar{5}$ $\bar{1}$ $\bar{1}$)

II-4. The double group T_d.

The double group T_d contains 48 elements. To each element R of the single group there correspond two operations in the double group, usually denoted by R and $\bar{R}$, where (cf. Eq. I-37)

$$R \equiv D(R)R \quad \text{and} \quad \bar{R} \equiv -D(R)R \,. \tag{II-17}$$

The 2 x 2 matrix D(R) was defined in Eq. (I-36) in terms of the Euler angles α, β, and γ. The character tables for the irreducible representations of the double group at all points of interest are given by Parmenter [Par 55] and Dresselhaus [Dre 55]. Slater gives the full matrices of the additional representations at Γ [Sla 65, Table A9-11] and the basis functions [op. cit., Eq. (A9-76)].

The basis functions for the additional representations of the double group are two-component spinors (cf. Sec. I-4). A function of this kind can be written

$$\psi = \begin{pmatrix} f_1(\underset{\sim}{r}) \\ f_2(\underset{\sim}{r}) \end{pmatrix} . \tag{II-18}$$

An operator R (Eq. II-17), acting upon ψ, will produce the following effect:

$$R\psi = \begin{pmatrix} D_{11}(R)R & D_{12}(R)R \\ D_{21}(R)R & D_{22}(R)R \end{pmatrix} \begin{pmatrix} f_1(\underset{\sim}{r}) \\ f_2(\underset{\sim}{r}) \end{pmatrix} \tag{II-19}$$

$$= \begin{pmatrix} D_{11}(R)\, f_1(\alpha^{-1}\underset{\sim}{r}) + D_{12}(R)\, f_2(\alpha^{-1}\underset{\sim}{r}) \\ D_{21}(R)\, f_1(\alpha^{-1}\underset{\sim}{r}) + D_{22}(R)\, f_2(\alpha^{-1}\underset{\sim}{r}) \end{pmatrix} .$$

An equivalent way of writing Eq. (II-18) is

$$\psi = f_1(\vec{r})\begin{pmatrix}1\\0\end{pmatrix} + f_2(\vec{r})\begin{pmatrix}0\\1\end{pmatrix}, \tag{II-20}$$

where $\begin{pmatrix}1\\0\end{pmatrix}$ and $\begin{pmatrix}0\\1\end{pmatrix}$ are column matrices operated upon by D(R). If we denote these matrices by α and β, respectively, [cf. Sla 60] Eq. (II-20) becomes

$$\psi = f_1\alpha + f_2\beta . \tag{II-21}$$

It is easy to see that the result of operating on α and β with D(R) is

$$\begin{aligned} D(R)\alpha &= D_{11}\alpha + D_{21}\beta , \\ D(R)\beta &= D_{12}\alpha + D_{22}\beta . \end{aligned} \tag{II-22}$$

Eq. (II-22) shows that the constant spinors α and β form a basis for the two-dimensional representation $D_{\frac{1}{2}}$ of the double group (cf. Sec. I-4).

In Table 17 we give the character table and basis functions for the additional representations of the double group at Γ. We give only one type of basis functions (Bloch functions) and one point (Γ), because this is all we need for our spin-orbit splitting calculation in the next chapter. The compatibility relations connecting the representations of the single group with the extra representations of the double group (cf. Eq. I-38) are also given. We see that in the presence of spin-orbit interaction a state Γ_{15} splits into $\Gamma_7+\Gamma_8$. The difference in energy between

TABLE 17

CHARACTER TABLE AND BASIS FUNCTIONS FOR THE ADDITIONAL REPRESENTATIONS OF THE DOUBLE GROUP AT Γ.

	E	$\bar{E}$	$6C_4^2$	$8C_3$	$8\bar{C}_3$	$6IxC_4$	$6Ix\bar{C}_4$	$12IxC_2$
Γ_6	2	-2	0	1	-1	$\sqrt{2}$	$-\sqrt{2}$	0
Γ_7	2	-2	0	1	-1	$-\sqrt{2}$	$\sqrt{2}$	0
Γ_8	4	-4	0	-1	1	0	0	0

Γ_i	Γ_1	Γ_2	Γ_{12}	Γ_{15}	Γ_{25}
$\Gamma_i \times D_{\frac{1}{2}}$	Γ_6	Γ_7	Γ_8	$\Gamma_7+\Gamma_8$	$\Gamma_6+\Gamma_8$

$$\Gamma_7 : -\frac{i}{\sqrt{3}}\left[(d_{yz}-id_{zx})\alpha - d_{xy}\beta\right], \quad -\frac{i}{\sqrt{3}}\left[(p_x-ip_y)\alpha - p_z\beta\right]$$

$$\Gamma_8 : \frac{i}{\sqrt{2}}\left[(d_{yz}+id_{zx})\alpha\right], \quad \frac{i}{\sqrt{2}}\left[(p_x+ip_y)\alpha\right]$$

these two states will give the spin-orbit splitting.

Chapter III

THE VALENCE BANDS

III-1. The tight-binding approximation for an ionic crystal.

We begin our investigation of the energy bands of the CuCl crystal by studying the valence bands in the "tight-binding" approximation [Blo 28; see also Fow 63, 63a and Bas 65]. In this approximation the trial function $f_i^\sigma(\underset{\sim}{r})$ (Eq.I-33) is expanded in terms of Bloch functions (Eq. II-7):

$$f_i^\sigma(\underset{\sim}{r}) = \sum_n a_{in}^\sigma F_n^\sigma(\underset{\sim}{r}), \qquad \text{(III-1)}$$

where

$$F_n^\sigma(\underset{\sim}{r}) = \eta_n^\sigma \sum_\nu e^{i\underset{\sim}{k}\cdot\underset{\sim}{R}_\nu} v_n^\sigma(\underset{\sim}{r} - \underset{\sim}{R}_\nu - \delta_n \underset{\sim}{\alpha}), \qquad \text{(III-2)}$$

and

$$v_n^\sigma(\underset{\sim}{r}') = \sum_{m'} c_{nm'}^\sigma u_{nlm'}(\underset{\sim}{r}'), \quad u_{nlm'}(\underset{\sim}{r}') = \frac{P_{nl}(r')}{r'} Q_l^{m'}\left(\frac{\underset{\sim}{r}'}{r'}\right). \qquad \text{(III-3)}$$

In Eq. (III-3) $P_{nl}(r')$ is the solution of the radial equation for an ion in the spherically averaged Madelung field (cf. Eq. III-25). $\Sigma_{m'} c_{nm'}^\sigma u_{nlm'}$ is a symmetrized combination of atomic orbitals, as given in Table 8.

The tight-binding method has been applied with success to the calculation of the valence bands of "tightly-bound" solids, such as rare gases or ionic crystals. One

argues that in such solids the crystal wave function for core and valence states should not differ too much from an atomic wave function, taking into account the crystal symmetry. Furthermore, the core functions are rather compact around the nuclei and they do not change considerably going from the free atom (or ion) to the crystal, except for a shift in energy equal to the Madelung energy. Also the Bloch functions formed from excited atomic states are not expected to mix very much with those formed from valence states, since they correspond to much higher energies. Thus one restricts the sum in Eq. (III-1) to Bloch functions coming from the outermost occupied atomic states. The choice depends on the particular atoms (or ions) forming the crystal. We will give and justify our choice for CuCl in the next section. In this section we derive the matrix elements of the secular determinant (cf. Sec. I-3) and in the next section we consider the approximations involved in calculating them.

We may choose the coefficient η_n^σ in Eq. (III-2) so that the functions F_n^σ are normalized to start with. Thus, we put

$$\eta_n^\sigma = \left(N \theta_n^\sigma\right)^{-\frac{1}{2}}, \tag{III-4}$$

where

$$\theta_n^\sigma = \sum_{0}^{N-1}{}_{\nu} \, e^{i \underline{k} \cdot \underline{R}_\nu} \langle v_n^\sigma(\underline{r}) \,|\, v_n^\sigma(\underline{r} - \underline{R}_\nu) \rangle \tag{III-5}$$

and N is the number of lattice sites in the crystal. The quantity θ_n^σ is real, since, as it can be easily seen, it is equal to its complex conjugate. We assume that the v_n^σ's are normalized.

The Hamiltonian and overlap matrix elements (cf. Eq. I-23) are

$$H_{np} = \langle F_n | H | F_p \rangle, \qquad O_{np} = \langle F_n | F_p \rangle ; \tag{III-6}$$

where we dropped the superscript σ, which is obviously the same for all the elements of a secular determinant (cf. Eq. I-33). We consider the overlap matrix elements first. From Eq. (III-6) and Eq. (III-2) we obtain

$$O_{np} = \eta_n \eta_p \sum_{\nu} \sum_{\nu'} e^{i \underset{\sim}{k} \cdot (\underset{\sim}{R}_{\nu'} - \underset{\sim}{R}_{\nu})} \langle v_n (\underset{\sim}{r} - \underset{\sim}{R}_{\nu} - \delta_n \underset{\sim}{d}) | v_p (\underset{\sim}{r} - \underset{\sim}{R}_{\nu'} - \delta_p \underset{\sim}{d}) \rangle$$

$$= (\theta_n \theta_p)^{-\frac{1}{2}} \sum_{\nu} e^{i \underset{\sim}{k} \cdot \underset{\sim}{R}_{\nu}} \langle v_n (\underset{\sim}{r}) | v_p (\underset{\sim}{r} - \underset{\sim}{R}_{\nu} - \gamma_{np} \underset{\sim}{d}) \rangle, \tag{III-7}$$

where $\gamma_{np} = \delta_p - \delta_n$. The possible values of γ_{np} are 0, 1, and -1, depending on the types of atoms on which the functions v_n and v_p are centered, remembering that $\underset{\sim}{d}$ is the displacement vector from atom A to atom B in the same unit cell (cf. Sec. I-5). We have

$$\begin{aligned} \gamma_{np} &= 0 \quad \text{for} \quad \langle A|A \rangle \text{ or } \langle B|B \rangle, \\ \gamma_{np} &= 1 \quad \text{"} \quad \langle A|B \rangle, \\ \gamma_{np} &= -1 \quad \text{"} \quad \langle B|A \rangle, \end{aligned} \tag{III-8}$$

$$\gamma_{pn} = -\gamma_{np} .$$

If we define a quantity h_{np} as follows:

$$h_{np} = \sum_{\nu}{}' \, e^{i \underline{k} \cdot \underline{R}_\nu} \langle v_n(\underline{r}) \mid v_p(\underline{r} - \underline{R}_\nu) \rangle, \quad \text{if } \gamma_{np} = 0,$$

$$h_{np} = \sum_{\nu} e^{i \underline{k} \cdot \underline{R}_\nu} \langle v_n(\underline{r}) \mid v_p(\underline{r} - \underline{R}_\nu - \gamma_{np} \underline{d}) \rangle, \quad \text{if } \gamma_{np} \neq 0, \tag{III-9}$$

we can write the overlap matrix element as

$$O_{np} = \frac{\delta_{np} + h_{np}}{\left[(1 + h_{nn})(1 + h_{pp})\right]^{\frac{1}{2}}} . \tag{III-10}$$

In Eq. (III-10) we have used the fact that

$$\langle v_n(\underline{r}) \mid v_p(\underline{r}) \rangle = \delta_{np} , \tag{III-11}$$

since v_n and v_p are normalized and belong to different representations, or to different rows of the same representation, of the full rotation group. For n = p, Eq. (III-10) gives $O_{nn} = 1$, as we expect, since the Bloch functions are normalized.

We now examine the Hamiltonian matrix elements H_{np}. We have (cf. Eq. III-7)

$$H_{np} = (\theta_n \theta_p)^{-\frac{1}{2}} \sum_{\nu} e^{i \underline{k} \cdot \underline{R}_\nu} \langle v_n(\underline{r}) \mid H \mid v_p(\underline{r} - \underline{R}_\nu - \gamma_{np} \underline{d}) \rangle . \tag{III-12}$$

By using Eqs. (I-12) and (I-44), we can write

$$H_{np} = (\theta_n \theta_p)^{-\frac{1}{2}} \sum_{\nu} e^{i \underline{k} \cdot \underline{R}_\nu} \langle v_n(\underline{r}) \mid -\nabla^2 + V_a(r) + M_a(\underline{r}) + \left[\Sigma' U\right]_o \mid v_p(\underline{r} - \underline{R}_\nu - \gamma_{np} \underline{d}) \rangle , \tag{III-13}$$

where $M_a(\underline{r})$ and $[\Sigma' U]_o$ are defined in Eqs. (I-45) and (I-46), respectively. The ionic-like potential $V_a(r)$ was discussed

in Sec. I-5. We now assume that $v_n(\underset{\sim}{r})$ satisfies the equation

$$\langle v_n(\underset{\sim}{r}) | \{-\nabla^2 + V_a(r) + M_a(r)\} = \varepsilon_n^a \langle v_n(\underset{\sim}{r}) | . \qquad \text{(III-14)}$$

In other words, we assume that $\langle v_n(\underset{\sim}{r}) |$ is an eigenvector of the central field Hamiltonian

$$H_a(\underset{\sim}{r}) = -\nabla^2 + V_a(r) + M_a(r), \qquad \text{(III-15)}$$

corresponding to the eigenvalue ε_n^a. It is obviously possible, in principle, to find a function $v_n(\underset{\sim}{r})$ satisfying Eq. (III-14), since v_n is a linear combination of orbitals which have the same quantum numbers $n\ell$ (cf. Eq. III-3), and therefore degenerate in a central field problem. By making use of Eq. (III-14) and neglecting the non-spherical terms of $M_a(\underset{\sim}{r})$ (cf. Eq. I-48), Eq. (III-13) becomes

$$H_{np} = (\theta_n \theta_p)^{-\frac{1}{2}} \sum_{\nu} e^{i\underset{\sim}{k}\cdot\underset{\sim}{R}_\nu} \left\{ \varepsilon_n^a \langle v_n(\underset{\sim}{r}) | v_p(\underset{\sim}{r}-\underset{\sim}{R}_\nu-\gamma_{np}\underset{\sim}{d}) \rangle + \langle v_n(\underset{\sim}{r}) | [\Sigma' U]_o | v_p(\underset{\sim}{r}-\underset{\sim}{R}_\nu-\gamma_{np}\underset{\sim}{d}) \rangle \right\}. \qquad \text{(III-16)}$$

If in Eq. (III-13) we operate on the function v_p at the right with the operator $H_a(\underset{\sim}{r}-\underset{\sim}{R}_\nu-\gamma_{np}\underset{\sim}{d})$ (cf. Eq. III-15), we obtain a result similar to that of Eq. (III-16), with ε_n^a replaced by ε_p^a and $[\Sigma' U]_o$ replaced by $[\Sigma' U]_{\underset{\sim}{R}_\nu+\gamma_{np}\underset{\sim}{d}}$, where $[\Sigma' U]_{\underset{\sim}{R}_\nu+\gamma_{np}\underset{\sim}{d}}$ denotes the sum of all short-range potentials, excluding the one around $\underset{\sim}{R}_\nu+\gamma_{np}\underset{\sim}{d}$. Thus, by operating on the left, we obtain Eq. (III-16); by operating on the right, we obtain

$$H_{mp} = (\theta_m \theta_p)^{-\frac{1}{2}} \sum_\nu e^{i \underset{\sim}{k} \cdot \underset{\sim}{R}_\nu} \left\{ \varepsilon_p^a \langle v_m(\underset{\sim}{r}) | v_p(\underset{\sim}{r} - \underset{\sim}{R}_\nu - \gamma_{mp} \underset{\sim}{d}) \rangle \right.$$

$$\left. + \langle v_m(\underset{\sim}{r}) | [\Sigma' U]_{\underset{\sim}{R}_\nu + \gamma_{mp} \underset{\sim}{d}} | v_p(\underset{\sim}{r} - \underset{\sim}{R}_\nu - \gamma_{mp} \underset{\sim}{d}) \rangle \right\} . \qquad \text{(III-17)}$$

In an exact calculation, the two expressions of H_{np} (Eqs. III-16 and 17) should yield the same numerical result, but the approximations used in the actual calculation may make the two results slightly different. We then take the average of the two expressions and write

$$H_{mp} = (\theta_m \theta_p)^{-\frac{1}{2}} \left\{ \frac{\varepsilon_m^a + \varepsilon_p^a}{2} \sum_\nu e^{i \underset{\sim}{k} \cdot \underset{\sim}{R}_\nu} \langle v_m(\underset{\sim}{r}) | v_p(\underset{\sim}{r} - \underset{\sim}{R}_\nu - \gamma_{mp} \underset{\sim}{d}) \rangle \right.$$

$$\left. + \frac{1}{2} \sum_\nu e^{i \underset{\sim}{k} \cdot \underset{\sim}{R}_\nu} \langle v_m(\underset{\sim}{r}) | [\Sigma' U]_o + [\Sigma' U]_{\underset{\sim}{R}_\nu + \gamma_{mp} \underset{\sim}{d}} | v_p(\underset{\sim}{r} - \underset{\sim}{R}_\nu - \gamma_{mp} \underset{\sim}{d}) \rangle \right\} . \qquad \text{(III-18)}$$

To simplify the notation, we introduce two new quantities, f_{np} and g_{np}, according to the following definitions:

$$f_{mp} = \langle v_m(\underset{\sim}{r}) | [\Sigma' U]_o | v_p(\underset{\sim}{r}) \rangle \delta_{o \gamma_{mp}} , \qquad \text{(III-19)}$$

and

$$g_{mp} = \frac{1}{2} \sum_\nu{}' e^{i \underset{\sim}{k} \cdot \underset{\sim}{R}_\nu} \langle v_m(\underset{\sim}{r}) | [\Sigma' U]_o + [\Sigma' U]_{\underset{\sim}{R}_\nu} | v_p(\underset{\sim}{r} - \underset{\sim}{R}_\nu) \rangle , \text{ if } \gamma_{mp} = 0 ,$$

$$g_{mp} = \frac{1}{2} \sum_\nu e^{i \underset{\sim}{k} \cdot \underset{\sim}{R}_\nu} \langle v_m(\underset{\sim}{r}) | [\Sigma' U]_o + [\Sigma' U]_{\underset{\sim}{R}_\nu + \gamma_{mp} \underset{\sim}{d}} | v_p(\underset{\sim}{r} - \underset{\sim}{R}_\nu + \gamma_{mp} \underset{\sim}{d}) \rangle , \text{ if } \gamma_{mp} \neq 0 . \qquad \text{(III-20)}$$

In Eq. (III-19), $\delta_{o\gamma_{np}}$ is the Kronecker δ symbol: $\delta_{o\gamma_{np}} = 1$, if $\gamma_{np} = 0$; $\delta_{o\gamma_{np}} = 0$, if $\gamma_{np} \neq 0$. The Hamiltonian matrix element can now be written

$$H_{mp} = \frac{\varepsilon_m^a + \varepsilon_p^a}{2} O_{mp} + \frac{f_{mp} + g_{mp}}{\left[(1 + h_{mm})(1 + h_{pp}) \right]^{\frac{1}{2}}} . \qquad \text{(III-21)}$$

We have expressed the matrix elements O_{np} and H_{np} in terms of three types of quantities: f_{np}, h_{np}, and g_{np}. The quantity f_{np} (Eq. III-19) does not depend explicitly on σ, the symmetry of the Bloch function. Since the only operations that leave $[\Sigma'U]_o$ invariant are those of the point group of the crystal, the functions v_n and v_p must be expressed in terms of basis functions for the irreducible representations of this group. Then, f_{np} can be different from zero only when v_n and v_p contain parts transforming according to the same row of the same representation of the point group of the crystal. From Eq. (III-19) we see that f_{np} is a sum of two-center integrals; but, as we will see in the next section, in some cases it can be reduced to a single one-center integral. The quantities h_{np} (Eq. III-9) and g_{np} (Eq. III-20) depend on σ and are far more difficult to calculate than f_{np}, since they contain both two- and three-center integrals and a sum over all lattice vectors $\underset{\sim}{R}_\nu$. All three quantities, f_{np}, h_{np}, and g_{np}, satisfy the relation

$$\zeta_{pn} = \zeta^*_{np} , \qquad \text{(III-22)}$$

where ζ is either f or h or g; that is, they are elements of a hermitian matrix. Thus, from Eqs. (III-10) and (III-21) we see that

$$O_{pn} = O^*_{np} \qquad \text{and} \qquad H_{pn} = H^*_{np} , \qquad \text{(III-23)}$$

as we expect, since the unity and Hamiltonian operators are hermitian operators.

In the next section we apply the previous results to CuCℓ and see how, through some approximations, the quantities f_{np}, h_{np}, and g_{np}, can be expressed in terms of a few types of integrals that are relatively easy to compute.

III-2. Application to copper chloride.

The considerations in the preceding section can be applied to any ionic crystal with two ions per basis, since they do not depend on a particular type of symmetry. We would now like to look closer at the point symmetry of the crystal potential $V(\underset{\sim}{r})$. To do this, we restrict ourselves to the zinc blende structure, which has the point group T_d (cf. Sec. II-1). The crystal potential $V(\underset{\sim}{r})$ must transform according to the representation Γ_1 of T_d (cf. Table 3). If we expand $V(\underset{\sim}{r})$ in a series of spherical harmonics (cf. Eq. I-47), we obtain

$$V(\underset{\sim}{r}) = a_0(r)\,Y_0^0 + a_3(r)\left(Y_3^2 - Y_3^{-2}\right) + a_4(r)\left[Y_4^0 + \sqrt{\tfrac{5}{14}}\left(Y_4^4 + Y_4^{-4}\right)\right] + (\text{terms with } \ell \geq 6), \tag{III-24}$$

since only the combinations of spherical harmonics transforming according to Γ_1 can be present in the expansion. Expansion (III-24) is also valid for $M_a(\underset{\sim}{r})$ and $[\Sigma' U]_o$, since both these terms have the same point symmetry as the total crystal potential $V(\underset{\sim}{r})$. In matrix elements of the type $\langle v_n(\underset{\sim}{r}) | V(\underset{\sim}{r}) | v_p(r) \rangle$, where v_n and v_p are s-, p-, or d-like

functions (ℓ=0,1,2), those terms with ℓ>4 in Eq. (III-24) give zero contribution [cf. Kno 64, Chap. 11]. If only s and p functions are involved, then only the spherically symmetric term $a_o(r)Y_o^o$ can give a nonzero contribution.

It has been found that, for the 3d function of copper, the contribution of the ℓ=4 term in the expansion of $M_a(\underset{\sim}{r})$ is about 0.01 eV in a crystal of symmetry O_h and nearest-neighbor distance 4.4 Bohr radii (NaF) [K.L. Yip, private communication]. This contribution is about three orders of magnitude smaller than that of the spherical part of $M_a(\underset{\sim}{r})$. This justifies the approximation of Eq. (I-48), in which we retain only the spherically symmetric (ℓ=0) term in the expansion of $M_a(\underset{\sim}{r})$ in spherical harmonics. (The Madelung potential for CuCl in the spherical approximation is calculated in Appendix B.) However, the contribution to the nonspherical terms due to the first and second nearest neighbors will be included in the parameters f_{nn} (Eq. III-19) by explicit calculation of the two-center integrals, and a comparison with the spherical approximation will be made.

In applying the tight-binding method to CuCl we restrict the sum in Eq. (III-1) to Bloch functions coming from the orbitals 3s and 3p of Cl^- and 3d of Cu^+. In Table 18 we give the atomic parameters ε_n^a (cf. Eq. III-14) for all the occupied states of Cu^+ and Cl^-. These parameters were obtained by solving the radial part of Eq. (III-14), which is

TABLE 18

ATOMIC PARAMETERS ϵ_n^a FOR Cu^+ AND Cl^-. VALENCE SCREENING POTENTIAL. RYDBERG UNITS. (KUT = 0).

Cu^+		Cl^-	
1s	-648.87	1s	-206.98
2s	-78.698	2s	-20.142
2p	-69.487	2p	-15.961
3s	-8.8244	3s	-1.5387
3p	-5.8767	3p	-0.66486
3d	-0.88927		

$$\left\{-\frac{d^2}{dr^2} + \frac{\ell(\ell+1)}{r^2} + V_a(r) + M_a(r)\right\} P_{n\ell}(r) = \varepsilon^a_{n\ell} P_{n\ell}(r), \qquad \text{(III-25)}$$

where $V_a(r)$ is the atomic potential defined in Eq. (I-58) and $M_a(r)$ is the Madelung potential obtained in Appendix B. Eq. (III-25) was solved for all occupied states in the ion by the self-consistent field method [Har 57; see also Her 63], which yields, besides $\varepsilon^a_{n\ell}$, the radial functions $P_{n\ell}(r)$, to be used in Eq. (III-3), and the potential $V_a(r)$. A FORTRAN program, ATOM, was used. This program, together with all other programs used in connection with the present work, is described in Appendix G.

The FORTRAN variable KUT [Her 63, p. 7-6] was set equal to zero, which means that the potential $V_a(r)$ used in Eq. (III-25) is that given by Eq. (I-59), where $V_o(r)$ is now the screened-valence potential given in Eq. (I-58). Thus, the one-ion potential used in determining the parameters ε^a_n and the radial functions $P_{n\ell}(r)$ is slightly different from the other one-ion potentials used in constructing our model crystal potential $V(\underset{\sim}{r})$ (Eq. I-40) [cf. Bas 65].

> "This is justified for valence electrons, because if one were to use the exact Hartree-Fock expression for exchange, with the crystal density matrix constructed in terms of atomic functions with small overlap, one would see that the contribution to the Coulomb potential which comes from the wave function [of the electron in consideration] would be canceled by an equal term in the exchange. This amounts to saying that an electron

> sees only the potential due to other electrons, but not due to itself. On the other hand, contributions to the potential due to other ions are well represented by the model potential, since this resembles the potential that an extra electron sees due to the ions."

We have quoted from the paper by Bassani, Knox, and Fowler [op. cit.]. Even though they use the Hartree-Fock atomic eigenvalues for the parameters ε_n^a, their argument is valid in our case too. We may add that, in a way, our calculation is more consistent, since we use essentially the same type of potential for all the ions, while they use a Hartree-Fock potential for the ion on which the atomic orbital in consideration is centered and a screened Hartree-Fock-Slater potential, similar to that of Eq. (I-58) with $\rho_{ac}=0$, $\rho_{av}=\rho_a$, and $\kappa\to\infty$, for the other ions.

From Table 18 we see that the energies of the states that we use in the expansion of our valence band wave functions are all within one rydberg range, separated by more than four rydbergs from the next lower state (3p of Cu^+). Thus, all the orbitals that we have neglected should be fairly compact and should not overlap in an appreciable way the neighbor orbitals. Therefore, their contribution to the valence bands should be negligible. Our calculation in the next chapter confirms this assumption.

Going back to the quantities f_{np}, h_{np}, and g_{np}, defined in the preceding section (Eqs. III-9, 19, 20), we

first notice that, because of our choice of atomic states made in this section, we can write

$$f_{np} = f_{nn}\,\delta_{np} \,. \qquad \text{(III-26)}$$

This is true because, in our case, the only states that could mix are the p and d states which transform according to Γ_{15} (cf. Table 8), but they are centered on different kinds of ions ($\gamma_{np}\neq 0$), therefore $f_{np}=0$ (cf. Eq. III-19). Thus, inspection of the basis functions for the small representations of Γ (Table 8) shows that we can have only four different quantities of the type f_{np}: $f_{ss}(\Gamma_1)$, $f_{pp}(\Gamma_{15})$, $f_{dd}(\Gamma_{15})$, and $f_{d'd'}(\Gamma_{12})$. Furthermore, by the considerations at the beginning of this section, in calculating f_{ss} and f_{pp} it is sufficient to retain the spherically symmetric part of $[\Sigma' U]_o$.

In calculating the quantitites f_{nn}, h_{np}, and g_{np}, we introduce the following approximations: (a) two-center integrals: we retain only those involving first and second nearest neighbors [cf. Fow 63a, Bas 65]; (b) three-center integrals: will not be explicitly calculated; however, some three-center contribution will be included in the two-center terms involving second nearest neighbors, by taking a spherical average of the short-range potentials due to nearest neighbors.

With these approximations, the quantities f_{nn}, h_{np}, and g_{np} can be written

$$f_{nn} \approx \langle v_n(\underset{\sim}{r}) | [\Sigma' U_1]_o + [\Sigma' U_2]_o | v_n(\underset{\sim}{r})\rangle \; ; \tag{III-27}$$

$$h_{np} \approx \sum_{|\underset{\sim}{R}_\nu| = |\underset{\sim}{a}_i|}{}' e^{i \underset{\sim}{k}\cdot \underset{\sim}{R}_\nu} \langle v_n(\underset{\sim}{r}) | v_p(\underset{\sim}{r} - \underset{\sim}{R}_\nu)\rangle, \qquad \text{if } \gamma_{np} = 0,$$

(III-28)

$$h_{np} \approx \sum_{|\underset{\sim}{R}_\nu + \gamma_{np}\underset{\sim}{d}| = |\underset{\sim}{d}|} e^{i \underset{\sim}{k}\cdot \underset{\sim}{R}_\nu} \langle v_n(\underset{\sim}{r}) | v_p(\underset{\sim}{r} - \underset{\sim}{R}_\nu - \gamma_{np}\underset{\sim}{d})\rangle, \quad \text{if } \gamma_{np} \neq 0;$$

$$g_{np} \approx \frac{1}{2} \sum_{|\underset{\sim}{R}_\nu| = |\underset{\sim}{a}_i|}{}' e^{i \underset{\sim}{k}\cdot \underset{\sim}{R}_\nu} \Big\{ \langle v_n(\underset{\sim}{r}) | U(\underset{\sim}{r} - \underset{\sim}{R}_\nu) + \overline{[\Sigma' U_1]}_{\underset{\sim}{R}_\nu} | v_p(\underset{\sim}{r} - \underset{\sim}{R}_\nu)\rangle$$
$$+ \langle v_n(\underset{\sim}{r}) | U(\underset{\sim}{r}) + \overline{[\Sigma' U_1]}_o | v_p(\underset{\sim}{r} - \underset{\sim}{R}_\nu)\rangle \Big\}, \qquad \text{if } \gamma_{np} = 0,$$

(III-29)

$$g_{np} \approx \frac{1}{2} \sum_{|\underset{\sim}{R}_\nu + \gamma_{np}\underset{\sim}{d}| = |\underset{\sim}{d}|} e^{i \underset{\sim}{k}\cdot \underset{\sim}{R}_\nu} \Big\{ \langle v_n(\underset{\sim}{r}) | U(\underset{\sim}{r} - \underset{\sim}{R}_\nu - \gamma_{np}\underset{\sim}{d}) | v_p(\underset{\sim}{r} - \underset{\sim}{R}_\nu - \gamma_{np}\underset{\sim}{d})\rangle$$
$$+ \langle v_n(\underset{\sim}{r}) | U(\underset{\sim}{r}) | v_p(\underset{\sim}{r} - \underset{\sim}{R}_\nu - \gamma_{np}\underset{\sim}{d})\rangle \Big\}, \qquad \text{if } \gamma_{np} \neq 0 .$$

In the above equations the subscript 1 in $\overline{[\Sigma' U_1]}_{\underset{\sim}{R}_\nu}$ means that the sum is restricted to the nearest neighbors of the ion centered at $\underset{\sim}{R}_\nu$; the bar means spherical average; $\underset{\sim}{a}_i$ is any one of the three basic lattice translation vectors defined in Eq. (II-1) ($|\underset{\sim}{a}_i| = \frac{a}{2}\sqrt{2}$).

We have to compute essentially three types of two-center integrals:

$$\int |v_n(\underset{\sim}{r})|^2 \, U(|\underset{\sim}{r} - \underset{\sim}{a}|) \, d\tau ,$$
$$\int v_n^*(\underset{\sim}{r}) \, v_p(\underset{\sim}{r} - \underset{\sim}{a}) \, d\tau , \tag{III-30}$$
$$\int v_n^*(\underset{\sim}{r}) \, \overline{U}(r) \, v_p(\underset{\sim}{r} - \underset{\sim}{a}) \, d\tau ,$$

where, for nearest neighbors, $|\underset{\sim}{a}| = |\underset{\sim}{d}| = \frac{a}{4}\sqrt{3}$, $\bar{U}(r) = U(r)$; for second nearest neighbors, $|\underset{\sim}{a}| = |\underset{\sim}{a}_i| = \frac{a}{2}\sqrt{2}$, $\bar{U}(r) = U(r) + \overline{[\Sigma' U_1]}_o$. An integral of the type $\int v_n^*(\underset{\sim}{r})\bar{U}(|\underset{\sim}{r}-\underset{\sim}{a}|)v_p(\underset{\sim}{r}-\underset{\sim}{a})d\tau$ can be reduced to the third type of Eq. (III-30) by a

translation of coordinates. It is convenient to expand the functions v_n and v_p in terms of spherical harmonics space-quantized with respect to the axis containing the two centers. Any of the above integrals can then be expressed in terms of two-center integrals involving functions of the type σ, π, or δ, where σ, π, δ refer to the component of the angular momentum along the direction of the axis (m=0,1,2 for σ, π, and δ, respectively). Slater and Koster [Sla 54] have tabulated the coefficients of this expansion in terms of ℓ,m, n, the direction cosines of the vector $\underset{\sim}{a}$. As an example, let $E_{x,xy}(\ell,m,n)$ represent an overlap integral (Eq. III-30, 2nd type) between a u_x and a u_{xy} function; then, Table I of Slater and Koster gives

$$E_{x,xy}(\ell,m,n) = \sqrt{3}\,\ell^2 m\,(pd\sigma) + m(1-2\ell^2)(pd\pi), \qquad \text{(III-31)}$$

where, in this case, (pdσ) and (pdπ) represent the following integrals:

$$(pd\sigma) = \int u^*_{p\sigma}(\underset{\sim}{r})\, u_{d\sigma}(\underset{\sim}{r}-\underset{\sim}{a})\, d\tau,$$
$$(pd\pi) = \int u^*_{p\pi}(\underset{\sim}{r})\, u_{d\pi}(\underset{\sim}{r}-\underset{\sim}{a})\, d\tau. \qquad \text{(III-32)}$$

For convenience, we introduce the following notation:

$$U_{\alpha\mu} = \int |u_{\alpha\mu}(\underset{\sim}{r})|^2\, U(|\underset{\sim}{r}-\underset{\sim}{a}|)\, d\tau,$$
$$S_{\alpha\beta\mu} = \int u^*_{\alpha\mu}(\underset{\sim}{r})\, u_{\beta\mu}(\underset{\sim}{r}-\underset{\sim}{a})\, d\tau, \qquad \text{(III-33)}$$
$$U_{\alpha\beta\mu} = \int u^*_{\alpha\mu}(\underset{\sim}{r})\, \bar{U}(r)\, u_{\beta\mu}(\underset{\sim}{r}-\underset{\sim}{a})\, d\tau,$$

where μ stands for σ, π, or δ. A subscript 1 or 2 will be added when necessary, to indicate whether the integral is between first or second nearest neighbors.

Quantities of the type written in Eq. (III-31) are listed in Tables 19 and 20 for all of the first- and second-nearest-neighbor positions in the zinc blende structure. The four quantities of the type f_{nn} are given here:

$$
\begin{aligned}
f_{ss} &= 4\,U_{ss\sigma_1} + 12\,U_{ss\sigma_2} = \int [P_{3s}(r)]^2 \left(\overline{[\Sigma' U_1]}_0 + \overline{[\Sigma' U_2]}_0 \right) dr, \\
f_{pp} &= 4\left[\frac{U_{pp\sigma} + 2\,U_{pp\pi}}{3}\right]_1 + 12\left[\frac{U_{pp\sigma} + 2\,U_{pp\pi}}{3}\right]_2 = \int [P_{3p}(r)]^2 \left(\overline{[\Sigma' U_1]}_0 + \overline{[\Sigma' U_2]}_0 \right) dr, \\
f_{dd} &= \frac{4}{9}\left[3\,U_{dd\sigma} + 2\,U_{dd\pi} + 4\,U_{dd\delta}\right]_1 + \left[3\,U_{dd\sigma} + 4\,U_{dd\pi} + 5\,U_{dd\delta}\right]_2, \\
f_{d'd'} &= \frac{4}{3}\left[2\,U_{dd\pi} + U_{dd\delta}\right]_1 + \frac{3}{2}\left[U_{dd\sigma} + 4\,U_{dd\pi} + 3\,U_{dd\delta}\right]_2 .
\end{aligned}
\qquad \text{(III-34)}
$$

The quantities h_{np} and g_{np} are too extensive to be listed here. The quantities of the type h_{np} are given in Appendix C. The quantities g_{np} can be obtained from the corresponding h_{np} by making the following substitution:

$$
S_{\alpha\beta\mu} \longrightarrow \frac{1}{2}\left[U_{\alpha\beta\mu} + (-1)^{\ell_\alpha + \ell_\beta} U_{\beta\alpha\mu}\right], \qquad \text{(III-35)}
$$

where ℓ_α and ℓ_β are the orbital quantum numbers of v_n and v_p, respectively.

This is all the theory we need; what is left is numerical computation. We have to calculate the quantities $U_{\alpha\mu}$, $S_{\alpha\beta\mu}$, and $U_{\alpha\beta\mu}$, defined in Eq. (III-33). The radial part of the function $u_{\alpha\mu}(\underset{\sim}{r})$ is $r^{-1}P_{n\ell}(r)$ (cf. Eq. III-3), and $P_{n\ell}(r)$ is obtained from the solution of Eq. (III-25). The short-range potential can be obtained from Eq. (I-42),

TABLE 19

QUANTITIES $E_{a,b}$ FOR NEAREST-NEIGHBOR POINTS IN THE ZINC BLENDE STRUCTURE. ORIGIN Cu^+.

$\underset{\sim}{R}_\nu + \underset{\sim}{d}$	$\frac{a}{4}(111)$	$\frac{a}{4}(1\bar{1}\bar{1})$	$\frac{a}{4}(\bar{1}1\bar{1})$	$\frac{a}{4}(\bar{1}\bar{1}1)$
Direction cosines	$\frac{1}{\sqrt{3}}, \frac{1}{\sqrt{3}}, \frac{1}{\sqrt{3}}$	$+\ -\ -$	$-\ +\ -$	$-\ -\ +$
$E_{xy,s}$	$\frac{1}{\sqrt{3}}(dso)$	$-$	$-$	$+$
$E_{xy,x}$	$\frac{1}{3}\left[(dp\sigma)+\frac{1}{\sqrt{3}}(dp\pi)\right]$	$-$	$+$	$-$
$E_{xy,y}$	$\frac{1}{3}\left[(dp\sigma)+\frac{1}{\sqrt{3}}(dp\pi)\right]$	$+$	$-$	$-$
$E_{xy,z}$	$\frac{1}{3}\left[(dp\sigma)-\frac{2}{\sqrt{3}}(dp\pi)\right]$	$+$	$+$	$+$
$E_{yz,s}$	$\frac{1}{\sqrt{3}}(dso)$	$+$	$-$	$-$
$E_{yz,x}$	$\frac{1}{3}\left[(dp\sigma)-\frac{2}{\sqrt{3}}(dp\pi)\right]$	$+$	$+$	$+$
$E_{yz,y}$	$\frac{1}{3}\left[(dp\sigma)+\frac{1}{\sqrt{3}}(dp\pi)\right]$	$-$	$-$	$+$
$E_{yz,z}$	$\frac{1}{3}\left[(dp\sigma)+\frac{1}{\sqrt{3}}(dp\pi)\right]$	$-$	$+$	$-$
$E_{zx,s}$	$\frac{1}{\sqrt{3}}(dso)$	$-$	$+$	$-$
$E_{zx,x}$	$\frac{1}{3}\left[(dp\sigma)+\frac{1}{\sqrt{3}}(dp\pi)\right]$	$-$	$-$	$+$
$E_{zx,y}$	$\frac{1}{3}\left[(dp\sigma)-\frac{2}{\sqrt{3}}(dp\pi)\right]$	$+$	$+$	$+$
$E_{zx,z}$	$\frac{1}{3}\left[(dp\sigma)+\frac{1}{\sqrt{3}}(dp\pi)\right]$	$+$	$-$	$-$
$E_{x^2-y^2,s}$	0	0	0	0
$E_{x^2-y^2,x}$	$\frac{1}{\sqrt{3}}(dp\pi)$	$+$	$-$	$-$
$E_{x^2-y^2,y}$	$-\frac{1}{\sqrt{3}}(dp\pi)$	$-$	$+$	$-$
$E_{x^2-y^2,z}$	0	0	0	0
$E_{3z^2-r^2,s}$	0	0	0	0
$E_{3z^2-r^2,x}$	$-\frac{1}{3}(dp\pi)$	$+$	$-$	$-$
$E_{3z^2-r^2,y}$	$-\frac{1}{3}(dp\pi)$	$-$	$+$	$-$
$E_{3z^2-r^2,z}$	$\frac{2}{3}(dp\pi)$	$-$	$-$	$+$

TABLE 20

QUANTITIES $E_{a,b}$ FOR NEXT-NEAREST-NEIGHBOR POINTS IN THE ZINC BLENDE STRUCTURE.

R_ν	$\frac{a}{2}(110)$	$\frac{a}{2}(1\bar{1}0)$	$\frac{a}{2}(\bar{1}10)$	$\frac{a}{2}(\bar{1}\bar{1}0)$	$\frac{a}{2}(101)$	$\frac{a}{2}(10\bar{1})$	$\frac{a}{2}(\bar{1}01)$	$\frac{a}{2}(\bar{1}0\bar{1})$	$\frac{a}{2}(011)$	$\frac{a}{2}(01\bar{1})$	$\frac{a}{2}(0\bar{1}1)$	$\frac{a}{2}(0\bar{1}\bar{1})$
Dir. cos.	$\frac{1}{\sqrt{2}}, \frac{1}{\sqrt{2}}, 0$	$\frac{1}{\sqrt{2}}, -\frac{1}{\sqrt{2}}, 0$	$-\frac{1}{\sqrt{2}}, \frac{1}{\sqrt{2}}, 0$	$-\frac{1}{\sqrt{2}}, -\frac{1}{\sqrt{2}}, 0$	$\frac{1}{\sqrt{2}}, 0, \frac{1}{\sqrt{2}}$	$\frac{1}{\sqrt{2}}, 0, -\frac{1}{\sqrt{2}}$	$-\frac{1}{\sqrt{2}}, 0, \frac{1}{\sqrt{2}}$	$-\frac{1}{\sqrt{2}}, 0, -\frac{1}{\sqrt{2}}$	$0, \frac{1}{\sqrt{2}}, \frac{1}{\sqrt{2}}$	$0, \frac{1}{\sqrt{2}}, -\frac{1}{\sqrt{2}}$	$0, -\frac{1}{\sqrt{2}}, \frac{1}{\sqrt{2}}$	$0, -\frac{1}{\sqrt{2}}, -\frac{1}{\sqrt{2}}$
E_{ss}	$(ss\sigma)$	+	+	+	+	+	+	+	+	+	+	+
E_{sx}	$\frac{1}{\sqrt{2}}(sp\sigma)$	+	−	−	+	+	−	−	0	0	0	0
E_{sy}	$\frac{1}{\sqrt{2}}(sp\sigma)$	−	+	−	0	0	0	0	+	+	−	−
E_{sz}	0	0	0	0	$\frac{1}{\sqrt{2}}(sp\sigma)$	−	+	−	+	−	+	−
E_{xx}	$\frac{1}{2}[(pp\sigma)+(pp\pi)]$	+	+	+	+	+	+	+	$(pp\pi)$	+	+	+
E_{yy}	$\frac{1}{2}[(pp\sigma)+(pp\pi)]$	+	+	+	$(pp\pi)$	+	+	+	$\frac{1}{2}[(pp\sigma)+(pp\pi)]$	+	+	+
E_{zz}	$(pp\pi)$	+	+	+	$\frac{1}{2}[(pp\sigma)+(pp\pi)]$	+	+	+	+	+	+	+
E_{xy}	$\frac{1}{2}[(pp\sigma)-(pp\pi)]$	−	−	+	0	0	0	0	0	0	0	0
E_{xz}	0	0	0	0	$\frac{1}{2}[(pp\sigma)-(pp\pi)]$	−	−	+	0	0	0	0
E_{yz}	0	0	0	0	0	0	0	0	$\frac{1}{2}[(pp\sigma)-(pp\pi)]$	−	−	+

TABLE 20

(cont'd)

R_ν	$\frac{a}{2}(110)$	$(1\bar{1}0)$	$(\bar{1}10)$	$(\bar{1}\bar{1}0)$	$\frac{a}{2}(101)$	$(10\bar{1})$	$(\bar{1}01)$	$(\bar{1}0\bar{1})$	$\frac{a}{2}(011)$	$(01\bar{1})$	$(0\bar{1}1)$	$(0\bar{1}\bar{1})$
Dir. cos.	$\frac{1}{\sqrt{2}}, \frac{1}{\sqrt{2}}, 0$	$+\ -\ 0$	$-\ +\ 0$	$-\ -\ 0$	$\frac{1}{\sqrt{2}}, 0, \frac{1}{\sqrt{2}}$	$+\ 0\ -$	$-\ 0\ +$	$-\ 0\ -$	$0, \frac{1}{\sqrt{2}}, \frac{1}{\sqrt{2}}$	$0\ +\ -$	$0\ -\ +$	$0\ -\ -$
$E_{xy,xy}$	$\frac{3}{4}\sigma+\frac{1}{4}\delta$	+	+	+	$\frac{1}{2}(\pi+\delta)$	+	+	+	+	+	+	+
$E_{xy,yz}$	0	0	0	0	$\frac{1}{2}(\pi-\delta)$	−	−	+	0	0	0	0
$E_{xy,zx}$	0	0	0	0	0	0	0	0	$\frac{1}{2}(\pi-\delta)$	−	−	+
E_{xy,x^2-y^2}	0	0	0	0	0	0	0	0	0	0	0	0
E_{yz,x^2-y^2}	0	0	0	0	0	0	0	0	$-\frac{3}{8}(\sigma-\delta)$	−	−	+
E_{zx,x^2-y^2}	0	0	0	0	$\frac{3}{8}(\sigma-\delta)$	−	−	+	0	0	0	0
$E_{xy,3z^2-r^2}$	$-\frac{\sqrt{3}}{4}(\sigma-\delta)$	−	−	+	0	0	0	0	0	0	0	0
$E_{yz,3z^2-r^2}$	0	0	0	0	0	0	0	0	$\frac{\sqrt{3}}{8}(\sigma-\delta)$	−	−	+
$E_{zx,3z^2-r^2}$	0	0	0	0	$\frac{\sqrt{3}}{8}(\sigma-\delta)$	−	−	+	0	0	0	0
$E_{x^2-y^2,x^2-y^2}$	$(dd\pi)$	+	+	+	$\frac{1}{16}(3\sigma+4\pi+9\delta)$	+	+	+	+	+	+	+
$E_{x^2-y^2,3z^2-r^2}$	0	0	0	0	$\frac{\sqrt{3}}{16}(\sigma-4\pi+3\delta)$	+	+	+	−	−	−	−
$E_{3z^2-r^2,3z^2-r^2}$	$\frac{1}{4}(\sigma+3\delta)$	+	+	+	$\frac{1}{16}(\sigma+12\pi+3\delta)$	+	+	+	+	+	+	+
$E_{yz,yz}$	$\frac{1}{2}(\pi+\delta)$	+	+	+	$\frac{1}{2}(\pi+\delta)$	+	+	+	$\frac{1}{4}(3\sigma+\delta)$	+	+	+
$E_{yz,zx}$	$\frac{1}{2}(\pi-\delta)$	−	−	+	0	0	0	0	0	0	0	0
$E_{zx,zx}$	$\frac{1}{2}(\pi+\delta)$	+	+	+	$\frac{1}{4}(3\sigma+\delta)$	+	+	+	$\frac{1}{2}(\pi+\delta)$	+	+	+

$\sigma \equiv (dd\sigma)$

$\pi \equiv (dd\pi)$

$\delta \equiv (dd\delta)$

once $V_a(r)$ is known. The contribution to the average short-range potential due to the γth shell, containing n ions of type a, is

$$\overline{[\Sigma' U_\gamma]}_0 = (Y_0^0)^2 \int [\Sigma' U_\gamma]_0 \, d\Omega$$

$$= \frac{\pi}{2} \int_0^\pi U_a(|\underset{\sim}{r} - \underset{\sim}{R}_\gamma|) \sin\theta \, d\theta, \qquad \underset{\sim}{R}_\gamma \equiv (0, 0, R_\gamma), \tag{III-36}$$

where R_γ is the radius of the shell (cf. Table 1). The first two shells contain, respectively, 4 ions at a distance $\frac{a}{4}\sqrt{3}$ and 12 ions at a distance $\frac{a}{2}\sqrt{2}$. Thus, their contribution is

$$\overline{[\Sigma' U_1]}_0 = 2 \int_0^\pi U_1(|\underset{\sim}{r} - \underset{\sim}{a}|) \sin\theta \, d\theta, \qquad \underset{\sim}{a} \equiv (0, 0, \tfrac{a}{4}\sqrt{3}),$$

$$\overline{[\Sigma' U_2]}_0 = 6 \int_0^\pi U_2(|\underset{\sim}{r} - \underset{\sim}{b}|) \sin\theta \, d\theta, \qquad \underset{\sim}{b} \equiv (0, 0, \tfrac{a}{2}\sqrt{2}). \tag{III-37}$$

The two-center integrals defined in Eq. (III-33) were computed numerically, by using the program DOUB (see Appendix G). For the integrals given in Eq. (III-37) we have used program AVERPOT. All the single integrals were performed by Simpson's rule. Once we have the quantities $U_{\alpha\mu}$, $S_{\alpha\beta\mu}$, and $U_{\alpha\beta\mu}$, we can calculate f_{nn}, h^σ_{np}, and g^σ_{np}, insert them in O_{np} and H_{np}, and solve the secular equation for the energy $E^\alpha_i(\underset{\sim}{k})$. For a given representation along Δ or Λ, we have to solve a secular equation for every value of $\underset{\sim}{k}(\rho)$, where $0<\rho<1$ (cf. Sec. II-2). If we let $\rho = 0$, we have the point Γ; while $\rho = 1$ gives X and L, respectively. We have

solved the secular equation at 21 points in the zone: Γ, 10 points along Δ (including X), and 10 points along Λ (including L). We have done this by letting ρ vary between 0 and 1 with an increment $\Delta\rho = \frac{1}{10}$.

To solve the secular equation (I-27), we multiply both members of this equation by $|\underset{\approx}{O}^{-1}|$ and diagonalize the matrix $\underset{\approx}{O}^{-1}\underset{\approx}{H}$. The program VALENCE computes the quantities f_{nn}, h^{σ}_{np}, g^{σ}_{np} and the elements O_{np} and H_{np} of the secular determinant, and then solves the secular equation by calling the subroutine DIAG. All the programs used in connection with the present work are described in Appendix G.

The potential used in the tight-binding calculation was the one with valence screening (Eq. I-58). The valence density ρ_v was that of the 3s and 3p electrons for $C\ell^-$, and that of the 3d electrons for Cu^+. In Table 21 we give the parameters $U_{\alpha\mu}$, $S_{\alpha\beta\mu}$, and $U_{\alpha\beta\mu}$. The quantities f_{nn} can be obtained from Eq. (III-34), once the values of $U_{\alpha\mu}$ are known. Their values are (in rydbergs)

$$f_{ss} = -0.42048, \qquad f_{pp} = -0.56975,$$
$$f_{dd} = -0.52556, \qquad f_{d'd'} = -0.51470. \tag{III-38}$$

If in Eq. (III-19) we take the spherical average of $[\Sigma' U]_o$, from the first two shells of nearest neighbors, we obtain

$$\bar{f}_{ss} = -0.42047, \qquad \bar{f}_{pp} = -0.56975, \tag{III-39}$$
$$\bar{f}_{dd} = \bar{f}_{d'd'} = -0.52122.$$

TABLE 21

TWO-CENTER INTEGRALS: $U_{\alpha\mu}$, $S_{\alpha\beta\mu}$, $U_{\alpha\beta\mu}$.

U_{s1} = -0.04292	S_{ss} = 0.00626	U_{ss} = -0.00712
U_{s2} = -0.02073	$S_{pp\sigma}$ = -0.10370	$U_{pp\sigma}$ = 0.11195
$U_{p\sigma 1}$ = -0.15011	$S_{pp\pi}$ = 0.02608	$U_{pp\pi}$ = -0.02151
$U_{p\pi 1}$ = -0.03176	$S_{dd\sigma}$ = 0.00217	$U_{dd\sigma}$ = -0.00304
$U_{p\sigma 2}$ = -0.03284	$S_{dd\pi}$ = -0.00092	$U_{dd\pi}$ = 0.00124
$U_{p\pi 2}$ = -0.01919	$S_{dd\delta}$ = 0.00010	$U_{dd\delta}$ = -0.00012
$U_{d\sigma 1}$ = -0.14011	S_{sp} = 0.04096	U_{sp} = -0.07164
$U_{d\pi 1}$ = -0.12782	S_{sd} = 0.04262	U_{sd} = -0.08363
$U_{d\delta 1}$ = -0.11472	$S_{pd\sigma}$ = -0.04849	$U_{pd\sigma}$ = 0.08273
$U_{d\sigma 2}$ = -0.00206	$S_{pd\pi}$ = 0.03957	$U_{pd\pi}$ = -0.03114
$U_{d\pi 2}$ = -0.00179		U_{ps} = 0.02354
$U_{d\delta 2}$ = -0.00157		U_{ds} = -0.02649
		$U_{dp\sigma}$ = -0.05259
		$U_{dp\pi}$ = 0.03211

By comparing Eqs. (III-38) and (III-39), we see that the nonspherical terms of $[\Sigma'U]_o$ make no contribution to f_{ss} and f_{pp}, as discussed previously in this section. For the d terms, however, there is a splitting of about 0.01 Ry in the tetrahedral field. This is connected to the fact that the representation D_1 of the rotation group splits into the representations Γ_{15} and Γ_{12} of the group T_d [cf. Kos 63]. Neglecting the nonspherical terms of the short-range sum $[\Sigma'U]_o$ is equivalent to taking a weighted average of the two values $f_{dd}(\Gamma_{15})$ and $f_{d'd'}(\Gamma_{12})$, remembering that Γ_{15} is triply degenerate and Γ_{12} is doubly degenerate. Thus,

$$\bar{f}_{dd} = \bar{f}_{d'd'} = \frac{1}{5}\left(3 f_{dd} + 2 f_{d'd'}\right). \qquad \text{(III-40)}$$

If we would use $\bar{f}_{dd}$ for f_{dd} or $f_{d'd'}$, we would introduce an error of less than 1.3%, as it can be seen from Eqs. (III-38) and (III-39). We expect the error introduced by neglecting the nonspherical terms of $M_a(\underset{\sim}{r})$ to be of the same order.

The energy bands and a discussion of the results are in Chapter V. In the next section we consider the spin-orbit splitting at the top of the valence bands in the tight-binding approximation.

III-3. Spin-orbit splitting.

In the tight-binding approximation the two scalar components of a spinor are Bloch functions. The overlap matrix element between two spinors ψ_i and ψ_j of the form

(II-21) is (cf. Eq. F-3)

$$O_{ij} = \langle f_{1i}\alpha + f_{2i}\beta \mid f_{1j}\alpha + f_{2j}\beta \rangle \qquad \text{(III-41)}$$
$$= \langle f_{1i} \mid f_{1j} \rangle + \langle f_{2i} \mid f_{2j} \rangle .$$

Since the f's are Bloch functions, the calculation of O_{ij} proceeds as in Sec. III-1 (see Eq. III-10). The Hamiltonian matrix element is

$$H_{ij} = \langle f_{1i}\alpha + f_{2i}\beta \mid H_o + H_{so} \mid f_{1j}\alpha + f_{2j}\beta \rangle$$
$$= \langle f_{1i} \mid H_o \mid f_{1j} \rangle + \langle f_{2i} \mid H_o \mid f_{2j} \rangle + \langle f_{1i}\alpha \mid H_{so} \mid f_{1j}\alpha \rangle \qquad \text{(III-42)}$$
$$+ \langle f_{1i}\alpha \mid H_{so} \mid f_{2j}\beta \rangle + \langle f_{2i}\beta \mid H_{so} \mid f_{1j}\alpha \rangle + \langle f_{2i}\beta \mid H_{so} \mid f_{2j}\beta \rangle .$$

The matrix elements involving the classical Hamiltonian H_o are identical to those considered in Sec. III-1 (see Eq. III-21). The matrix elements of the spin-orbit interaction are derived in Appendix F. There, we assume that the atomic orbitals v_n centered on different ions do not overlap and replace $\underset{\sim}{\nabla} V(\underset{\sim}{r})$ with $\underset{\sim}{\nabla} V_a(r)$. The same approximation can be used if there is a little overlap between the v's, due to the fact that $\underset{\sim}{\nabla} V_a(r)$ is large near the nucleus and drops off much faster than $V_a(r)$ [cf. Fow 63]. However, in Eq. F-22 we must include a factor $(\theta_i \theta_j)^{-\frac{1}{2}}$ (see Eq. III-5), which accounts for the overlap of the v's.

We limit our analysis to the top of the valence bands, which occurs at Γ_{15} if spin-orbit interaction is not included (see Fig. 6). In the presence of spin-orbit

interaction, this state splits into Γ_7 and Γ_8 (see Table 17). The basis functions for these representations are given in Table 17. Only the orbitals 3p of Cl^- and 3d of Cu^+ are involved. Thus we have to calculate only two integrals of the type ξ_{ij} (see Eq. F-19): $\xi_{3p,3p}$ and $\xi_{3d,3d}$.

At Γ_7 or Γ_8, a basis function can be written

$$\psi_n^\sigma = \eta_n^\sigma \sum_\nu v_n^\sigma (\underset{\sim}{r} - \underset{\sim}{R}_\nu - \delta_n \underset{\sim}{d}, \zeta), \tag{III-43}$$

where the v's are now spin-orbitals (cf. Eq. I-6). If we express the angular part of v in terms of spherical harmonics, from Table 17 and Table 7 we obtain

$$\begin{aligned}
\Gamma_7: \quad v_{3d} &= \frac{P_{3d}(r)}{r} \frac{1}{\sqrt{6}} \left[2\, Y_2^1 \alpha + (Y_2^2 - Y_2^{-2}) \beta \right], \\
v_{3p} &= \frac{P_{3p}(r)}{r} \frac{-i}{\sqrt{3}} \left[\sqrt{2}\, Y_1^{-1} \alpha - Y_1^0 \beta \right]; \\
\Gamma_8: \quad v_{3d} &= \frac{P_{3d}(r)}{r} \left[- Y_2^{-1} \alpha \right], \\
v_{3p} &= \frac{P_{3p}(r)}{r} \left[-i\, Y_1^1 \alpha \right].
\end{aligned} \tag{III-44}$$

The matrix elements of the secular equation for these two representations are

$$\begin{aligned}
\Gamma_8: \quad O_{dd} &= O_{dd}(\Gamma_{15}), & H_{dd} &= H_{dd}(\Gamma_{15}) - \frac{1}{c^2} \frac{\xi_{dd}}{\theta_d(\Gamma_{15})}, \\
O_{pp} &= O_{pp}(\Gamma_{15}), & H_{pp} &= H_{pp}(\Gamma_{15}) + \frac{1}{c^2} \frac{\xi_{pp}}{\theta_p(\Gamma_{15})}, \\
O_{dp} &= O_{dp}(\Gamma_{15}), & H_{dp} &= H_{dp}(\Gamma_{15}); \\
\Gamma_7: \quad O_{dd} &= O_{dd}(\Gamma_{15}), & H_{dd} &= H_{dd}(\Gamma_{15}) + \frac{1}{c^2} \frac{2\,\xi_{dd}}{\theta_d(\Gamma_{15})}, \\
O_{pp} &= O_{pp}(\Gamma_{15}), & H_{pp} &= H_{pp}(\Gamma_{15}) - \frac{1}{c^2} \frac{2\,\xi_{pp}}{\theta_p(\Gamma_{15})}, \\
O_{dp} &= O_{dp}(\Gamma_{15}), & H_{dp} &= H_{dp}(\Gamma_{15}).
\end{aligned} \tag{III-45}$$

We have used atomic units in Eq. (III-45), thus c = 274.074 (cf. Eq. I-39). By $O_{dd}(\Gamma_{15})$ we mean the dd overlap matrix element at Γ_{15}. The rest of the notation is evident. All the quantities in Eq. (III-45), except ξ_{dd} and ξ_{pp}, can be obtained from the tight-binding calculation without spin-orbit interaction (see Sec. III-1 and 2). The integrals $\xi_{dd} \equiv \xi_{3d,3d}$ and $\xi_{pp} \equiv \xi_{3p,3p}$ must be computed numerically (cf. Appendix F). The numerical values of these quantities are given here in rydbergs:

$$O_{dd}(\Gamma_{15}) = O_{pp}(\Gamma_{15}) = 1, \qquad O_{dp}(\Gamma_{15}) = 0.1407,$$
$$H_{dd}(\Gamma_{15}) = -1.4178, \quad H_{pp}(\Gamma_{15}) = -1.0353, \quad H_{dp}(\Gamma_{15}) = -0.2650, \tag{III-46}$$
$$\theta_d(\Gamma_{15}) = 1.0034, \qquad \theta_p(\Gamma_{15}) = 0.7939,$$
$$\frac{1}{c^2}\xi_{dd} = 0.00480, \qquad \frac{1}{c^2}\xi_{pp} = 0.00309.$$

By solving the secular equation, we obtain

$$E_1(\Gamma_8) = -0.9948, \qquad E_2(\Gamma_8) = -1.4326,$$
$$E_1(\Gamma_7) = -1.0054, \qquad E_2(\Gamma_7) = -1.4194. \tag{III-47}$$

Thus, the spin-orbit splitting at the top of the valence bands is

$$E_1(\Gamma_8) - E_1(\Gamma_7) = 0.0106\ R_Y \simeq 0.14\ eV. \tag{III-48}$$

This result will be discussed in Sec. V-3.

Chapter IV

THE MIXED-BASIS METHOD

IV-1. The mixed-basis method.

In this chapter we undertake the study of the valence and conduction bands of CuCℓ by a method which essentially involves no other approximation besides the use of a model crystal potential. This is the "mixed-basis" (MB) method, developed by Kunz [Kun 69], based on an idea first suggested by Brown [Bro 62]. In this method, the advantages of the linear variation function technique (cf. Sec. I-3) are fully employed, and the number of functions in the truncated basis set can be increased until a "satisfactory" convergence is achieved.

In the MB method the truncated basis set for the expansion of the trial function $f_i^\sigma(\underset{\sim}{r})$ (cf. Eq. I-33) consists of two types of functions: Bloch functions and plane waves. We have performed the symmetry analysis for these two types of functions in Sec. II-3 and here we assume that they have the correct symmetry. Thus, we can write

$$f_i^\sigma(\underset{\sim}{r}) = \sum_n^N a_{in}^\sigma F_n^\sigma(\underset{\sim}{r}) + \sum_m^M b_{im}^\sigma S_m^\sigma(\underset{\sim}{r}), \qquad \text{(IV-1)}$$

where $F_n^\sigma(\underset{\sim}{r})$ is a symmetrized Bloch function, as in Eq. (II-7), and $S_n^\sigma(\underset{\sim}{r})$ is a symmetrized combination of plane waves,

as in Eq. (II-15). We assume that all the functions in the expansion (IV-1) are linearly independent and normalized, but not necessarily orthogonal. According to the results of Sec. I-3, we will have to solve a secular equation, whose determinant is of order N+M and is schematically of the form

$$\left|\begin{array}{c|c} \underset{(N\times N)}{\langle F|H-E|F\rangle} & \underset{(N\times M)}{\langle F|H-E|S\rangle} \\ \hline \underset{(M\times N)}{\langle S|H-E|F\rangle} & \underset{(M\times M)}{\langle S|H-E|S\rangle} \end{array}\right| , \qquad \text{(IV-2)}$$

where the number of elements in each block is shown.

The tight-binding approximation, described in Chap. III, can be considered a special case of the MB method in which all coefficients b_{im}^{σ} in Eq. (IV-1) are put equal to zero. The main difference is that in the tight-binding approximation we restrict the sum to a small fixed number N of Bloch functions (cf. Sec. III-1). In this way, we are not making full use of the characteristics of the linear variation function method. To do this, we should increase the number N, by adding Bloch functions coming from excited atomic states of increasing energy, and study the convergence of the band energy E_i versus N. This is possible, in principle, but a rigorous calculation of the tight-binding matrix elements is extremely hard, because of the large number of two- and three-center integrals involved [cf. Sla 54]. Therefore, we are forced to introduce some approximations (cf. Sec. III-2) and it is not always possible to estimate how much they affect the results. Besides, it is not clear

how meaningful a study of the convergence of E vs N is, if the matrix elements of the secular determinant are not calculated exactly. This is the reason why we call the tight-binding an "approximation." It will soon become clear why, on the other hand, we call the mixed-basis a "method."

In the MB method we keep N, the number of Bloch functions, fixed, and vary M, the number of sets of plane waves. Plane waves are mathematically much easier to handle and matrix elements between plane waves can be calculated rigorously with little (computer) effort. Furthermore, with a "good" choice of Bloch functions, we may need only relatively few plane waves to obtain a satisfactory convergence. On the other hand, the computation of matrix elements between Bloch functions can be greatly simplified by choosing atomic-like orbitals which do not overlap, thus reducing all three-center integrals to zero. If we can choose the orbitals so that they do not overlap the atomic potential at a neighboring site, even the two-center integrals will be eliminated. We have a large freedom in the choice of the atomic-like orbitals $v(\underset{\sim}{r})$ from which the Bloch functions are formed. There are only two practical restrictions: first, that they have the correct symmetry; second, that they do not require a very large number of plane waves to yield a good convergence for the states of interest.

If the Bloch functions used in Eq. (IV-1) are orthonormal core eigenstates of the crystal Hamiltonian, the MB

method is equivalent to the OPW (orthogonalized-plane-wave) method.* To show this [cf. Bro 62, 58], assume that the N functions F_n in Eq. (IV-1) satisfy the following equations:

$$\begin{aligned} &\langle F_n | F_{n'} \rangle = \delta_{nn'} , \\ &H|F_n\rangle = E_n |F_n\rangle , \qquad n,n' = 1,2,\ldots,N . \end{aligned} \tag{IV-3}$$

That is, they are orthonormal and they are eigenfunctions of the crystal Hamiltonian corresponding to the lowest N eigenvalues E_n ($E_1<E_2<\ldots<E_N$). We note, in passing, that the orthogonality condition is a consequence of the second of Eqs. (IV-3) [cf. Dir 58, §9]. For f_i (Eq. IV-1) to be an eigenfunction of the same Hamiltonian H, corresponding to an eigenvalue $E_i>E_N$, it must be

$$\{H-E_i\}|f_i\rangle = 0 . \tag{IV-4}$$

Substituting Eq. (IV-1) for f_i, we obtain

$$\sum_n a_{in}(E_n-E_i)|F_n\rangle = -\sum_m b_{im}(H-E_i)|S_m\rangle , \tag{IV-5}$$

where we have made use of the second of Eqs. (IV-3). Multiplying both sides of Eq. (IV-5) by $\langle F_{n'}|$, and making use of the first of Eqs. (IV-3) and of the conjugate imaginary of the second, we get

$$\sum_n a_{in}(E_n-E_i)\delta_{nn'} = -\sum_m b_{im}(E_{n'}-E_i)\langle F_{n'}|S_m\rangle . \tag{IV-6}$$

---

*See Woo 57 or Cal 64 for a description of the OPW method.

Thus,

$$a_{in'} = -\Sigma_m b_{im} \langle F_{n'} | S_m \rangle . \qquad \text{(IV-7)}$$

Putting this result into Eq. (IV-1) yields

$$f_i(\underset{\sim}{r}) = \Sigma_m b_{im} \left[S_m(\underset{\sim}{r}) - \Sigma_n \langle F_n | S_m \rangle F_n(\underset{\sim}{r}) \right], \qquad \text{(IV-8)}$$

which is a well known form of the OPW wavefunction [cf., e.g., Bas 63; Fow 63, 63a].

The result of the preceding paragraph is a trivial consequence of the orthogonality theorem of quantum mechanics [Dir 58, §9], since we imposed that $f_i(\underset{\sim}{r})$ be an eigenfunction of H corresponding to an eigenvalue E_i different from all eigenvalues E_n of the core states F_n. The point to note, according to Brown [Bro 62], is that "the orthogonalization condition [which is explicit in Eq. (IV-8)] need not be invoked a priori...Omitting the orthogonalization conditions achieves a great simplification in form without any loss of accuracy" [loc. cit.]. The most important advantage of the MB method over the OPW method is that the Bloch functions in Eq. (IV-1) need not be exact core eigenfunctions of the crystal Hamiltonian, while the OPW method strongly relies upon this assumption. As Callaway has shown [Cal 55], the OPW method may lead to serious errors if the core (Bloch) functions are not good eigenfunctions of the crystal Hamiltonian. These errors reflect the fact that the trial function is restricted to the wrong subspace of Hilbert space.

The MB method has no such drawback, since the wavefunction in Eq. (IV-1) is not restricted to any subspace. The variational method applied to this function will then yield all the core states, as well as the valence and conduction states.

Another advantage of the MB method is that relativistic effects can be included in a "nonperturbative" way [see Kun 69]. We have not calculated relativistic effects, but in Appendix F we show how the spin-orbit interaction can be incorporated in this method.

In the next section we describe a method to construct nonoverlapping atomic-like orbitals for the Bloch sums. In Section 3 we form the matrix elements of the secular determinant (Eq. IV-2). Finally, in Section 4, we apply this method to CuCℓ. The results and a discussion of them are in Chapter V.

IV-2. Cutoff orbitals.

The atomic-like orbitals v, from which the Bloch functions are formed, can be written (cf. Eq. III-3)

$$v_n^\sigma(\underset{\sim}{r}) = r^{-1} P_{n\ell}(r) \sum_{m'} c^\sigma_{nm'} Q_\ell^{m'}\left(\frac{\underset{\sim}{r}}{r}\right). \qquad \text{(IV-9)}$$

While the angular part $\Sigma c^\sigma_{nm'} Q_\ell^{m'}$ is determined by the symmetry of v_n^σ, the radial function $P_{n\ell}(r)$ can be chosen at our convenience, provided that the following conditions are satisfied [cf., e.g., Per 39]:

$$P_{n\ell}(0) = 0,$$
$$\int_0^\infty |P_{n\ell}(r)|^2 dr = 1. \qquad \text{(IV-10)}$$

We can then choose $P_{n\ell}(r)$ so that it satisfies Eq. (III-25) for $r \leq r_c$ and joins on smoothly to a smooth function which goes to zero at $r = r_m > r_c$ [cf. Bro 62]. The parameter r_m can be chosen so that orbitals centered on different sites do not overlap. When there is mixing between functions coming from both types of atoms, this condition implies that

$$r_m^A + r_m^B \leq d_{AB}, \qquad \text{(IV-11)}$$

where r_m^A and r_m^B are the cutoff radii for type A and B ions, respectively, and d_{AB} is the nearest-neighbor distance. Deegan and Twose [Dee 67] have used similar cutoff functions in their modified OPW method, and we use their method to construct such functions, as described in Appendix C of their paper [loc. cit.].

The unorthogonalized cutoff (CO) radial function, denoted by $S_{n\ell}^{CO}(r)$, is defined as follows:

$$S_{n\ell}^{CO}(r) \equiv P_{n\ell}(r) \qquad \text{for } 0 \leq r \leq r_c,$$
$$S_{n\ell}^{CO}(r) \equiv b\{1 + \cos[q(r - r_o)]\} \qquad \text{for } r_c \leq r \leq r_m, \qquad \text{(IV-12)}$$

where $P_{n\ell}(r)$ is the solution of Eq. (III-25), corresponding to the eigenvalue $\varepsilon_{n\ell}^a$. The three parameters b, q, and r_o are chosen to satisfy the three conditions that the tail match

$P_{n\ell}(r)$ continuously with continuous first derivative at r_c and vanish identically at r_m. Specifically,

$$b = \frac{P_{n\ell}(r_c)}{1 + \cos[q(r_c - r_o)]}, \quad q = \frac{\pi}{r_m - r_o}, \tag{IV-13}$$

and r_o is determined by a trial-and-error procedure, so that

$$\left.\frac{d P_{n\ell}(r)}{dr}\right|_{r=r_c} = \left.\frac{d}{dr}\left\{b\left[1 + \cos q(r - r_o)\right]\right\}\right|_{r=r_c} \tag{IV-14}$$

$$= -bq \sin\left[q(r_c - r_o)\right].$$

The CO function is then orthogonalized to the inner-core functions, so the final (orthonormal) CO function is

$$P^{CO}_{n\ell}(r) = \left(O^{CO}_{n\ell}\right)^{-\frac{1}{2}}\left[S^{CO}_{n\ell}(r) - \sum_{n'} \omega^{n'}_{n\ell} P_{n'\ell}(r)\right], \tag{IV-15}$$

where $$\omega^{n'}_{n\ell} = \int_0^\infty P_{n'\ell}(r)\, S^{CO}_{n\ell}(r)\, dr, \tag{IV-16}$$

and the summation is over inner-core states of angular momentum ℓ. $O^{CO}_{n\ell}$ is a normalization factor, so that the second condition in Eq. (IV-10) is satisfied. Explicitly,

$$O^{CO}_{n\ell} = \int_0^\infty \left[S^{CO}_{n\ell}(r)\right]^2 dr - \sum_{n'} \left(\omega^{n'}_{n\ell}\right)^2. \tag{IV-17}$$

In Eq. (IV-17) we have made use of the orthonormality of the inner-core radial functions $P_{n\ell}(r)$.

We have chosen the parameter r_c to be approximately

$$r_c \approx \frac{2}{3} r_m. \qquad \text{(IV-18)}$$

Since in general both types of atoms contribute to the basis functions, the parameters r_m^A and r_m^B can be varied, subject to condition (IV-11), so as to optimize the basis functions, that is, to minimize the eigenvalues of the secular equation. In cases such as Γ_{12} for CuCl, in which only one ion (Cu^+) contributes to the basis functions, r_m for Cu^+ can be as large as half the Cu^+-Cu^+ distance and Eq. (IV-11) becomes meaningless.

Obviously, we do not need to apply the cutoff to those functions that do not extend beyond r_m. The choice of the functions to which to apply the cutoff is sometimes arbitrary. We first solve Eq. (III-25) for all occupied states, for each type of ion, to obtain radial functions and potentials. If the potentials centered on two nearest-neighbor ions do not extend too far into each other's region, we might apply the cutoff to all those functions that overlap the nearest-neighbor potential. If this is unpractical or impossible, as in our case, we must content ourselves with nonoverlapping orbitals. In this case, the following criterion may be used. Define a value of r, say r_{max}, for each function $P_{n\ell}(r)$, such that for $r>r_{max}$ the value of the function is negligible (say, $<10^{-3}$). Then discard functions for decreasing r_{max}, starting with the one corresponding to the largest r_{max}, until there are no overlapping functions

left. These non-overlapping functions can be left unchanged, and we refer to them as the core functions. The remaining functions are cut off, so that they do not overlap.

The overlap and Hamiltonian matrix elements for the core functions are similar to those derived in Chapter III (cf. Eqs. III-10 and 21), but, due to the fact that functions centered on different ions do not overlap, the quantities h_{np} and g_{np} are identically zero. We then obtain

$$O_{np} = \delta_{np} , \tag{IV-19}$$

$$H_{np} = \varepsilon_n^a \delta_{np} + f_{np} . \tag{IV-20}$$

The matrix elements involving CO functions require particular care. The overlap matrix element is the same as in Eq. (IV-19), since we have explicitly orthonormalized the CO functions (cf. Eq. IV-15). For the same reason, the Hamiltonian matrix element between a core and a CO function can be written in the form (IV-20). For the Hamiltonian matrix elements involving only CO functions, on the other hand, we cannot use Eq. (III-21), because this implies Eq. (III-14), which is not valid for CO functions. Therefore we have to start with Eq. (III-13), which for nonoverlapping functions becomes

$$H_{np} = \langle v_n(\underset{\sim}{r}) | -\nabla^2 + V_a(r) + M_a(\underset{\sim}{r}) + [\Sigma' U]_a | v_p(\underset{\sim}{r}) \rangle \delta_{o\gamma_{np}} , \tag{IV-21}$$

where $\delta_{o\gamma_{np}}$ is the Kronecker δ symbol (cf. Eq. III-19) and

γ_{np} is defined by Eq. (III-8). Eq. (IV-21) can be written

$$H_{np} = \langle v_n(\underset{\sim}{r}) | -\nabla^2 + V_a(r) + M_a(r) | v_p(\underset{\sim}{r}) \rangle \delta_{o\gamma_{np}} + f_{np} , \qquad \text{(IV-22)}$$

where f_{np}, if we neglect the nonspherical terms of $M_a(\underset{\sim}{r})$, is defined as in Eq. (III-19). Substituting Eq. (IV-9) for $v(\underset{\sim}{r})$ yields

$$H_{np} = \left[\int_o^\infty P_n^{co}(r) \left\{ -\frac{d^2}{dr^2} + \frac{\ell(\ell+1)}{r^2} + V_a(r) + M_a(r) \right\} P_p^{co}(r)\, dr \right] \times \delta_{\ell_n \ell_p} \delta_{m_n m_p} \delta_{o\gamma_{np}} + f_{np} . \qquad \text{(IV-23)}$$

The factor $\delta_{\ell_n \ell_p} \delta_{m_n m_p}$ comes from the integration over the angular coordinates θ and ϕ, and expresses the fact that the two functions must belong to the same row of the same representation of the full rotation group (cf. Sec. I-2).

If all the CO functions centered on the same ion correspond to different angular momentum quantum numbers ℓ, Eq. (IV-23) reduces to

$$H_{np} = \left[\int_o^\infty P_n^{co}(r) \left\{ -\frac{d^2}{dr^2} + \frac{\ell(\ell+1)}{r^2} + V_a(r) + M_a(r) \right\} P_n^{co}(r)\, dr \right] \delta_{np} + f_{np} . \qquad \text{(IV-24)}$$

The integral in Eq. (IV-24) is calculated in Appendix D (see Eq. D-8). Accordingly, we obtain

$$H_{np} = (O_{n\ell}^{co})^{-1} \left\{ \varepsilon_{n\ell}^2 \int_o^{r_c} \left[S_{n\ell}^{co}(r) \right]^2 dr + (bq)^2 \int_{r_c}^{r_m} \left[1 + \cos q(r - r_o) \right] \cos q(r - r_o)\, dr \right.$$
$$\left. + \int_{r_c}^{r_m} \left[S_{n\ell}^{co}(r) \right]^2 \left[\frac{\ell(\ell+1)}{r^2} + V_a(r) + M_a(r) \right] dr - \sum_{n'} \varepsilon_{n'\ell}^2 \left(\omega_{n\ell}^{n'} \right)^2 \right\} \delta_{np} + f_{np} . \qquad \text{(IV-25)}$$

If we retain only the spherical part of $[\Sigma'U]_o$, in consistency with retaining only the spherical part of the Madelung potential, we can write f_{np} in Eq. (IV-25) as

$$f_{np} \approx \bar{f}_{np} = \int_0^\infty [P_n^{co}(r)]^2 \overline{[\Sigma'U]}_o \, dr \, \delta_{np} . \qquad \text{(IV-26)}$$

In our CuCℓ calculation we have applied the cutoff to the 3s and 3p functions of chlorine and to the 3s, 3p, and 3d functions of copper. Thus, Eqs. (IV-24 and 25) are valid in our case.

In this section we have considered the matrix elements of the form <F|H - E|F>, appearing in Eq. (IV-2). The remaining matrix elements, involving plane waves, are considered in the next section.

IV-3. <u>Matrix elements of the secular equation</u>.

In the MB method we have to calculate three types of matrix elements [cf. Kun 69]:

$$\text{type 1:} \quad \langle F_n | Op | F_{n'} \rangle , \qquad \text{(IV-27)}$$

$$\text{type 2:} \quad \langle F_n | Op | S_m \rangle , \qquad \text{(IV-28)}$$

$$\text{type 3:} \quad \langle S_m | Op | S_{m'} \rangle , \qquad \text{(IV-29)}$$

where Op = H for Hamiltonian matrix elements, and Op = 1 for overlap matrix elements. A Bloch function $F_n(\underset{\sim}{r})$ will be written (cf. Eqs. III-2, 4, 5)

$$F_n(\underset{\sim}{r}) = i^{\ell} N^{-\frac{1}{2}} \sum_{\nu} e^{i \underset{\sim}{k} \cdot \underset{\sim}{R}_\nu} v_n(\underset{\sim}{r} - \underset{\sim}{R}_\nu - \delta_n \underset{\sim}{d}) , \qquad \text{(IV-30)}$$

where the phase factor i^{ℓ} has been introduced for convenience. In Eq. (IV-30) we have used the fact that $\theta_n = 1$ (see Eq. III-5), since the orbitals v centered on different sites do not overlap (cf. Sec. IV-2). A S.C.P.W. will be written (cf. Eq. II-15)

$$S_m(\underset{\sim}{r}) = (N\Omega\Theta_m)^{-\frac{1}{2}} \sum_n \Gamma^{\alpha}_{\gamma\gamma}(R_n)\, e^{i\alpha_n^{-1}(\underset{\sim}{k}+\underset{\sim}{h}_\mu)\cdot\underset{\sim}{r}} , \qquad \text{(IV-31)}$$

where we have made use of the unitary property of the representation matrices ($\Gamma^{\dagger}(R) = \Gamma^{-1}(R)$). Ω is the volume of the primitive cell (see Sec. II-1) and Θ_m is obtained by imposing the normalization condition on S_m. Specifically,

$$\Theta_m = \sum_n \sum_{n'} \Gamma^{\alpha}_{\gamma\gamma}(R_n)^{*}\, \Gamma^{\alpha}_{\gamma\gamma}(R_{n'})\, \delta_{\alpha_n^{-1}(\underset{\sim}{k}+\underset{\sim}{h}_\mu),\, \alpha_{n'}^{-1}(\underset{\sim}{k}+\underset{\sim}{h}_\mu)} . \qquad \text{(IV-32)}$$

It is easy to see from Eq. (IV-32) that $\Theta_m^* = \Theta_m$; thus Θ_m is real.

Type 1: The matrix elements between Bloch functions of the form (IV-30) are the same as those derived in the preceding section. We rewrite them in the form:

$$\langle F_n \mid F_{n'} \rangle = \delta_{n,n'} , \qquad \text{(IV-33)}$$

$$\langle F_n \mid H \mid F_{n'} \rangle = \varepsilon'_n \delta_{nn'} + f_{nn'} . \qquad \text{(IV-34)}$$

The quantity ε'_n in Eq. (IV-34) is defined as follows:

$$\varepsilon'_n = \varepsilon^{a}_{n\ell} \qquad \text{for core functions,}$$

$$\varepsilon'_n = \varepsilon^{CO}_{n\ell} = (O^{CO}_{n\ell})^{-1}\left\{\varepsilon^2_{n\ell}\int_0^{r_c}\left[S^{CO}_{n\ell}(r)\right]^2 dr + (bq)^2\int_{r_c}^{r_m}\left[1+\cos q(r-r_c)\right]\cos q(r-r_c)\,dr\right.$$

$$\left. + \int_{r_c}^{r_m}\left[S^{CO}_{n\ell}(r)\right]^2\left[\frac{\ell(\ell+1)}{r^2} + V_a(r) + M_a(r)\right]dr - \sum_{n'}\varepsilon^2_{n'\ell}\left(\omega^{n'}_{n\ell}\right)^2\right\} \qquad \text{(IV-35)}$$

for CO functions.

All the quantities in Eq. (IV-35) have been defined in the preceding section (cf. Eq. IV-25).

Type 2: The matrix elements between Bloch functions and S.C.P.W.'s (Eq. IV-28) are derived in Appendix D. We report here the results:

$$\langle F_n | S_m\rangle = 4\pi(\Omega\Theta_m)^{-\frac{1}{2}}\left[\sum_R \Gamma^{\kappa}_{\gamma\gamma'}(R)\, e^{i\delta_m \underset{\sim}{K}_R\cdot\underset{\sim}{d}} \sum_m c^{*}_{nm}\, Q^{m*}_{\ell}\left(\frac{\underset{\sim}{K}_R}{K}\right)\right]$$

$$\times \int_0^{\infty} r\, P_m(r)\, j_\ell(Kr)\, dr, \qquad \text{(IV-36)}$$

$$\langle F_n | H | S_m\rangle = (K^2 + E^2_M)\langle F_n | S_m\rangle + 4\pi(\Omega\Theta_m)^{-\frac{1}{2}}\left[\sum_R \Gamma^{\kappa}_{\gamma\gamma'}(R)\, e^{i\delta_m \underset{\sim}{K}_R\cdot\underset{\sim}{d}} \sum_m c^{*}_{nm}\, Q^{m*}_{\ell}\left(\frac{\underset{\sim}{K}_R}{K}\right)\right]$$

$$\times \int_0^{\infty} r\, P_m(r)\, j_\ell(Kr)\left\{V_a(r) + \left[\overline{\Sigma' U}\right]_0\right\} dr, \qquad \text{(IV-37)}$$

where

$$\underset{\sim}{K}_R = \alpha^{-1}(\underset{\sim}{k} + \underset{\sim}{h}_\mu) \quad \text{and} \quad K = |\underset{\sim}{K}_R| = |\underset{\sim}{k} + \underset{\sim}{h}_\mu|\,. \qquad \text{(IV-38)}$$

$j_\ell(\rho)$ is the spherical Bessel function of order l. The first three j's are given here [cf. Sch 68, p. 85]:

$$j_0(\rho) = \frac{\sin\rho}{\rho},$$

$$j_1(\rho) = \frac{\sin\rho}{\rho^2} - \frac{\cos\rho}{\rho}, \qquad \text{(IV-39)}$$

$$j_2(\rho) = \left(\frac{3}{\rho^3} - \frac{1}{\rho}\right)\sin\rho - \frac{3}{\rho^2}\cos\rho\,.$$

Type 3: The matrix elements between S.C.P.W.'s are also derived in Appendix D. The result is:

$$\langle S_m | S_{m'} \rangle = (\Omega_m \Omega_{m'})^{-\frac{1}{2}} \sum_n \sum_{n'} \Gamma^n_{\gamma\gamma}(R_n)^* \, \Gamma^{n'}_{\gamma\gamma}(R_{n'}) \, \delta_{\underset{\sim}{K}_n, \underset{\sim}{K}_{n'}} , \tag{IV-40}$$

$$\langle S_m | H | S_{m'} \rangle = | \underset{\sim}{k} + \underset{\sim}{h}_\mu |^2 \langle S_m | S_{m'} \rangle + (\Omega_m \Omega_{m'})^{-\frac{1}{2}} \sum_n \sum_{n'} \Gamma^n_{\gamma\gamma}(R_n)^* \, \Gamma^{n'}_{\delta\gamma}(R_{n'}) \, v(\underset{\sim}{K}_n - \underset{\sim}{K}_{n'}) , \tag{IV-41}$$

where $\underset{\sim}{K}_n = \underset{\sim}{K}_{R_n} = \alpha_n^{-1}(\underset{\sim}{k} + \underset{\sim}{h}_\mu)$ (cf. Eq. IV-38). In Eq. (IV-41), $v(\underset{\sim}{K})$ is the Fourier coefficient of the crystal potential $V(\underset{\sim}{r})$, defined as follows:

$$v(\underset{\sim}{K}) = (N\Omega)^{-1} \int_c e^{-i \underset{\sim}{K} \cdot \underset{\sim}{r}} V(\underset{\sim}{r}) \, d\tau , \tag{IV-42}$$

where $\int_c$ means that the integral extends over the entire crystal, whose volume is $N\Omega$. As shown in Appendix E, Eq. (IV-42) can be written

$$v(\underset{\sim}{K}) = v_A(\underset{\sim}{K}) + e^{-i \underset{\sim}{K} \cdot \underset{\sim}{d}} v_B(\underset{\sim}{K}) , \tag{IV-43}$$

where

$$v_a(\underset{\sim}{K}) = \Omega^{-1} \int_c e^{-i \underset{\sim}{K} \cdot \underset{\sim}{r}} V_a(r) \, d\tau . \tag{IV-44}$$

Separating $V_a(r)$ in its long- and short-range parts (cf. Eq. I-42), Eq. (IV-44) becomes (see Appendix E)

$$v_a(\underset{\sim}{K}) = v_a(K) = -\frac{8\pi z_a}{\Omega K^2} + \frac{4\pi}{\Omega K} \int_0^\infty r \sin(Kr) \, U_a(r) \, dr \quad \text{for } K > 0 ,$$

$$v_a(0) = \frac{4\pi}{\Omega} \int_0^\infty r^2 U_a(r) \, dr . \tag{IV-45}$$

Now that we have obtained all matrix elements in the mixed-basis method, it may be interesting to review the assumptions and approximations made in deriving them. At the beginning of this chapter, we claimed that "essentially" the only approximation in this method was the use of a model crystal potential. Actually, we have also assumed that the crystal potential can be written as a sum of spherical potentials centered around each ion (cf. Eqs. I-40, 41). We believe that this is the only assumption intrinsic to the MB method in its present form. In deriving the matrix elements involving Bloch functions, we have also neglected the nonspherical terms in the expansion of the crystal potential in spherical harmonics (Eq. III-24). This approximation is not intrinsic to the method, but it reduces considerably the labor of computation, without introducing any serious error in most cases. In our case, we believe that the error introduced by the spherical approximation is negligible, as discussed in Section III-2.

As an improvement to the present form of the MB method, we suggest consideration of some of the nonspherical terms of the potential $V(\underset{\sim}{r})$, which in some cases might give a non negligible contribution. In the matrix elements of type 1, this can be done through the quantity f_{np} (cf. Eq. IV-34), which can be redefined to include the nonspherical terms of the Madelung potential, as follows:

$$f_{np} = \langle v_n(\underset{\sim}{r}) \mid M_a^{NS}(\underset{\sim}{r}) + [\Sigma' U]_o \mid v_p(\underset{\sim}{r}) \rangle \delta_{o\gamma_{np}} . \qquad \text{(IV-46)}$$

In Eq. (IV-46), by $M_a^{NS}(\underset{\sim}{r})$ we denote the nonspherical part of the Madelung potential (cf. Eq. I-48):

$$M_a^{NS}(\underset{\sim}{r}) = M_a(\underset{\sim}{r}) - M_a(r) = \sum_{\ell>0} \sum_{-\ell}^{\ell}{}_m \; a_{\ell m}^{M_a}(r)\, Y_\ell^m(\theta,\phi) \,. \qquad \text{(IV-47)}$$

In the matrix elements of type 2, we have to add to Eq. (IV-37) the following term:

$$\langle F_n \,|\, V^{NS}(\underset{\sim}{r}) \,|\, S_m \rangle \,, \qquad \text{(IV-48)}$$

where $V^{NS}(\underset{\sim}{r})$ is the nonspherical part of the total crystal potential. As shown in Appendix D, the matrix element in Eq. (IV-48) is given explicitly by

$$\begin{aligned} \langle F_n \,|\, V^{NS}(\underset{\sim}{r}) \,|\, S_m \rangle \;=\; & (-i)^{\ell} (\Omega \mathcal{O}_m)^{-\frac{1}{2}} \sum_R \Gamma^*_{\gamma\gamma}(R)\, e^{i\delta_n \underset{\sim}{K}_R \cdot \underset{\sim}{d}} \\ & \times \sqrt{4\pi} \sum_{-\ell}^{\ell}{}_m \sum_{\ell_1}^{\infty} \sum_{|\ell-\ell_1|}^{\ell+\ell_1}{}_{\ell_2} \sum_{m-\ell_2}^{m+\ell_2}{}_{m_1} i^{\ell_2}\, c^*_{\ell m}\, Y^{m-m_1\,*}_{\ell_2}(\theta,\phi)_{\underset{\sim}{K}_R} \\ & \times \sqrt{\frac{(2\ell_1+1)(2\ell_2+1)}{2\ell+1}}\; (\ell_1 \ell_2\, m_1 m_2 \,|\, \ell m)\,(\ell_1 \ell_2\, 00 \,|\, \ell 0) \\ & \times \int_0^\infty r\, P_n(r)\, \overset{v}{a}_{\ell_1 m_1}(r)\, j_{\ell_2}(\kappa r)\, dr \,. \end{aligned} \qquad \text{(IV-49)}$$

In Eq. (IV-49), $c_{\ell m}$ are the coefficients of the expansion of $v_n(\underset{\sim}{r})$ in spherical (not cubic!) harmonics (cf. Eq. II-8) and $(\ell_1 \ell_2 m_1 m_2 \,|\, \ell m)$ are Clebsch-Gordan coefficients. These coefficients are tabulated in Condon and Shortley's book [Con 64, Tables $1^3, 2^3, 3^3, 4^3$]. They use the notation $(j_1 j_2 m_1 m_2 \,|\, j_1 j_2 j m)$, which corresponds to $(j_1 j_2 m_1 m_2 \,|\, j m)$ in our notation.

All other quantities in Eq. (IV-49) have been defined previously.

In the following section, we apply the MB method to the calculation of the band structure of CuCℓ.

IV-4. Application to CuCℓ.

In applying the MB method to CuCℓ, we first solved the atomic problem (Eq. III-25) to obtain radial functions $P_{n\ell}(r)$, atomic energy parameters $\varepsilon^a_{n\ell}$ and potentials $V_a(r)$. The program ATOM (see Appendix G) was again used for this purpose, but the variable KUT was this time set equal to 1 (cf. Sec. III-2). This ensures that the Hamiltonian H is the same in all MB matrix elements. The resulting atomic functions, energies, and potentials are given in Tables 22 and 23.

The atomic potentials $V_a(r)$ obtained from the solution of Eq. (III-25) were used to construct the crystal potential, according to Eq. (I-40), although this is not a restriction of the MB method [cf. Kun 69]. The Fourier coefficients $v_a(K)$ were then obtained by using Eq. (IV-45). This is done in program PAULI, described in Appendix H. In calculating the average short-range potential $\overline{[\Sigma' U]}_o$, we considered only the contribution of the first three shells of nearest neighbors. The contribution of the first two shells is given in Eq. (III-37). The third shell contains 12 ions at a distance $a\sqrt{11}/4$ (cf. Table 1); its contribution can be

TABLE 22

RADIAL FUNCTIONS, ENERGIES AND POTENTIAL FOR Cu^+.
VALENCE SCREENING POTENTIAL. ATOMIC UNITS. (KUT=1)

r	$P_{3s}(r)$	$P_{3p}(r)$	$P_{3d}(r)$	rV(r)
0.0000	0.0000	0.0000	0.0000	-58.000
0.0065	0.1946	0.0105	0.0001	-56.666
0.0137	0.3275	0.0422	0.0006	-55.156
0.0209	0.3918	0.0885	0.0021	-53.680
0.0281	0.4037	0.1441	0.0049	-52.263
0.0418	0.3280	0.2614	0.0142	-49.747
0.0562	0.1687	0.3833	0.0304	-47.329
0.0706	-0.0213	0.4896	0.0532	-45.129
0.0850	-0.2096	0.5727	0.0822	-43.134
0.1124	-0.5010	0.6574	0.1519	-39.809
0.1412	-0.6724	0.6473	0.2402	-36.789
0.1700	-0.7055	0.5549	0.3369	-34.133
0.1988	-0.6270	0.4047	0.4361	-31.768
0.2536	-0.2871	0.0390	0.6155	-27.878
0.3112	0.1689	-0.3587	0.7751	-24.405
0.3689	0.5926	-0.6990	0.8968	-21.478
0.4265	0.9241	-0.9554	0.9811	-19.051
0.5360	1.2679	-1.2158	1.0547	-15.397
0.6513	1.3178	-1.2515	1.0454	-12.465
0.7665	1.1933	-1.1519	0.9862	-10.258
0.8818	1.0019	-0.9959	0.9040	-8.6097
1.1008	0.6415	-0.6870	0.7345	-6.5086
1.3313	0.3680	-0.4325	0.5734	-5.1490
1.5619	0.2015	-0.2620	0.4418	-4.2627
1.7924	0.1073	-0.1552	0.3386	-3.6558
2.2304	0.0311	-0.0555	0.2033	-2.9475
2.6915	0.0081	-0.0183	0.1191	-2.5490
3.1526	0.0021	-0.0060	0.0703	-2.3317
3.6136	0.0005	-0.0019	0.0421	-2.2093
4.4896		-0.0002	0.0184	-2.1037
5.4118	ε_{3s}=-8.6845		0.0091	-2.0609
6.3339		ε_{3p}=-5.7387	0.0045	-2.0371
7.2561			0.0022	-2.0224
9.0081				-2.0000
			ε_{3d}= -0.7439	

TABLE 23

RADIAL FUNCTIONS, ENERGIES, AND POTENTIAL FOR Cl^-.
VALENCE SCREENING POTENTIAL. ATOMIC UNITS. (KUT=1).

r	$P_{3s}(r)$	$P_{3p}(r)$	rV(r)
0.0000	0.0000	0.0000	-34.000
0.0077	0.0898	0.0026	-33.327
0.0164	0.1624	0.0110	-32.544
0.0250	0.2111	0.0238	-31.754
0.0336	0.2399	0.0400	-30.974
0.0499	0.2517	0.0772	-29.553
0.0671	0.2210	0.1212	-28.159
0.0844	0.1625	0.1660	-26.870
0.1016	0.0884	0.2091	-25.681
0.1343	-0.0661	0.2800	-23.676
0.1687	-0.2165	0.3338	-21.880
0.2031	-0.3349	0.3641	-20.329
0.2376	-0.4143	0.3721	-18.952
0.3030	-0.4619	0.3357	-16.686
0.3719	-0.3968	0.2454	-14.683
0.4407	-0.2576	0.1251	-12.969
0.5096	-0.0821	-0.0074	-11.459
0.6404	0.2626	-0.2521	-9.5974
0.7782	0.5605	-0.4632	-7.9511
0.9159	0.7585	-0.6118	-6.4666
1.0536	0.8633	-0.7024	-5.1472
1.3153	0.8843	-0.7585	-3.1276
1.5908	0.7803	-0.7261	-1.6301
1.8662	0.6414	-0.6575	-0.6182
2.1417	0.5092	-0.5812	0.0635
2.6650	0.3150	-0.4488	0.8218
3.2159	0.1854	-0.3367	1.2278
3.7669	0.1069	-0.2453	1.4552
4.3178	0.0583	-0.1656	1.6099
5.3645	0.0156	-0.0663	1.7981
6.4663	0.0040	-0.0263	1.8909
7.5681	0.0010	-0.0107	1.9390
8.6700	0.0003	-0.0045	1.9654
10.763		-0.0009	1.9886
12.967		-0.0002	2.0000

obtained by using Eq. (III-36) with n = 12 and $R_\gamma = a\sqrt{11}/4$:

$$\overline{[\Sigma' U_3]} = 6 \int_0^\pi U_3(|\underset{\sim}{r} - \underset{\sim}{\varrho}|) \sin\theta \, d\theta, \qquad \underset{\sim}{\varrho} \equiv (0, 0, \tfrac{a}{4}\sqrt{11}); \qquad \text{(IV-50)}$$

The contribution of the first three shells of nearest neighbors to the average short-range potential is given in Table 24 for $C\ell^-$ at the origin, and in Table 25 for Cu^+ at the origin.

All the quantities obtained so far depend only on the type of potential used (cf. Sec. I-5), but they are independent of the particular representation, the cutoff parameter, the number of basis functions used, etc. It is then convenient to store them, while in the process of testing for the best cutoff parameters or studying the convergence of the variational energies.

As mentioned in Sec. IV-2, we applied the Deegan and Twose cutoff to the 3s and 3p functions of $C\ell^-$ and to the 3s, 3p, and 3d functions of Cu^+. We have used the same cutoff parameter r_m for all functions centered on the same atom, which is a logical thing to do for a given representation. Obviously, we can use a different cutoff parameter when solving a secular equation for a different representation. However, we must be careful when comparing the results, and pay special attention to the convergence curves, as we will see in Chapter V. In Fig. 5 we show a CO function ($3p^-$) and the corresponding function without cutoff. The value r_m = 2.2a.u. was chosen for both $C\ell^-$ and Cu^+ (nearest-neighbor

TABLE 24

AVERAGE SHORT-RANGE POTENTIALS OF THE FIRST THREE SHELLS OF NEAREST-NEIGHBORS OF Cl^-. VALENCE SCREENING POTENTIAL. ATOMIC UNITS.

r	$r[\Sigma' U_1]$	$r[\Sigma' U_2]$	$r[\Sigma' U_3]$
0.0000	0.0000	0.0000	0.0000
0.0077	-0.0008	-0.0009	0.0000
0.0164	-0.0016	-0.0020	0.0000
0.0250	-0.0024	-0.0030	0.0000
0.0336	-0.0033	-0.0041	0.0000
0.0499	-0.0049	-0.0060	0.0000
0.0671	-0.0065	-0.0081	0.0000
0.0844	-0.0082	-0.0102	0.0000
0.1016	-0.0099	-0.0123	0.0000
0.1343	-0.0131	-0.0162	0.0000
0.1687	-0.0165	-0.0204	0.0000
0.2031	-0.0199	-0.0246	0.0000
0.2376	-0.0233	-0.0288	0.0000
0.3030	-0.0298	-0.0368	0.0000
0.3719	-0.0368	-0.0452	0.0000
0.4407	-0.0440	-0.0538	0.0000
0.5096	-0.0513	-0.0624	0.0000
0.6404	-0.0657	-0.0789	0.0000
0.7782	-0.0820	-0.0968	0.0000
0.9159	-0.0994	-0.1152	0.0000
1.0536	-0.1186	-0.1343	-0.0005
1.3153	-0.1608	-0.1727	-0.0043
1.5908	-0.2166	-0.2170	-0.0093
1.8662	-0.2895	-0.2665	-0.0151
2.1417	-0.3875	-0.3226	-0.0218
2.6650	-0.6892	-0.4540	-0.0376
3.2159	-1.3348	-0.6434	-0.0599
3.7669	-2.9008	-0.9036	-0.0901
4.3178	-7.9493	-1.2711	-0.1323
5.3645	-1.9368	-2.6695	-0.2920
6.4663	-0.5155	-7.7510	-0.8275
7.5681	-0.1829	-12.446	-3.1348
8.6700	-0.0800	-3.8755	-10.468
10.763	-0.0139	-0.8755	-0.6264
12.967		-0.2471	-0.1056
15.171		-0.0733	-0.0134
17.374		-0.0184	

TABLE 25

AVERAGE SHORT-RANGE POTENTIALS OF THE FIRST THREE SHELLS OF NEAREST NEIGHBORS OF Cu^+. VALENCE SCREENING POTENTIAL. ATOMIC UNITS.

r	$r[\Sigma' U_1]$	$r[\Sigma' U_2]$	$r[\Sigma' U_3]$
0.0000	0.0000	0.0000	0.0000
0.0065	-0.0021	-0.0002	-0.0004
0.0137	-0.0045	-0.0005	-0.0007
0.0209	-0.0068	-0.0008	-0.0011
0.0281	-0.0092	-0.0011	-0.0015
0.0418	-0.0137	-0.0016	-0.0023
0.0562	-0.0184	-0.0021	-0.0030
0.0706	-0.0231	-0.0027	-0.0038
0.0850	-0.0278	-0.0032	-0.0046
0.1124	-0.0368	-0.0042	-0.0061
0.1412	-0.0463	-0.0053	-0.0076
0.1700	-0.0557	-0.0063	-0.0092
0.1988	-0.0652	-0.0072	-0.0107
0.2536	-0.0833	-0.0088	-0.0137
0.3112	-0.1024	-0.0102	-0.0169
0.3689	-0.1217	-0.0115	-0.0200
0.4265	-0.1411	-0.0129	-0.0232
0.5360	-0.1784	-0.0156	-0.0293
0.6513	-0.2185	-0.0186	-0.0358
0.7665	-0.2597	-0.0218	-0.0424
0.8818	-0.3021	-0.0252	-0.0492
1.1008	-0.3875	-0.0324	-0.0626
1.3313	-0.4860	-0.0408	-0.0776
1.5619	-0.5969	-0.0503	-0.0937
1.7924	-0.7250	-0.0611	-0.1112
2.2304	-1.0408	-0.0859	-0.1492
2.6915	-1.5513	-0.1196	-0.1982
3.1526	-2.4160	-0.1646	-0.2599
3.6136	-3.9449	-0.2301	-0.3394
4.4896	-9.4732	-0.4749	-0.5690
5.4118	-3.3243	-1.2001	-0.9879
6.3339	-1.4020	-3.7592	-1.8296
7.2561	-0.7307	-15.439	-4.0743
9.0081	-0.2570	-1.2551	-8.5473
10.852	-0.0925	-0.2291	-1.5536
12.697	-0.0331	-0.0597	-0.4976
14.541	-0.0102	-0.0023	-0.1766
18.045			-0.0232

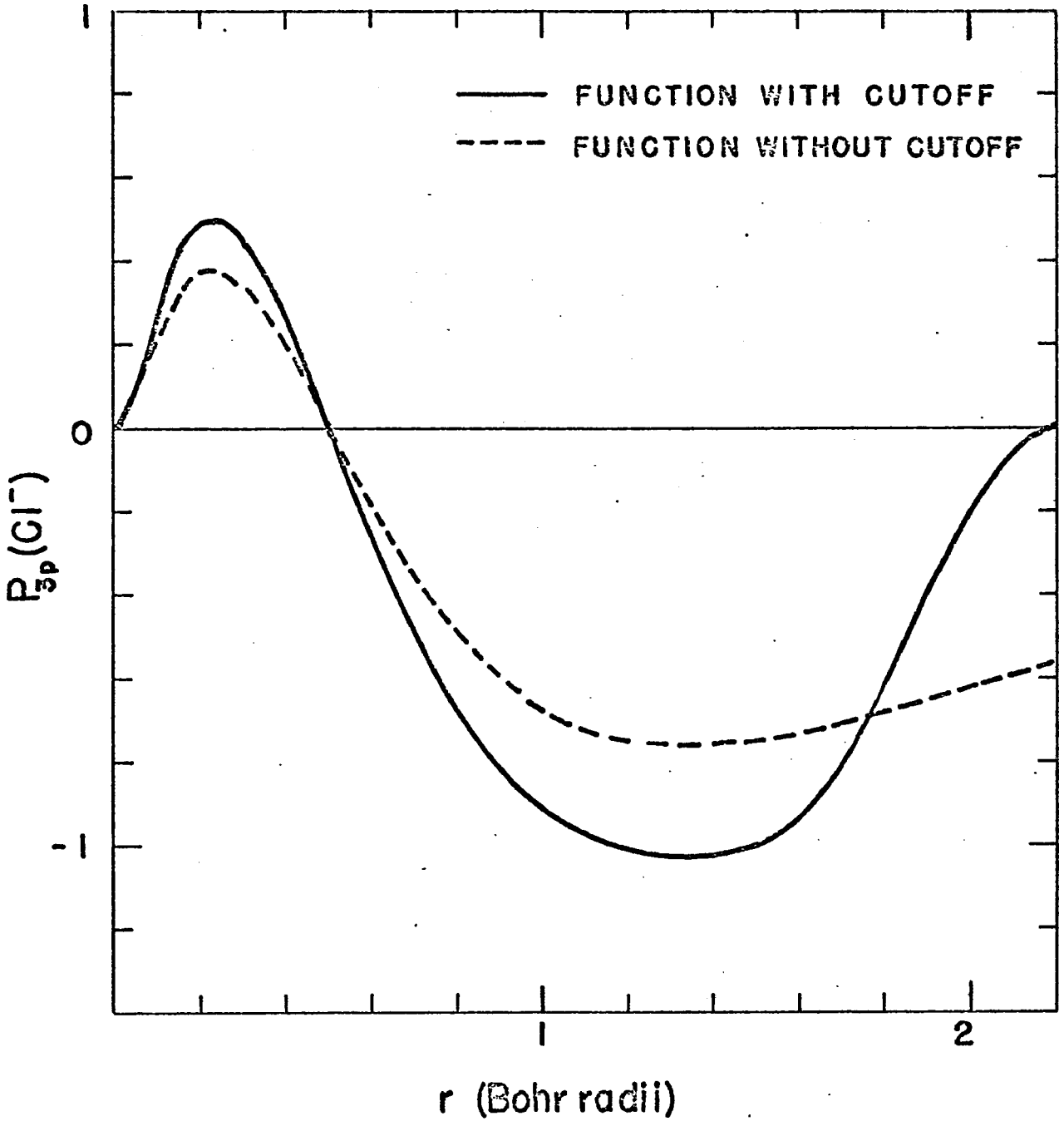

Fig. 5 - Radial function 3p of Cl^-. The cutoff is introduced in the way described by Deegan and Twose [Dee 67]. The functions shown are normalized, so that $\int_0^\infty [P_{3p}(r)]^2 dr = 1$.

distance = 4.43a.u.). Other cutoff parameters have been tried, as discussed in Chapter V. The subroutine DTCO (see Appendix H) forms the CO functions and calculates the CO energy parameters ε_n^{CO} (Eq. IV-35).

The quantities $\bar{f}_{nn}$ can be calculated at this point and added to the energy parameters ε_n', since they are independent of σ, the symmetry of the wave function (cf. Sec. III-1). The matrix elements of type 1 (Eqs. IV-33,34) are then easily obtained.

The procedure to follow is now the following: choose a value of $\underset{\sim}{k}$; for every "interesting" representation (cf. Sec. II-3) of the group of $\underset{\sim}{k}$ select the Bloch functions and S.C.P.W.'s belonging to the same row of this representation; then compute the matrix elements and solve the secular equation. The computation of all matrix elements is done in subroutine BETA (see Appendix H). The secular equation is then solved in subroutine DIAG, as in the tight-binding calculation (cf. Sec. III-2). To study the convergence of the roots of the secular equation, we may delete the last, say, n rows and columns before solving the secular equation. These n rows and columns must correspond to plane waves with the highest values of $|\underset{\sim}{k} + \underset{\sim}{h}_\mu|$. We then solve the remaining secular equation, add a few rows and columns of increasing $|\underset{\sim}{k} + \underset{\sim}{h}_\mu|$, and solve the expanded secular equation, and so forth until the last row and column have been included. It is advisable to write the S.C.P.W.'s in Eq. IV-1 in order of

increasing $|\underset{\sim}{k} + \underset{\sim}{h}_{\mu}|$, to make the convergence study easier.

We have obtained the energy bands of CuCℓ using two different types of exchange in the atomic potentials: the Slater exchange (Eq. I-49), and the screened-valence exchange (Eq. I-57). We have written the atomic potential in the form of Eq. (I-58), from which the two types of potentials can be derived, as described in connection with that equation.

The results of the MB calculation are in Chapter V. We have not included any relativistic effects in our calculation. A prescription to include them in the MB method is given in Kunz's paper [Kun 69]. In including spin-orbit effects in OPW or MB calculations authors generally assume that the matrix elements of the spin-orbit interaction involving plane waves are negligible [cf. Liu 62, Kun 69]. This might not be a valid assumption in the MB method in its most general form, since the plane wave contribution may be determinant in the valence wavefunctions. The spin-orbit interaction can be included in a straightforward manner in the MB method, as shown in Appendix F.

Chapter V

RESULTS, DISCUSSION, CONCLUSIONS

V-1. Tight-binding results.

The data used in the present calculation are given in Table 26. They are divided into two categories: the first category contains experimental data; the second, data derived from the first category. All other quantities needed in this calculation can be obtained from these data.

The valence bands of CuCℓ in the tight-binding approximation are shown in Fig. 6. The top of the valence bands is at Γ_{15}. At this point the wave function can be written

$$\phi_{\Gamma_{15}}(\underset{\sim}{r}) = c_1 F_x(\underset{\sim}{r}) + c_2 F_{yz}(\underset{\sim}{r}), \qquad \text{(V-1)}$$

where F_x and F_{yz} are Bloch functions formed, respectively, from the 3p orbital of symmetry x centered on $C\ell^-$ and from the 3d orbital of symmetry yz centered on Cu^+. The coefficients c_1 and c_2 for the normalized wave function can be obtained by the method described in Section I-3. In this case we get, apart from a constant phase factor,

$$c_1 = 0.9977, \qquad c_2 = -0.2962. \qquad \text{(V-2)}$$

TABLE 26

DATA FOR CuCl.

	Crystal	Ions
	Structure: zinc blende [a]	Cl^- Cu^+
Experimental	Lattice constant: $a = 5.41$ Å [b] $= 10.23$ a.u.	Atomic number Z: 17 29
	Dielectric constant : $\kappa = 3.57$	Ionicity (assumed) : -1 +1
Derived	Madelung constant: $\alpha_a = 3.78293$ [c]	Configuration Cl^-: $1s^2 2s^2 2p^6 3s^2 3p^6$, Cu^+: $1s^2 2s^2 2p^6 3s^2 3p^6 3d^{10}$

a - [Wyc 48]

b - [Sla 65]

c - [Tos 64]

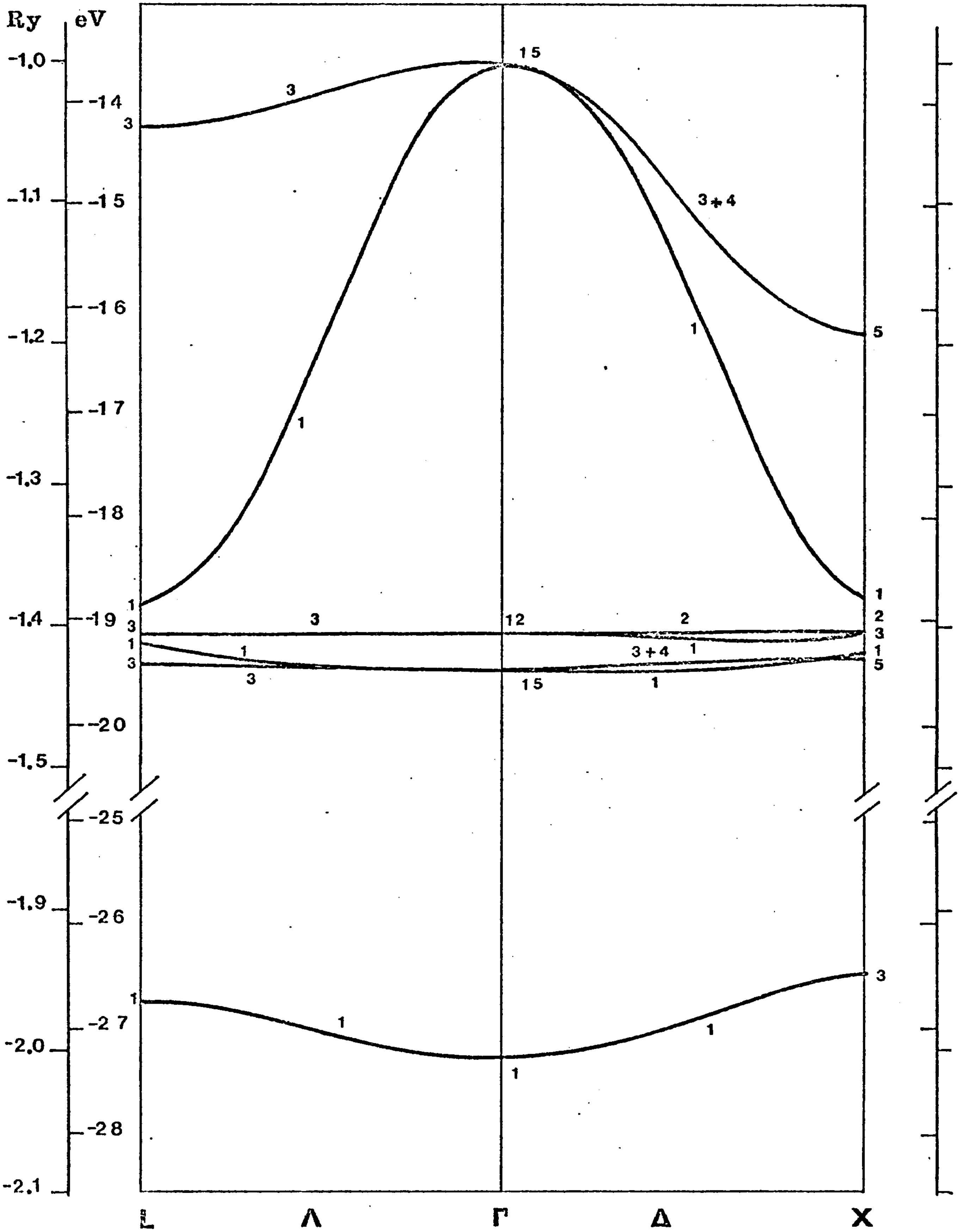

Fig. 6 - Valence bands of CuCl in the tight-binding approximation. Valence screening potential. The origin is on the Cu^+ ion.

Thus the 3p state of Cl^- contributes about 77% of the total wave function at the top of the valence band.

The first valence band is fairly wide (about 5.2 eV). The width of a band depends on the overlap parameters h_{np} and g_{np} (Eqs. III-9, 20). If there would be no overlap between atomic orbitals centered on different ions, all quantities of the type h_{np} and g_{np} would be zero and the bands would have zero width; in other words, there would be no bands, but only a shifting and eventually a splitting of the atomic levels. The large width of the first valence band is related to the large overlap between p functions (cf. Table 22) and confirms the p character of this band. It must be added that, perhaps, we have overestimated some three-center integrals in taking the spherical average of the nearest-neighbor short-range potentials. The separation between the first two bands is about 0.2 eV.

The second and third bands are separated by less than 0.03 eV and have a total width of about 0.4 eV. This clearly shows their d character, since the overlap between d functions is relatively small.

The lowest valence band is the s band. Its width is approximately 0.9 eV and it is separated by 7.0 eV from the higher valence bands.

V-2. Mixed-basis results.

The MB valence and conduction bands are shown in Fig. 7 for the HFS potential (Eq. I-50), and in Fig. 8 for the HFS-with-valence-screening potential (Eq. I-58). Attention should be given to the fact that the points shown in these figures are upper bounds to the exact energies for the Hamiltonian used (cf. Sec. I-3). How close these values are to the exact energies may be estimated by studying the convergence curves. In Figs. 9 and 10 we plot the energy versus number of basis functions for those points where the convergence was the poorest. In the curves not shown, the energy varied by less than 0.1 eV when we added the last ten sets of plane waves (or S.C.P.W.'s).

We notice that the convergence curves for the two types of potentials are very similar; on the other hand, according to our experience, they depend strongly on the cutoff parameters used (cf. Sec. IV-2). In the bands shown, we have used the values $r_c = 1.5$ and $r_m = 2.2$ (in Bohr radii) for both $C\ell^-$ and Cu^+. We tried $r_m = 2.0$ for Cu^+ and $r_m = 2.4$ for $C\ell^-$, $r_m = 1.8$ for Cu^+ and $r_m = 2.6$ for $C\ell^-$. Our conclusion was that, by "compressing" the $C\ell^-$ functions, and consequently "expanding" the Cu^+ functions, we were getting better convergence and lower energies. We have not tried to expand the positive ion functions beyond the value of 2.2 a.u., except at Γ_{12}, where only the 3d orbital of copper

Figs. 7 and 8 - Mixed-basis energy bands for CuCl. The superscript on Λ and Δ gives ρ^{-1} (cf. Sec. II-2). The origin is on Cl^-. Fig. 7: Slater potential. Fig. 8: Valence screening potential.

Figs. 9 and 10- Energy versus number of basis functions for some points of Figs. 7 and 8, respectively. For each curve we give the number of basis functions corresponding to the first point in the curve and the irreducible representation. Each letter corresponds to a representation in the following way:

a: Γ_1	f: X_4	k: Δ_2^2	p: Δ_2^4
b: Γ_{15}	g: X_5	ℓ: $\Delta_3^2+\Delta_4^2$	q: $\Delta_3^4+\Delta_4^4$
c: Γ_{12}	h: L_1	m: Λ_1^2	r: Λ_1^4
d: X_1	i: L_3	n: Λ_3^2	s: $\Lambda\Lambda_3^4$
e: X_3	j: Δ_1^2	o: Δ_1^4	

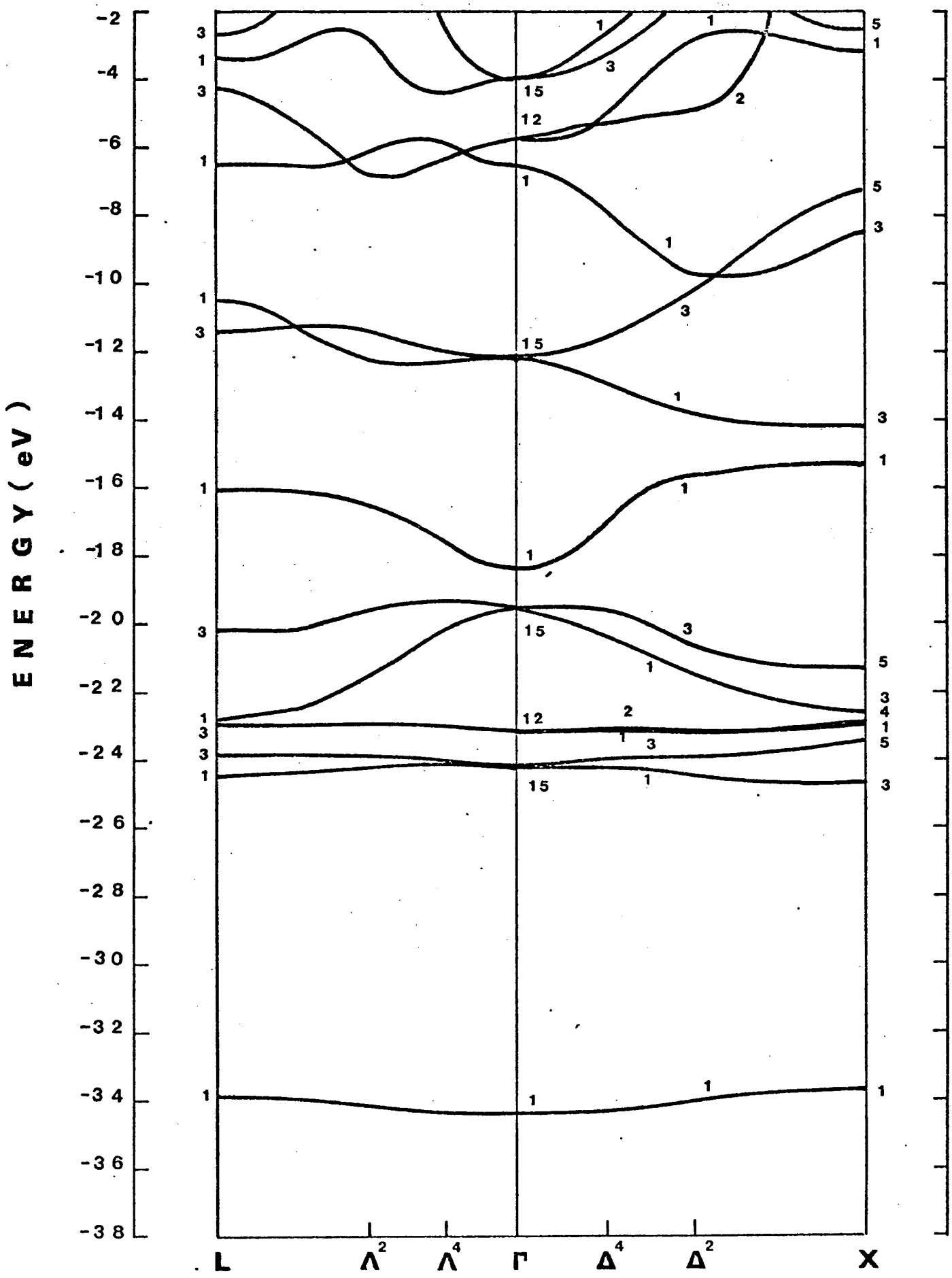

Fig. 7 - (Caption on p. 126)

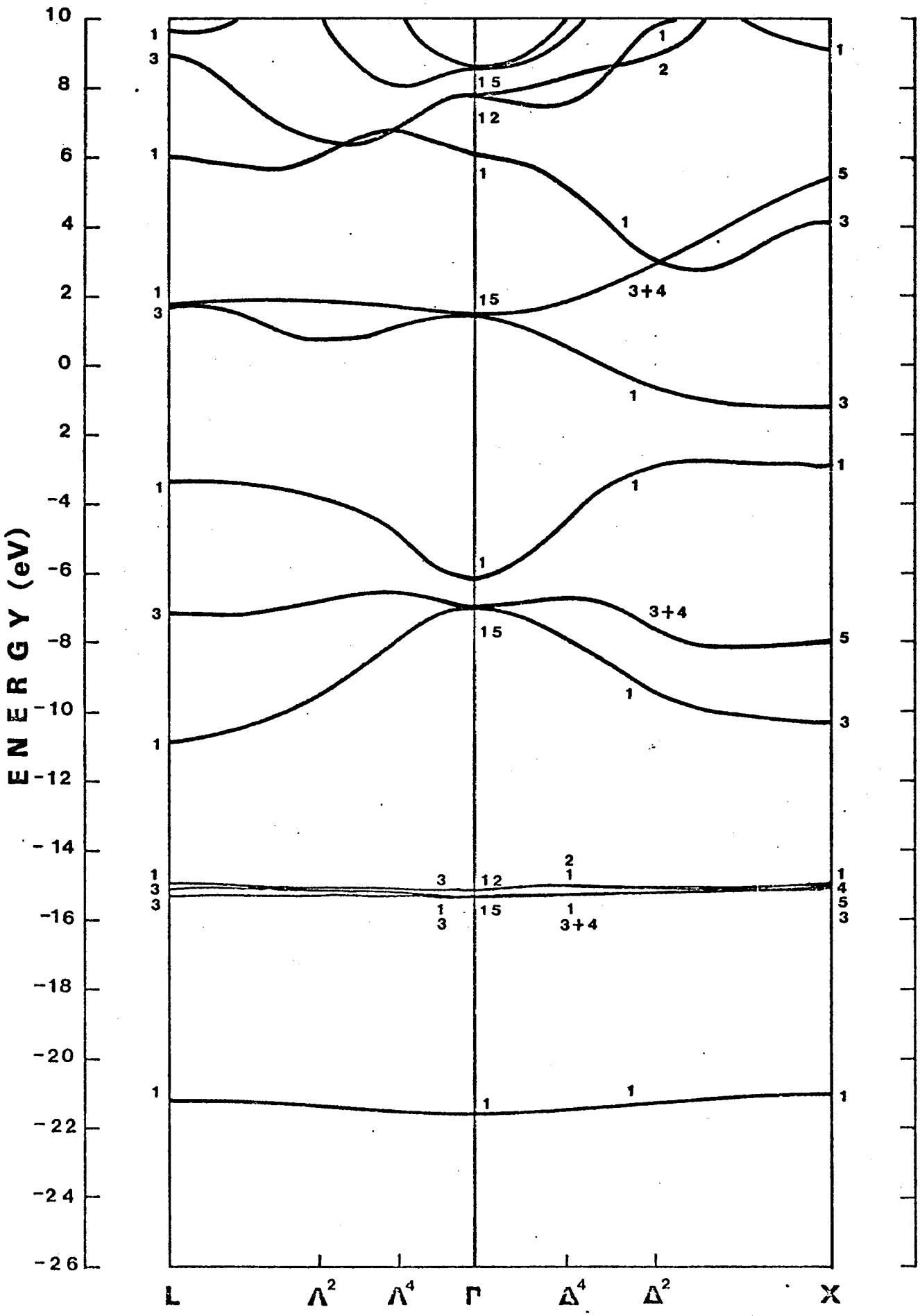

Fig. 8 - (Caption on p. 126)

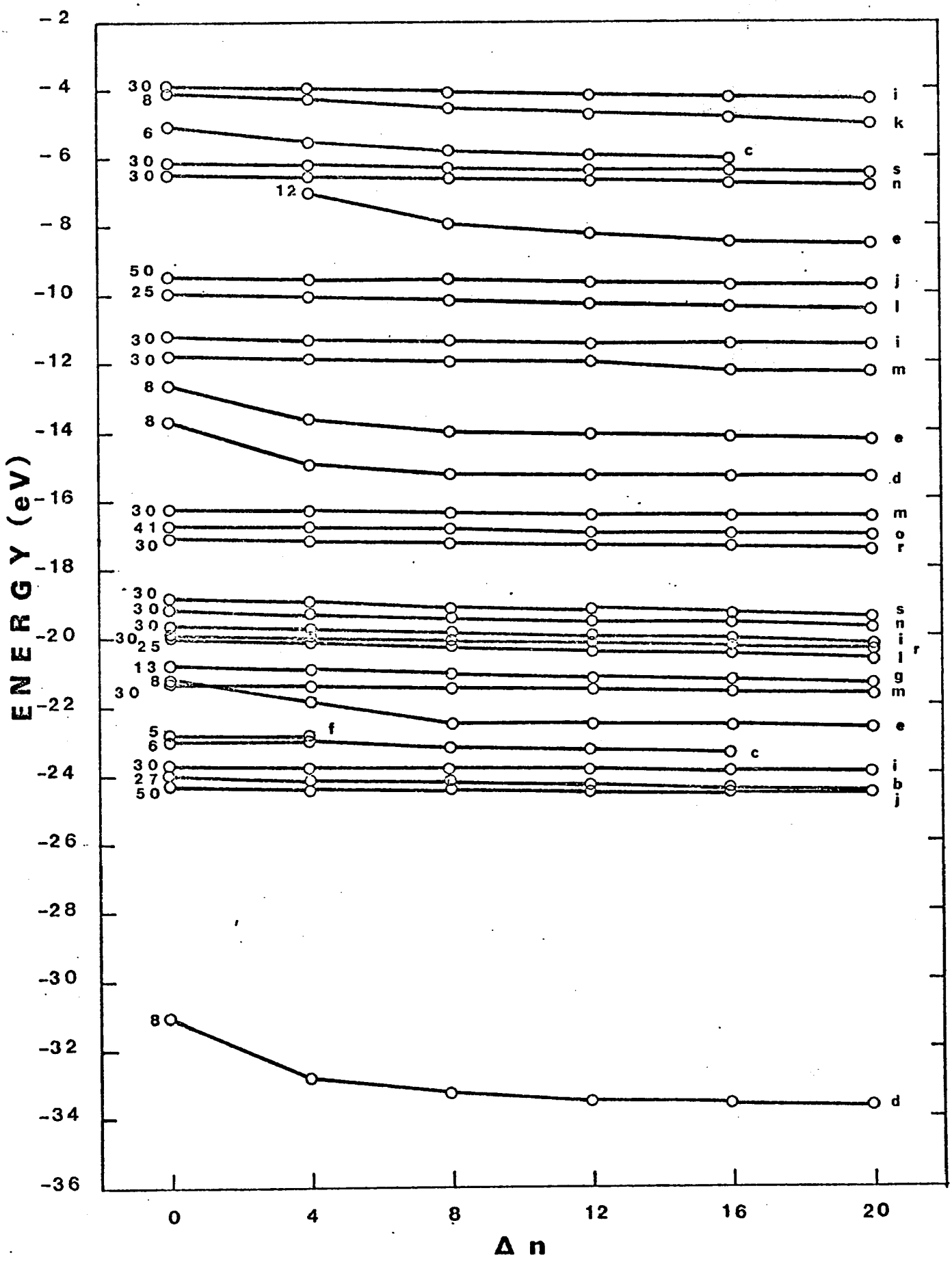

Fig. 9 - (Caption on p. 126)

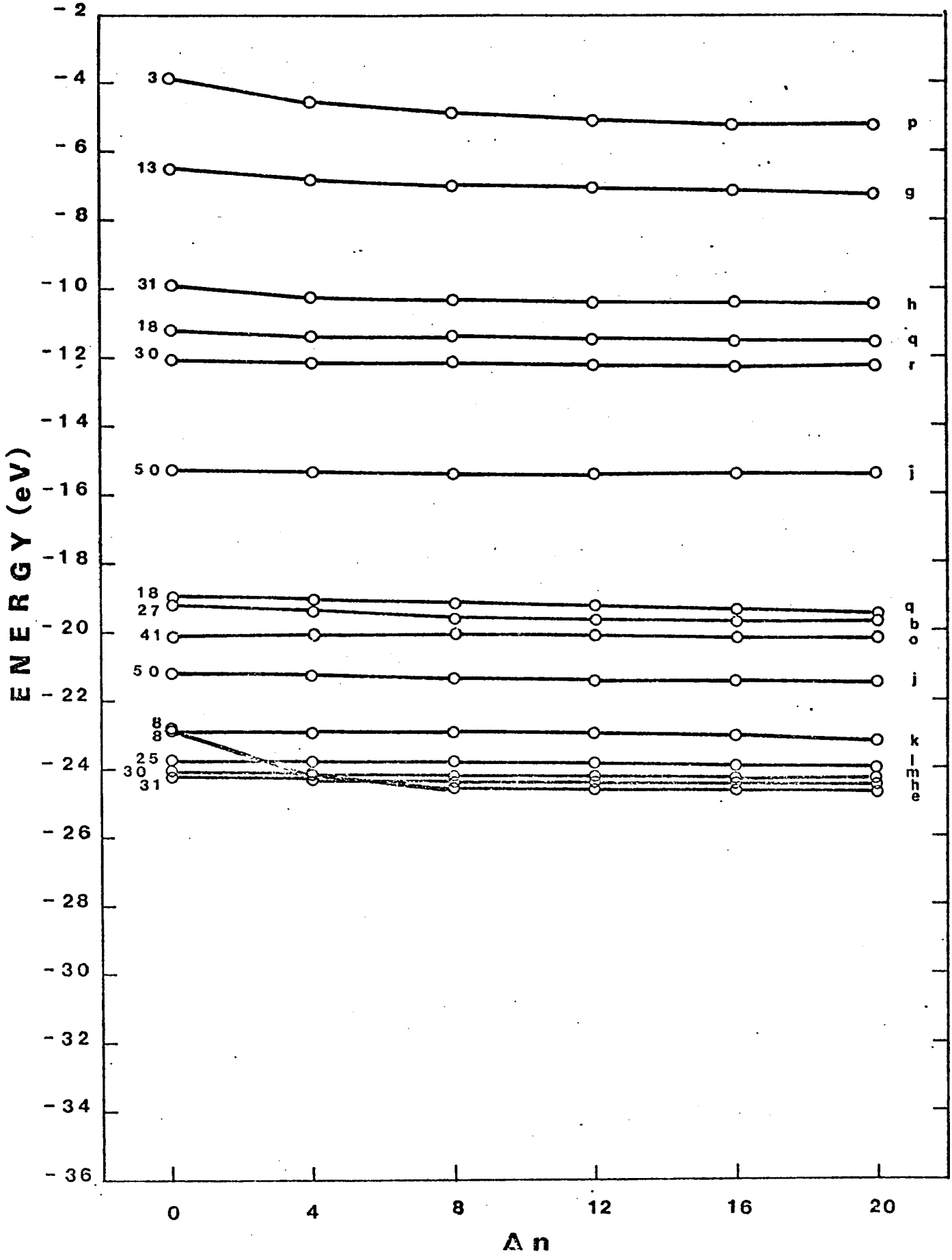
ENERGY (eV)
-2
-4
-6
-8
-10
-12
-14
-16
-18
-20
-22
-24
-26
-28
-30
-32
-34
-36
0
4
8
12
16
20
An
3
13
31
18
30
50
18
27
41
50
8
8
25
30
31
p
g
h
q
r
j
q
b
o
j
k
l
m
h
e

Fig. 9 - (cont'd).

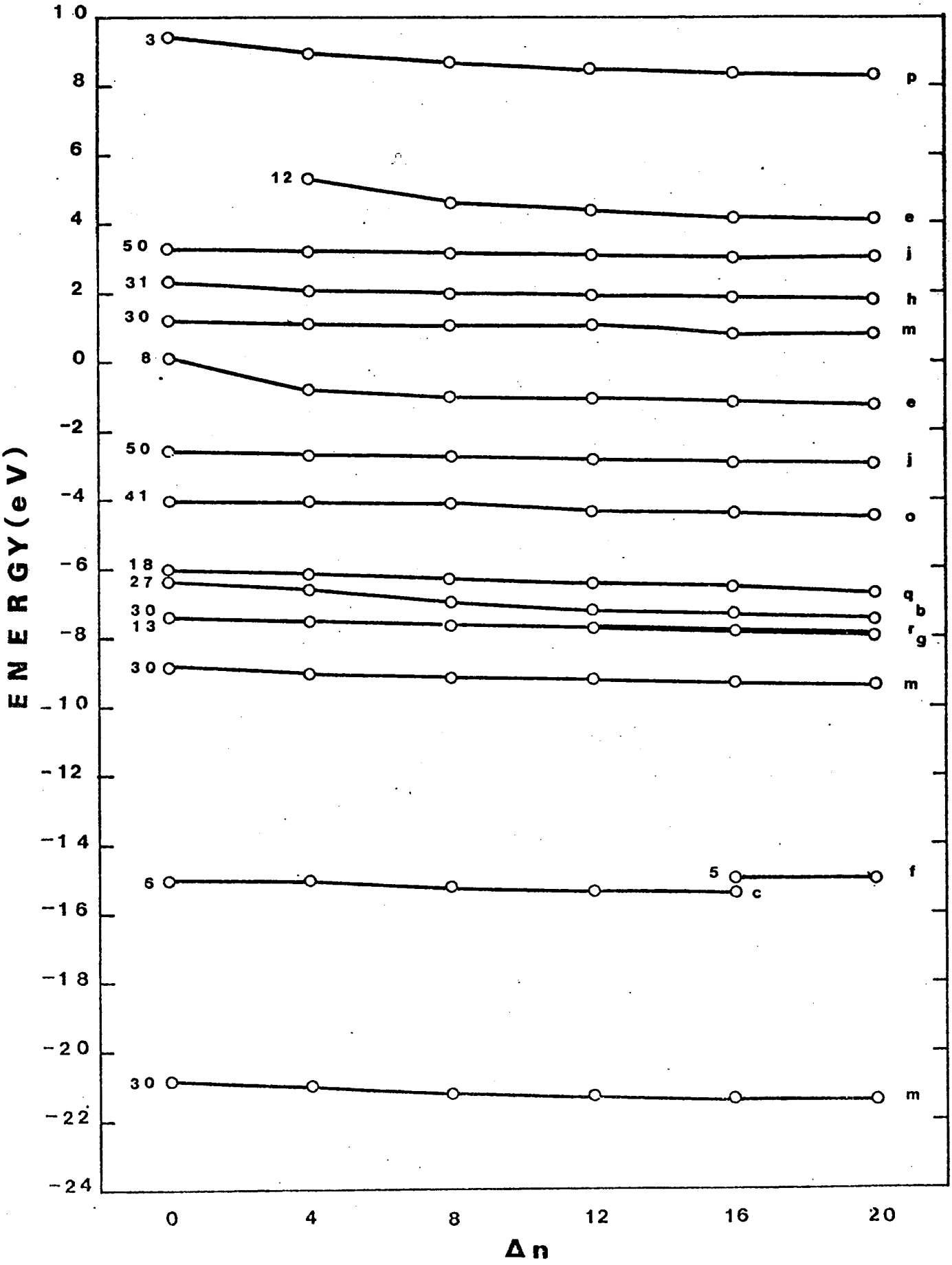

Fig. 10 - (Caption on p. 126).

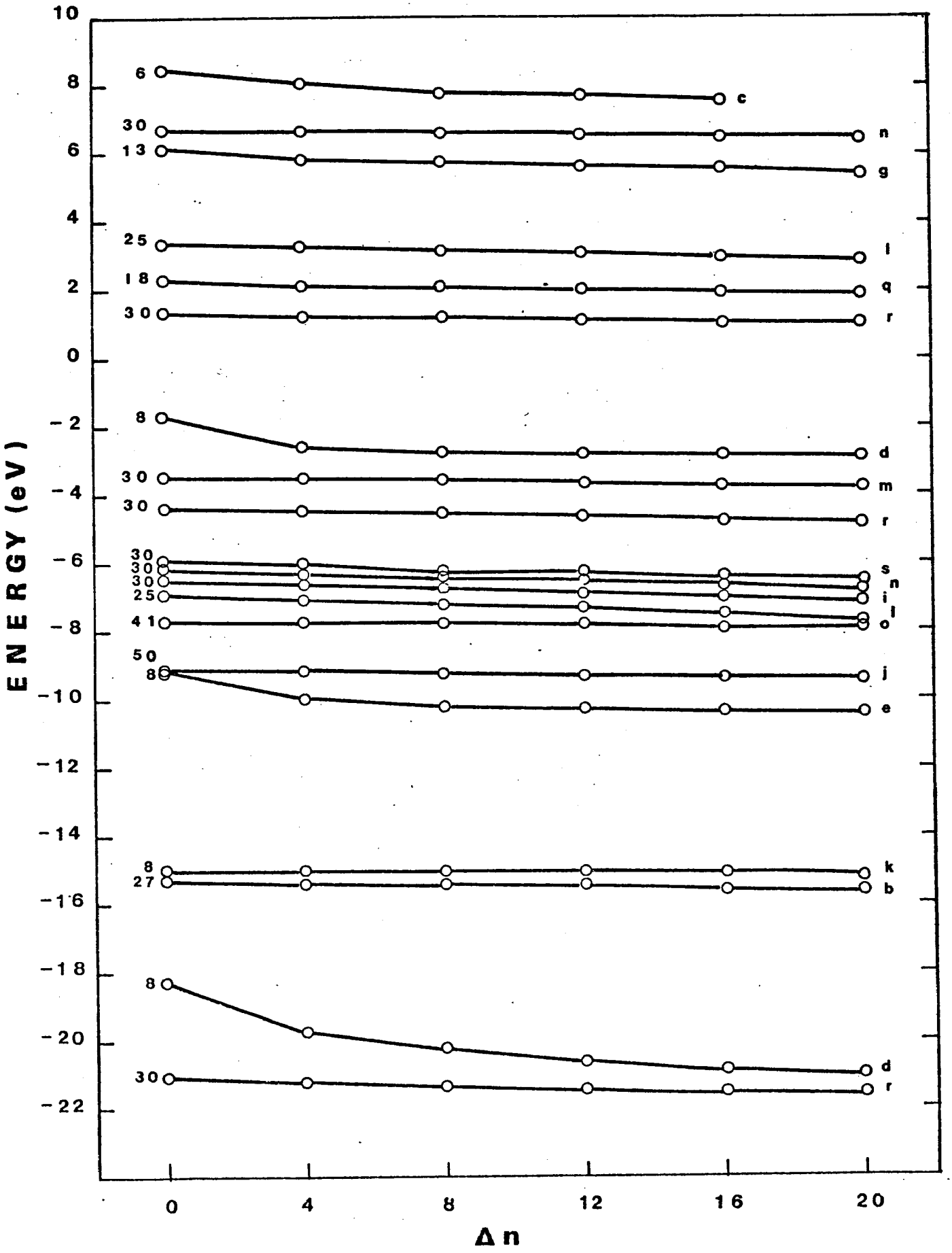
10
8
6
4
2
0
-2
-4
-6
-8
-10
-12
-14
-16
-18
-20
-22
ENERGY (eV)
0
4
8
12
16
20
Δn
6
c
30
13
n
g
25
18
30
l
q
r
8
30
30
d
m
r
30
30
30
25
41
s
n
i
l
o
50
8
j
e
8
27
k
b
8
30
d
r

Fig. 10 - (cont'd).

contributes to the basis functions. Here, by using r_m = 3.6 a.u., the valence state for the screened potential converged to -16.0 eV, with a change of less than 0.01 eV with the inclusion of the last 18 sets of plane waves. By comparison with the corresponding point in Fig. 8 (Γ_{12}:-15.4 eV), we estimate that the second valence band is converged within less than 1 eV. Special care must be used in including all S.C.P.W.'s of low kinetic energy, as mentioned in Sec. IV-4; otherwise, a study of the convergence curve is meaningless.

The bands in Figs. 7 and 8 have some similarities, apart from a shift of approximately 12 eV of the "screened" bands with respect to the "Slater" bands. This is comforting, since we should be skeptical about results that depend too strongly on the details of the potential used [cf. Fow 63]. For convenience we, using the tight-binding language, call the lowest valence band the "s-band," the middle bands the "d-bands," and the highest valence band the "p-band." The most noticeable difference between the two potentials is that with the screened potential the d-bands are narrower and lowered by about 3 eV relative to the s and p-bands. This is a consequence of the fact that the 3d state of Cu^+ is less screened than the 3s and 3p states of $C\ell^-$. As we recall from Chapter III (Sec. III-2), we have applied the screening factor only to the 3d state of Cu^+, and to the 3s and 3p states of $C\ell^-$. The screening, as it is apparent by comparing the two figures, pushes the bands up.

The energy gap between valence and conductions bands is 1.0 eV for the Slater potential, and 0.3 eV for the screened potential. However, from Figs. 9 and 10 we see that the convergence of the top valence band is slower than that of the conduction band. Therefore, we expect the energy gap to widen with the use of a better and/or larger basis set of functions.

As can be seen from Figs. 7 and 8, the shape and relative position of the conduction bands are not too sensitive to the form of the potential used. We also found that they do not vary too much by using different cutoffs for the atomic orbitals. Thus, we conclude that our conduction bands are very accurate.

We have also computed the effective mass at the bottom of the conduction bands by simply fitting a quadratic curve to the points Γ_1, Λ_1^4, and Δ_1^4. We use the equation

$$E(\underset{\sim}{k}) - E_o = \frac{m_o}{m^*} k^2 \quad (Ry), \tag{V-3}$$

where E_o is the energy at Γ_1, the bottom of the conduction bands, $m_o = \frac{1}{2}$ a.u. is the free electron mass, and m* is the effective mass. The result is

$$m^* \approx 0.23\, m_o \tag{V-4}$$

for the Slater potential, and

$$m^* \approx 0.17\, m_o \qquad \text{(V-5)}$$

for the screened potential. In both cases, the values along Λ and Δ agree within 0.003 m_o.

V-3. Comparison with Song's calculation and with experiment.

Song has done a theoretical study of the energy bands of copper chloride [Son 67, 67a]. His approach is semi-empirical, since he uses some experimental parameters in his calculation. He uses the tight-binding method for the valence bands and the orthogonalized-plane-wave (OPW) method for the conduction bands. In the OPW calculation he introduces an adjustable parameter in the exchange potential so as to fit the experimental value of the energy gap. He also uses the experimental values for the atomic energies ε_{3d} of Cu^+ and ε_{3p} of $C\ell^-$ (without Madelung potential). His treatment of the crystal potential is not too accurate, especially for the Madelung part, which we treat almost exactly.

As we mentioned at the beginning of this chapter, our calculation involves no other experimental data besides the structure of the crystal, the lattice constant, and the kind of ions constituting the crystal. However, the idea of using an adjustable parameter in the potential should be taken in consideration, since, as our mixed-basis results show, the fundamental energy gap and the overall structure of the bands depend on the potential used.

Due to the nature of the different approaches, it is hard to compare our results with those of Song's calculation. Nevertheless, we want to compare the main features. Song finds that the highest valence band is very narrow (~0.6 eV) and is formed mainly from the 3d orbital of Cu^+, with a contribution of the 3p orbital of $C\ell^-$ which is of the order of 21% at Γ_{15}. In our tight-binding calculation we obtain a very wide band (5.2 eV), probably due to an inaccurate approximation of the three-center integrals, and we find that the contribution of the 3p orbital of $C\ell^-$ is approximately 77% at Γ_{15}. However, our mixed-basis calculation, which is considerably more accurate, still yields a fairly wide band (3.5 eV for the Slater potential, and 4.3 eV for the screened potential). The wavefunction at Γ_{15}, in the top valence band, has a determinant contribution of plane waves, due to the drastic cutoff of the 3p orbital of $C\ell^-$. Comparison of the two MB bands (see Sec. V-2) leads us to conclude that the top valence band is mainly p-like, while the second band is mainly d-like.

Song finds a separation of about 3 eV between the first two valence bands. We obtain a separation of 0.01 eV for the Slater potential and 4.1 eV for the screened potential. The first value is not too meaningful since it is one order of magnitude smaller than our convergence error.

The bottom of the conduction bands is at Γ_1, in agreement with Song's speculation. The separation of the

first two conduction bands is 1.1 eV for the Slater potential, and 1.7 eV for the screened potential, as compared to the value of ~2 eV obtained by Song's qualitative interpolation.

Our spin-orbit splitting does not agree in sign with Song's and is almost doubled in value. He obtains $\Delta E(\Gamma_8-\Gamma_7)=$ = -0.08 eV; our result is 0.14 eV (see Sec. III-3).

Song also reports some experimental results related to the energy bands of CuCℓ. We will use some of these data, but refer to his work [Son 67] for a more detailed discussion and a presentation of the experimental curves.

Bonnelle has investigated the absorption and emission of soft X rays for some compounds of copper [Bon 67]. For CuCℓ, he evaluates the width of the fundamental energy gap to be approximately 3 eV, as compared to our "first-principle" results of 1.0 eV and 0.3 eV with the Slater and screened potential, respectively.

The width of the first valence band, according to Bonnelle, is approximately 1.5 eV. We obtain 3.5 eV and 4.3 eV with the two potentials. Our results also disagree with his interpretation of the first valence band as coming mainly from the 3d orbital of Cu^+, as we already mentioned.

The emission experiments give a value of approximately 3.7 eV for the separation between the first two valence bands. We obtain 4.1 eV with the screened potential and a negligible separation with the Slater potential.

The absorption measurements show a separation of about 2 eV between the first two conduction bands. Our values are 1.1 eV and 1.7 eV with the Slater and screened potential, respectively.

Considering other experimental data, the value of the spin-orbit splitting deduced from the exciton spectra is $\Delta E(\Gamma_7-\Gamma_8) = 0.072$ eV [Car 63; Nik 62]. We obtain -0.14 eV.

Song evaluates an adjusted experimental value of the effective mass of the electron as 0.28 m_o. His calculated value is 0.50 m_o. We obtain 0.23 m_o and 0.17 m_o with the two potentials, respectively (cf. Sec. V-2).

V-4. Summary and Conclusions.

We have calculated the energy bands of CuCl by using two different methods: the tight-binding method for the valence bands, and the mixed-basis method, which yields core, valence, and conduction bands. We have shown how the mixed-basis method is a rather general and rigorous method within the one-electron approximation. Since the MB matrix elements can be computed quite rigorously, the results can be directly associated with the potential used and several effective one-electron potentials can be tested. We have also compared the MB method to the OPW method and have shown how the latter is a special case of the MB method, but has some disadvantages that are not present in the MB method. In the OPW method, for instance, it is important that the

Bloch functions be exact eigenfunctions of the crystal Hamiltonian, otherwise serious errors might occur. In the MB method there is no such restriction. The two methods, however, share the advantage of allowing a rather general form of the crystal potential. In both methods it is also easy to study the convergence of the energy versus number of basis functions by adding more plane waves in the expansion of the wavefunction.

In the matrix elements involving Bloch functions we neglected the nonspherical terms in the expansion of the crystal potential in spherical harmonics. However, we showed how these terms can be included in the MB method.

We have not included any relativistic effects in our MB calculation, but we derived the matrix elements of the spin-orbit interaction involving plane waves, which are usually neglected in OPW or MB calculations.

A FORTRAN program, originally written by Kunz for calculations on alkali halides, was modified by us so that it could be applied to any ionic crystal. This program performs most of the MB calculation and allows us to study the convergence of the energy.

We solved secular equations of order up to 70 and found that the convergence was often within a few tenths of an electron-volt. It is important to examine the convergence curves when comparing the results with the experiment.

The comparison with the experimental data showed a general qualitative agreement, but the quantitative agreement was sometimes poor. However, we believe that this agreement can be improved by using a better effective potential. If not, we must conclude that either some of the data used and assumed are not correct, or the one-electron approximation does not describe the system accurately enough to give good quantitative agreement with experiment.

Appendix A

SYMMETRIZED COMBINATIONS OF BLOCH FUNCTIONS

Let

$$F(\underset{\sim}{r}) = \eta \sum_{\nu} e^{i \underset{\sim}{k}\cdot\underset{\sim}{R}_{\nu}} v(\underset{\sim}{r} - \underset{\sim}{R}_{\nu} - \delta\underset{\sim}{d}) \tag{A-1}$$

be a Bloch sum of atomic-like orbitals centered at $\underset{\sim}{R}_{\nu} + \delta\underset{\sim}{d}$ (cf. Eq. II-7).* For $F(\underset{\sim}{r})$ to belong to the γ^{th} row of the (unitary) irreducible representation Γ_{α} of the group of $\underset{\sim}{k}$, it must be

$$P^{\alpha}_{\gamma\gamma} F(\underset{\sim}{r}) = F(\underset{\sim}{r}), \tag{A-2}$$

where $P^{\alpha}_{\gamma\gamma}$ is the projection operator for the γth row of Γ_{α} (cf. Sec. II-3). Explicitly,

$$P^{\alpha}_{\gamma\gamma} = \frac{d_{\alpha}}{g} \sum_{R} \Gamma^{\alpha}_{\gamma\gamma}(R)^{*} R \ . \tag{A-3}$$

Operating on $F(\underset{\sim}{r})$ with the operator R yields (cf. Eq. II-3)

$$\begin{aligned} R F(\underset{\sim}{r}) &= \eta \sum_{\nu} e^{i \underset{\sim}{k}\cdot\underset{\sim}{R}_{\nu}} v(\alpha^{-1}\underset{\sim}{r} - \underset{\sim}{R}_{\nu} - \delta\underset{\sim}{d}) \\ &= \eta \sum_{\nu} e^{i\alpha\underset{\sim}{k}\cdot\alpha\underset{\sim}{R}_{\nu}} v(\alpha^{-1}\underset{\sim}{r} - \underset{\sim}{R}_{\nu} - \delta\underset{\sim}{d}) \ . \end{aligned} \tag{A-4}$$

*In Eq. (A-1) we have eliminated those superscripts and subscripts that are not relevant to the following discussion.

In the last step of Eq. (A-4) we made use of Eq. (II-14). If we now define

$$\underset{\sim}{R}_{\nu'} = \alpha \underset{\sim}{R}_{\nu} \qquad \text{and} \qquad \underset{\sim}{d}' = \alpha \underset{\sim}{d} \ , \tag{A-5}$$

and recall that (cf. Sec. I-2)

$$\alpha \underset{\sim}{k} = \underset{\sim}{k} + \underset{\sim}{h}_{\mu} \ , \tag{A-6}$$

where $\underset{\sim}{h}_{\mu}$ is a reciprocal lattice vector, Eq. (A-4) can be written

$$R\,F(\underset{\sim}{r}) = \eta \sum_{\nu'} e^{i \underset{\sim}{k} \cdot \underset{\sim}{R}_{\nu'}} \, v\left[\alpha^{-1}(\underset{\sim}{r} - \underset{\sim}{R}_{\nu'} - \delta \underset{\sim}{d}')\right] . \tag{A-7}$$

In Eq. (A-7) we used the fact that $\exp(i\underset{\sim}{h}_{\mu} \cdot \underset{\sim}{R}_{\nu'}) = 1$, since $\underset{\sim}{R}_{\nu'}$ is a lattice translation vector (cf. Eq. A-5). We now notice that to each $\underset{\sim}{R}_{\nu'}$ there corresponds another lattice translation vector $\underset{\sim}{R}_{\rho}$, such that

$$\underset{\sim}{R}_{\nu'} + \delta \underset{\sim}{d}' = \underset{\sim}{R}_{\rho} + \delta \underset{\sim}{d} \ . \tag{A-8}$$

By substituting Eq. (A-8) in Eq. (A-7), we obtain

$$\begin{aligned} R\,F(\underset{\sim}{r}) &= \eta \sum_{\rho} e^{i \underset{\sim}{k} \cdot \underset{\sim}{R}_{\rho}} \, e^{i \underset{\sim}{k} \cdot \delta (\underset{\sim}{d} - \underset{\sim}{d}')} \, v\left[\alpha^{-1}(\underset{\sim}{r} - \underset{\sim}{R}_{\rho} - \delta \underset{\sim}{d})\right] \\ &= \eta \sum_{\nu} e^{i \underset{\sim}{k} \cdot \underset{\sim}{R}_{\nu}} \, e^{i \underset{\sim}{k} \cdot \delta (\underset{\sim}{d} - \alpha \underset{\sim}{d})} \, v\left[\alpha^{-1}(\underset{\sim}{r} - \underset{\sim}{R}_{\nu} - \delta \underset{\sim}{d})\right] . \end{aligned} \tag{A-9}$$

With the use of Eq. (A-9), application of the projection operator (A-3) to $F(\underset{\sim}{r})$ now yields

$$P^{\alpha}_{\gamma\gamma} F(\underset{\sim}{r}) = \eta \sum_{\nu} e^{i \underset{\sim}{k} \cdot \underset{\sim}{R}_{\nu}} \frac{d_{\alpha}}{g} \sum_{R} \Gamma^{\alpha}_{\gamma\gamma}(R)^{*} e^{i \underset{\sim}{k} \cdot \delta (\underset{\sim}{d} - \alpha \underset{\sim}{d})} \, v\left[\alpha^{-1}(\underset{\sim}{r} - \underset{\sim}{R}_{\nu} - \delta \underset{\sim}{d})\right] \tag{A-10}$$

By comparing Eq. (A-10) with Eq. (A-1), we see that, for Eq. (A-2) to be satisfied, it must be

$$v(\underset{\sim}{r}) = \frac{d_\alpha}{g} \sum_R \Gamma^\alpha_{\gamma\gamma}(R)^* e^{i\underset{\sim}{k}\cdot\delta(\underset{\sim}{d}-\alpha\underset{\sim}{d})} R v(\underset{\sim}{r}) \equiv P^\beta_{\gamma\gamma} v(\underset{\sim}{r}) . \qquad \text{(A-11)}$$

That is, for $F(\underset{\sim}{r})$ to belong to the γth row of the representation Γ_α, $v(\underset{\sim}{r})$ must belong to the γth row of the representation Γ_β, where

$$\Gamma_\beta(R) = \Gamma_\alpha(R)\, e^{-i\underset{\sim}{k}\cdot\delta(\underset{\sim}{d}-\alpha\underset{\sim}{d})} . \qquad \text{(A-12)}$$

It is easy to show that Γ_β is an irreducible representation of the group of operators R, if Γ_α is. From Eq. (A-8) we see that $\delta(\underset{\sim}{d} - \alpha\underset{\sim}{d})$ is a lattice translation; thus, for any two rotations α_n and α_m in the group,

$$e^{-i\underset{\sim}{k}\cdot\delta(\underset{\sim}{d}-\alpha_m\underset{\sim}{d})} = e^{-i\underset{\sim}{k}\cdot\delta(\alpha_n\underset{\sim}{d}-\alpha_n\alpha_m\underset{\sim}{d})} . \qquad \text{(A-13)}$$

Then, the product of the two matrices of Γ_β corresponding to the operators R_n and R_m is

$$\begin{aligned}\Gamma_\beta(R_n)\Gamma_\beta(R_m) &= \Gamma_\alpha(R_n)\, e^{-i\underset{\sim}{k}\cdot\delta(\underset{\sim}{d}-\alpha_n\underset{\sim}{d})}\Gamma_\alpha(R_m)\, e^{-i\underset{\sim}{k}\cdot\delta(\underset{\sim}{d}-\alpha_m\underset{\sim}{d})} \\ &= \Gamma_\alpha(R_n)\Gamma_\alpha(R_m)\, e^{-i\underset{\sim}{k}\cdot\delta(\underset{\sim}{d}-\alpha_n\underset{\sim}{d})}\, e^{-i\underset{\sim}{k}\cdot\delta(\alpha_n\underset{\sim}{d}-\alpha_n\alpha_m\underset{\sim}{d})} \qquad \text{(A-14)} \\ &= \Gamma_\alpha(R_nR_m)\, e^{-i\underset{\sim}{k}\cdot\delta(\underset{\sim}{d}-\alpha_n\alpha_m\underset{\sim}{d})} = \Gamma_\beta(R_nR_m) .\end{aligned}$$

Eq. (A-14) proves that the matrices $\Gamma_\beta(R)$ form a representation of the group of $\underset{\sim}{k}$. That this representation is irreducible is obvious from Eq. (A-12), since we assumed that Γ_α is irreducible.

The result in Eq. (A-12), although independently derived, agrees with a result derived some time ago by Bell [Bel 54].

Appendix B

MADELUNG POTENTIAL IN THE SPHERICAL APPROXIMATION

In this Appendix we assume that the origin is on a positive ion. The γth shell of nearest neighbors contains n_γ ions of charge $(-1)^\gamma e z_a$, where z_a is the ionicity of the positive ion. In the spherical approximation, these point charges can be replaced by a uniform distribution of charges over the surface of a sphere of radius r_γ, the radius of the shell. Thus, inside the first shell the Madelung potential is constant and equals the Madelung energy E_M, where

$$E_M = \frac{2 z_a \alpha_a}{a} \quad (Ry) , \tag{B-1}$$

and α_a is the Madelung constant referred to the lattice parameter a [cf. Tos 64]. The Madelung constant depends only on the crystal structure. For example, for the zinc blende structure $\alpha_a = 3.78293$ [loc. cit.].

As is well known from electrostatics, if we have a distribution of charges which is spherically symmetric about the origin, the potential energy at a distance r from the origin is the sum of two contributions: the contribution of the charges inside the sphere of radius r, which is the same as if all these charges were concentrated at the origin; and

the contribution of the charges outside the sphere, which is constant inside the sphere. Thus, the Madelung energy (Eq. B-1) must be equal to

$$E_M = -2z_a \sum_i^{\infty} (-1)^i \frac{n_i}{r_i} = -\frac{2z_a}{a} \sum_i^{\infty} (-1)^i \frac{n_i}{x_i} , \qquad \text{(B-2)}$$

where the dimensionless quantity x is defined as x = r/a. In Eq. (B-2) we have assumed an infinite crystal.

In the region between the γth and γ+1th shells, the potential can be obtained by subtracting from E_M the contribution at the origin due to the first γ shells, and adding their contribution at r ($r_\gamma \leq r \leq r_{\gamma+1}$). Thus, if we denote by $M_\gamma(r)$ the Madelung potential inside this region, we have

$$M_\gamma(r) = E_M + \frac{2z_a}{a}\left[\sum_i^{\gamma} (-1)^i \frac{n_i}{x_i} - \frac{1}{x}\sum_i^{\gamma} (-1)^i n_i\right]. \qquad \text{(B-3)}$$

By using Eq. (B-1), Eq. (B-3) can be written

$$M_\gamma(r) = \frac{2z_a}{a}\left[\alpha_a + \sum_i^{\gamma} (-1)^i \frac{n_i}{x_i} - \frac{1}{x}\sum_i^{\gamma} (-1)^i n_i\right] . \qquad \text{(B-4)}$$

The quantity in brackets in Eq. (B-4) depends only on the crystal structure and it is shown in Fig. 11 for the zinc blende structure. The quantities n_i and x_i are given in Table 1.

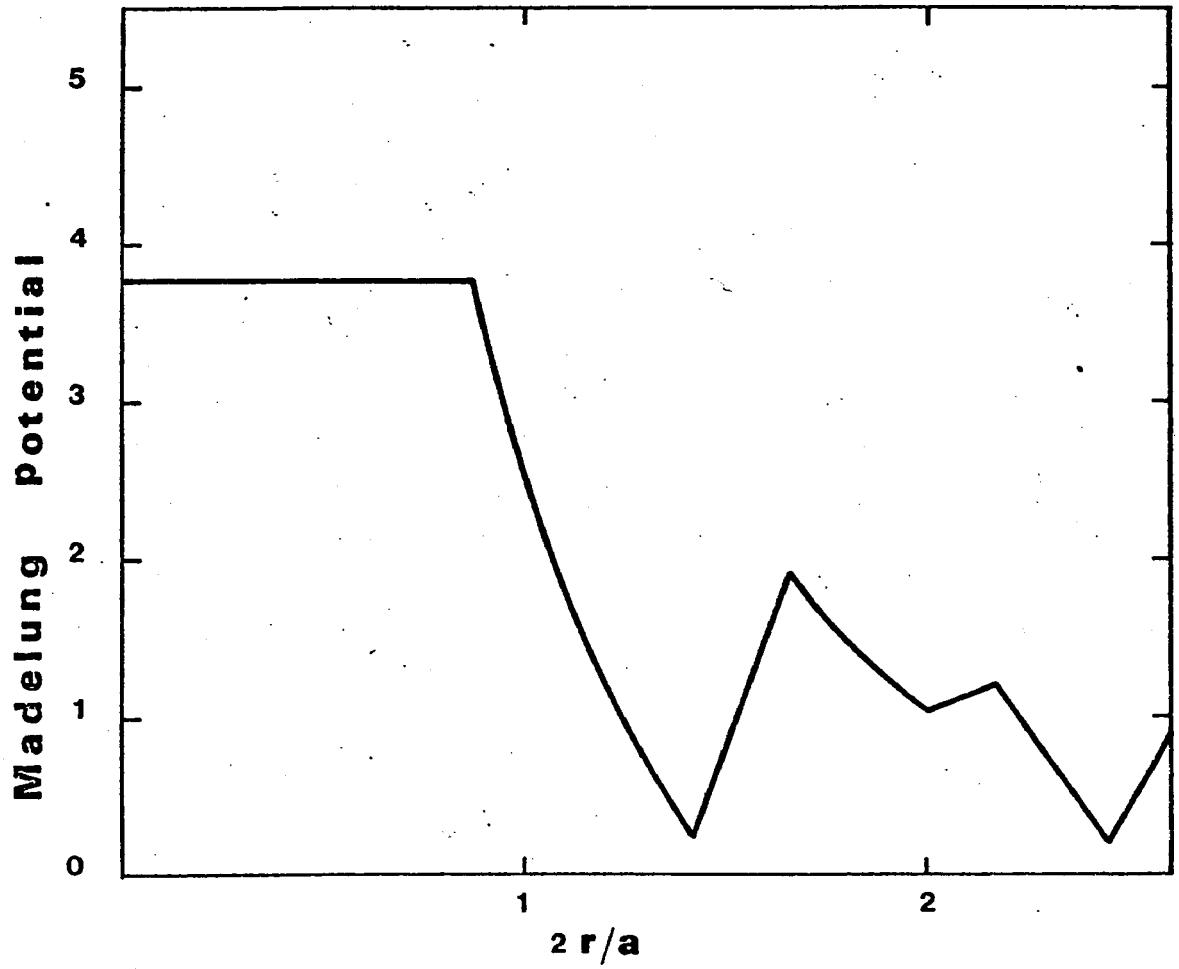

Fig. 11 - Spherical Madelung potential for the zinc blende structure. a is the lattice constant. The quantities on the axes are dimensionless.

Appendix C

TIGHT-BINDING QUANTITIES h^{σ}_{np}

The quantities h^{σ}_{np}, defined in Eq. (III-9), reduce to the form (III-28) if we restrict the summation to those two-center integrals involving first or second nearest neighbors (cf. Sec. III-2). By using Tables 19 and 20, these quantities can be expressed in terms of a few parameters of the form $S_{\alpha\beta\mu}$, defined in Eq. (III-33). We list here the quantities h^{σ}_{np} for those representations used in the tight-binding calculation. For each representation we also give the basis functions belonging to a particular row of that representation (cf. Table 8). The origin of the coordinates is taken at Cu^{+}.

$$\Gamma: \quad \underset{\sim}{k} = 0$$

Γ_1 : u_s

$$h_{ss} = 12\, S_{ss\sigma}$$

Γ_{15} : u_x, u_{yz}

$$h_{pp} = 4\,(S_{pp\sigma} + 2\,S_{pp\pi})$$

$$h_{dd} = 3\,S_{dd\sigma} + 4\,S_{dd\pi} + S\,S_{dd\delta}$$

$$h_{pd} = -\frac{4}{3}\left(S_{pd\sigma} - \frac{2}{\sqrt{3}}\,S_{pd\pi}\right)$$

Γ_{12} : $u_{x^2-y^2}$

$$h_{d'd'} = \frac{3}{2} S_{dd\sigma} + 6 S_{dd\pi} + \frac{9}{2} S_{dd\delta}$$

$$X : \quad \underset{\sim}{k} = \frac{2\pi}{a} (100)$$

X_1 : u_x , $u_{3x^2-r^2}$

$$h_{pp} = -4 S_{pp\sigma}$$

$$h_{d'd'} = \frac{1}{2} S_{dd\sigma} - 6 S_{dd\pi} + \frac{3}{2} S_{dd\delta}$$

$$h_{pd'} = -\frac{8}{3} S_{pd\pi}$$

X_2 : $u_{y^2-z^2}$

$$h_{d'd'} = -\frac{3}{2} S_{dd\sigma} + 2 S_{dd\pi} - \frac{9}{2} S_{dd\delta}$$

X_3 : u_s , u_{yz}

$$h_{ss} = -4 S_{ss\sigma}$$

$$h_{dd} = 3 S_{dd\sigma} - 4 S_{dd\pi} - 3 S_{dd\delta}$$

$$h_{sd} = \frac{4}{\sqrt{3}} S_{sd\sigma}$$

X_5 : $\frac{1}{\sqrt{2}} (u_y + u_z)$, $\frac{1}{\sqrt{2}} (u_{zx} + u_{xy})$

$$h_{pp} = -4 S_{pp\pi}$$

$$h_{dd} = -3 S_{dd\sigma} - S_{dd\delta}$$

$$h_{pd} = -\frac{4}{3} (S_{pd\sigma} + \frac{1}{\sqrt{3}} S_{pd\pi})$$

$$\Delta: \quad \underline{k} = \rho \frac{2\pi}{a}(100), \qquad 0 < \rho < 1$$

Δ_1: u_s, u_x, u_{yz}, $u_{3x^2-r^2}$

$$h_{ss} = 4 S_{ss\sigma} + 8 S_{ss\sigma} \cos(\pi\rho)$$

$$h_{pp} = 4 S_{pp\pi} + 4(S_{pp\sigma} + S_{pp\pi}) \cos(\pi\rho)$$

$$h_{dd} = 3 S_{dd\sigma} + S_{dd\delta} + 4(S_{dd\pi} + S_{dd\delta}) \cos(\pi\rho)$$

$$h_{d'd'} = S_{dd\sigma} + 3 S_{dd\delta} + \frac{1}{2}(S_{dd\sigma} + 12 S_{dd\pi} + 3 S_{dd\delta}) \cos(\pi\rho)$$

$$h_{sp} = 4\sqrt{2}\, i\, S_{sp\sigma} \sin(\pi\rho)$$

$$h_{sd} = \frac{2}{\sqrt{3}} S_{sd\sigma}(1 - e^{i\pi\rho})$$

$$h_{sd'} = 0$$

$$h_{pd} = -\frac{2}{3}\left(S_{pd\sigma} - \frac{2}{\sqrt{3}} S_{pd\pi}\right)(1 + e^{i\pi\rho})$$

$$h_{pd'} = -\frac{4}{3} S_{pd\pi}(1 - e^{i\pi\rho})$$

$$h_{dd'} = 0$$

Δ_2: $u_{y^2-z^2}$

$$h_{d'd'} = 4 S_{dd\pi} + \frac{1}{2}(3 S_{dd\sigma} + 4 S_{dd\pi} + 9 S_{dd\delta}) \cos(\pi\rho)$$

Δ_3: $\frac{1}{\sqrt{2}}(u_y - u_z)$, $\frac{1}{\sqrt{2}}(u_{zx} - u_{xy})$

$$h_{pp} = 2(S_{pp\sigma} + S_{pp\pi}) + 2(S_{pp\sigma} + 3 S_{pp\pi}) \cos(\pi\rho)$$

$$h_{dd} = 2(S_{dd\pi} + S_{dd\delta}) + (3 S_{dd\sigma} + 2 S_{dd\pi} + 3 S_{dd\delta}) \cos(\pi\rho)$$

$$h_{pd} = \frac{2}{\sqrt{3}} S_{pd\pi} - \frac{2}{3}\left(2 S_{pd\sigma} - \frac{1}{\sqrt{3}} S_{pd\pi}\right) e^{i\pi\rho}$$

Δ_4: $\frac{1}{\sqrt{2}}(u_y + u_z)$, $\frac{1}{\sqrt{2}}(u_{zx} + u_{xy})$

$$h_{pp}, h_{dd} = \text{same as for } \Delta_3$$

$$h_{pd} = -\frac{2}{3}\left(2 S_{pd\sigma} - \frac{1}{\sqrt{3}} S_{pd\pi}\right) + \frac{2}{\sqrt{3}} S_{pd\pi} e^{i\pi\rho}$$

$L, \Lambda: \ \rho \frac{2\pi}{a}\left(\frac{1}{2}\frac{1}{2}\frac{1}{2}\right); \quad L: \rho = 1, \quad \Lambda: 0 < \rho < 1$

$\Lambda_1: \ u_s, \ \frac{1}{\sqrt{3}}(u_x + u_y + u_z), \ \frac{1}{\sqrt{3}}(u_{xy} + u_{yz} + u_{zx})$

$$h_{ss} = 6\, S_{ss\sigma}\left[1 + \cos(\pi\rho)\right]$$

$$h_{pp} = 6\, S_{pp\pi} + 2\,(2\, S_{pp\sigma} + S_{pp\pi})\cos(\pi\rho)$$

$$h_{dd} = \frac{3}{2}(S_{dd\sigma} + 3\, S_{dd\delta}) + \frac{1}{2}(3\, S_{dd\sigma} + 8\, S_{dd\pi} + S_{dd\delta})\cos(\pi\rho)$$

$$h_{sp} = -2\sqrt{6}\, i\, S_{sp\sigma}\sin(\pi\rho)$$

$$h_{sd} = 2i\, S_{sd\sigma}\sin\left(\frac{\pi}{2}\rho\right) e^{i\pi\rho}$$

$$h_{pd} = -S_{pd\sigma}\, e^{i\frac{3\pi}{2}\rho} - \frac{1}{3}\left(S_{pd\sigma} - \frac{8}{\sqrt{3}}\, S_{pd\pi}\right) e^{i\frac{\pi}{2}\rho}$$

$\Lambda_3: \ \frac{1}{\sqrt{2}}(u_x - u_y), \ \frac{1}{\sqrt{2}}(u_{yz} - u_{zx}), \ u_{x^2-y^2}$

$$h_{pp} = 3\,(S_{pp\sigma} + S_{pp\pi}) + (S_{pp\sigma} + 5\, S_{pp\pi})\cos(\pi\rho)$$

$$h_{dd} = \frac{1}{2}(3\, S_{dd\sigma} + 6\, S_{dd\pi} + 3\, S_{dd\delta}) + \frac{1}{2}(3\, S_{dd\sigma} + 2\, S_{dd\pi} + 7\, S_{dd\delta})\cos(\pi\rho)$$

$$h_{d'd'} = \frac{3}{4}(S_{dd\sigma} + 4\, S_{dd\pi} + 3\, S_{dd\delta})\left[1 + \cos(\pi\rho)\right]$$

$$h_{pd} = \frac{1}{\sqrt{3}}\, S_{pd\pi}\, e^{i\frac{3\pi}{2}\rho} - \frac{1}{3}\left(4\, S_{pd\sigma} - \frac{5}{\sqrt{3}}\, S_{pd\pi}\right) e^{i\frac{\pi}{2}\rho}$$

$$h_{pd'} = -\frac{2}{\sqrt{6}}\, S_{pd\pi}\left(e^{i\frac{3\pi}{2}\rho} - e^{i\frac{\pi}{2}\rho}\right)$$

$$h_{dd'} = \frac{3}{2\sqrt{2}}(S_{dd\sigma} - S_{dd\delta})\left[1 - \cos(\pi\rho)\right]$$

Appendix D

MIXED-BASIS MATRIX ELEMENTS

The basis functions for the mixed-basis expansion are, as in Eqs. (IV-30) and (IV-31),

$$F_n(\underset{\sim}{r}) = i^{\ell} N^{-\frac{1}{2}} \sum_{\nu} e^{i \underset{\sim}{k} \cdot \underset{\sim}{R}_{\nu}} v_n(\underset{\sim}{r} - \underset{\sim}{R}_{\nu} - \delta_n \underset{\sim}{d}), \tag{D-1}$$

$$S_m(\underset{\sim}{r}) = (N \Omega \Theta_m)^{-\frac{1}{2}} \sum_{R} \Gamma^{\alpha}_{\gamma\gamma}(R)\, e^{i \alpha^{-1} (\underset{\sim}{k} + \underset{\sim}{h}_{\mu}) \cdot \underset{\sim}{r}}, \tag{D-2}$$

where the F's are Bloch functions and the S's are combinations of plane waves. As stated at the beginning of Sec. IV-3, we have to calculate three types of matrix elements (see Eqs. IV-27, 28, 29). We derive them here.

Type 1: $\langle F_n | Op | F_{n'} \rangle$. According to Sec. IV-2, we need only to calculate the following integral (cf. Eq. IV-24)

$$\varepsilon_n^{CO} = \int_0^{\infty} P_n^{CO}(r) \left\{ -\frac{d^2}{dr^2} + \frac{\ell(\ell+1)}{r^2} + V_2(r) + M_2(r) \right\} P_n^{CO}(r)\, dr, \tag{D-3}$$

where the orthonormal cutoff function $P_n^{CO}(r)$ is defined in Eq. (IV-15) as

$$P_n^{CO}(r) = (O_n^{CO})^{-\frac{1}{2}} \left[S_n^{CO}(r) - \sum_{n'} \omega_n^{n'} P_{n'}(r) \right]. \tag{D-4}$$

The angular momentum quantum number ℓ is the same for all functions appearing in Eq. (D-4). The unorthogonalized cut-off function $S_n^{CO}(r)$ is defined in Eq. (IV-12) as

$$\begin{aligned} S_n^{CO}(r) &\equiv P_n(r) && \text{for} \quad 0 \le r \le r_c \,, \\ S_n^{CO}(r) &\equiv b\left\{1+\cos\left[q(r-r_0)\right]\right\} && \text{for} \quad r_c \le r \le r_m \,. \end{aligned} \tag{D-5}$$

Eq. (D-3), by using Eq. (D-4) for $P_n^{CO}(r)$, becomes

$$\varepsilon_n^{CO} = (O_n^{CO})^{-1}\left\{\int_0^\infty S_n^{CO}(r)\left[-\frac{d^2}{dr^2}+\frac{\ell(\ell+1)}{r^2}+V_\ell(r)+M_\ell(r)\right]S_n^{CO}(r)\,dr - \sum_{n'}\varepsilon_{n'}^{a}\,(\omega_n^{n'})^2\right\}, \tag{D-6}$$

where use was made of the orthonormality of the core functions $P_{n'}(r)$. The $\varepsilon_{n'}^{a}$'s are the core energy eigenvalues and $\omega_n^{n'}$ is defined in Eq. (IV-16). By using Eq. (D-5), the integral in Eq. (D-6) yields

$$\begin{aligned} &\int_0^\infty S_n^{CO}(r)\left[-\frac{d^2}{dr^2}+\frac{\ell(\ell+1)}{r^2}+V_\ell(r)+M_\ell(r)\right]S_n^{CO}(r)\,dr \\ &= \varepsilon_n^2\int_0^{r_c}\left[S_n^{CO}(r)\right]^2 dr + (bq)^2\int_{r_c}^{r_m}\left[1+\cos q(r-r_0)\right]\cos\left[q(r-r_0)\right]dr \\ &\quad + \int_{r_c}^{r_m}\left[S_n^{CO}(r)\right]^2\left\{\frac{\ell(\ell+1)}{r^2}+V_\ell(r)+M_\ell(r)\right\}dr \,. \end{aligned} \tag{D-7}$$

Thus, we obtain (cf. Eqs. IV-25 and 35)

$$\begin{aligned} \varepsilon_n^{CO} = (O_n^{CO})^{-1}\Big\{&\varepsilon_n^2\int_0^{r_c}\left[S_n^{CO}(r)\right]^2 dr + (bq)^2\int_{r_c}^{r_m}\left[1+\cos q(r-r_0)\right]\cos\left[q(r-r_0)\right]dr \\ &+ \int_{r_c}^{r_m}\left[S_n^{CO}(r)\right]^2\left[\frac{\ell(\ell+1)}{r^2}+V_\ell(r)+M_\ell(r)\right]dr - \sum_{n'}\varepsilon_{n'}^{a}\,(\omega_n^{n'})^2\Big\}. \end{aligned} \tag{D-8}$$

Type 2: $\langle F_n|\mathrm{Op}|S_m\rangle$. For this type of matrix element we will make use of the following expansion [cf. Mes 68, App. B]

$$e^{i\underset{\sim}{K}\cdot\underset{\sim}{r}} = 4\pi \sum_{\ell'}^{\infty} \sum_{-\ell'}^{+\ell'} i^{\ell'} j_{\ell'}(Kr)\, Y_{\ell'}^{m'*}(\theta,\phi)_{\underset{\sim}{K}}\, Y_{\ell'}^{m'}(\theta,\phi)_{\underset{\sim}{r}} , \qquad \text{(D-9)}$$

where $j_{\ell'}(\ell)$ is a spherical Bessel function (see Eq. IV-39). The overlap matrix element, introducing the abbreviation $\underset{\sim}{K}_R = \alpha^{-1}(\underset{\sim}{k}+\underset{\sim}{h}_\mu)$, is

$$\begin{aligned}
\langle F_n | S_m\rangle &= (-i)^{\ell} N^{-1} (\Omega\Theta_m)^{-\frac{1}{2}} \sum_R \Gamma^{\alpha}_{\gamma\gamma}(R) \sum_\nu e^{-i\underset{\sim}{k}\cdot\underset{\sim}{R}_\nu} \langle v_m(\underset{\sim}{r}-\underset{\sim}{R}_\nu-\delta_{m\alpha}\underset{\sim}{d})|e^{i\underset{\sim}{K}_R\cdot\underset{\sim}{r}}\rangle \\
&= (-i)^{\ell} N^{-1} (\Omega\Theta_m)^{-\frac{1}{2}} \sum_R \Gamma^{\alpha}_{\gamma\gamma}(R) \sum_\nu e^{-i\underset{\sim}{k}\cdot\underset{\sim}{R}_\nu} e^{i\underset{\sim}{K}_R\cdot(\underset{\sim}{R}_\nu-\delta_{m\alpha}\underset{\sim}{d})} \langle v_m(\underset{\sim}{r}-\underset{\sim}{R}_\nu-\delta_{m\alpha}\underset{\sim}{d})|e^{i\underset{\sim}{K}_R\cdot(\underset{\sim}{r}-\underset{\sim}{R}_\nu-\delta_{m\alpha}\underset{\sim}{d})}\rangle \\
&= (-i)^{\ell} N^{-1} (\Omega\Theta_m)^{-\frac{1}{2}} \sum_R \Gamma^{\alpha}_{\gamma\gamma}(R) \sum_\nu e^{i(\underset{\sim}{K}_R-\underset{\sim}{k})\cdot\underset{\sim}{R}_\nu} e^{i\underset{\sim}{K}_R\cdot\delta_{m\alpha}\underset{\sim}{d}} \langle v_m(\underset{\sim}{r})|e^{i\underset{\sim}{K}_R\cdot\underset{\sim}{r}}\rangle \\
&= (-i)^{\ell} (\Omega\Theta_m)^{-\frac{1}{2}} \sum_R \Gamma^{\alpha}_{\gamma\gamma}(R)\, e^{i\underset{\sim}{K}_R\cdot\delta_{m\alpha}\underset{\sim}{d}} \langle v_m(\underset{\sim}{r})|e^{i\underset{\sim}{K}_R\cdot\underset{\sim}{r}}\rangle . \qquad \text{(D-10)}
\end{aligned}$$

In the last step we made use of the fact that $\underset{\sim}{K}_R - \underset{\sim}{k}$ is a reciprocal lattice vector [cf. Cal 64, Sec. 1.6]. By using Eq. (II-8) for $v_n(\underset{\sim}{r})$ and Eq. (D-9) for $e^{i\underset{\sim}{K}_R\cdot\underset{\sim}{r}}$, we obtain

$$\begin{aligned}
\langle F_n | S_m\rangle &= (-i)^{\ell} (\Omega\Theta_m)^{-\frac{1}{2}} \sum_R \Gamma^{\alpha}_{\gamma\gamma}(R)\, e^{i\underset{\sim}{K}_R\cdot\delta_{m\alpha}\underset{\sim}{d}}\; 4\pi \sum_{\underset{\sim}{m}} c^{\alpha}_{\underset{\sim}{m}m} \sum_{\ell'}\sum_{m'} i^{\ell'} Y_{\ell'}^{m'*}(\theta,\phi)_{\underset{\sim}{K}_R} \\
&\quad \times \int_0^{\infty} r\, P_m(r)\, j_{\ell'}(Kr)\, dr \iint Y_{\ell}^{m*}(\theta,\phi)\, Y_{\ell'}^{m'}(\theta,\phi)\, \sin\theta\, d\theta\, d\phi \\
&= 4\pi (\Omega\Theta_m)^{-\frac{1}{2}} \Big[\sum_R \Gamma^{\alpha}_{\gamma\gamma}(R)\, e^{i\delta_{m\alpha}\underset{\sim}{K}_R\cdot\underset{\sim}{d}} \sum_{\underset{\sim}{m}} c^{\alpha}_{\underset{\sim}{m}m}\, Y_{\ell}^{m*}(\theta,\phi)_{\underset{\sim}{K}_R}\Big] \int_0^{\infty} r\, P_m(r)\, j_{\ell}(Kr)\, dr , \qquad \text{(D-11)}
\end{aligned}$$

which, after replacing the spherical harmonics with the cubic harmonics (cf. Table 7), yields Eq. (IV-36). Notice that the coefficients c_{nm} in Eq. (D-11) and in Eq. (IV-36) are not the same, even though we have used the same notation for simplicity.

The Hamiltonian matrix element is

$$\begin{aligned} \langle F_n | H | S_m \rangle &= \langle F_n | -\nabla^2 + V(\underset{\sim}{r}) | S_m \rangle \\ &= K^2 \langle F_n | S_m \rangle + \langle F_n | V(\underset{\sim}{r}) | S_m \rangle , \end{aligned} \tag{D-12}$$

where $K = |\underset{\sim}{K}_R|$ is independent of R: S_m is an eigenfunction of the kinetic energy operator with eigenvalue K^2 (in a.u.). The matrix element of the crystal potential, by going through the same steps as in Eq. (D-10), yields

$$\langle F_n | V(\underset{\sim}{r}) | S_m \rangle = (-i)^{\ell} (\Omega \Theta_m)^{-\frac{1}{2}} \sum_R \Gamma^{\kappa}_{\gamma\gamma}(R)\, e^{i\delta_n \underset{\sim}{K}_R \cdot \underset{\sim}{d}} \langle v_n(\underset{\sim}{r}) | V(\underset{\sim}{r} + \delta_n \underset{\sim}{d}) | e^{i \underset{\sim}{K}_R \cdot \underset{\sim}{r}} \rangle . \tag{D-13}$$

By writing the crystal potential as in Eq. (I-44) and retaining only the spherical terms, we obtain

$$\begin{aligned} \langle F_n | V(\underset{\sim}{r}) | S_m \rangle &= (-i)^{\ell} (\Omega \Theta_m)^{-\frac{1}{2}} \sum_R \Gamma^{\kappa}_{\gamma\gamma}(R)\, e^{i\delta_n \underset{\sim}{K}_R \cdot \underset{\sim}{d}} \langle v_n(\underset{\sim}{r}) | V_a(r) + M_a(r) + [\Sigma' U]_0 | e^{i \underset{\sim}{K}_R \cdot \underset{\sim}{r}} \rangle \\ &= E^a_M \langle F_n | S_m \rangle + 4\pi (\Omega \Theta_m)^{-\frac{1}{2}} \Big[\sum_R \Gamma^{\kappa}_{\gamma\gamma}(R)\, e^{i\delta_n \underset{\sim}{K}_R \cdot \underset{\sim}{d}} \sum_m c^{\kappa}_{nm} Y^{m\kappa}_{\ell}(\theta,\phi)_{\underset{\sim}{K}_R} \Big] \\ &\quad \times \int_0^{\infty} r P_n(r)\, j_{\ell}(Kr) \left\{ V_a(r) + [\Sigma' U]_0 \right\} dr . \end{aligned} \tag{D-14}$$

In Eq. (D-14) we used the fact that $M_a(r)$ is constant inside the first shell (cf. Appendix B) and that $v_n(\underset{\sim}{r})$ is zero outside. Thus we can replace $M_a(r)$ with the Madelung energy E_M^a. The Madelung energy is positive around a positive ion and negative around a negative ion, but the absolute value is the same. Substituting Eq. (D-14) into Eq. (D-12), and replacing spherical harmonics with cubic harmonics, yields Eq. (IV-37).

Type 3: $\langle S_m | Op | S_{m'} \rangle$. The calculation of the overlap matrix element is straightforward. From Eq. (D-2) we obtain

$$\langle S_m | S_{m'} \rangle = (N\Omega)^{-1} (\Omega_m \Omega_{m'})^{-\frac{1}{2}} \sum_n \sum_{n'} \Gamma_{\gamma\gamma}^{\alpha}(R_n)^* \Gamma_{\gamma\gamma}^{\alpha}(R_{n'}) \langle e^{i \underset{\sim}{K}_n \cdot \underset{\sim}{r}} | e^{i \underset{\sim}{K}_{n'} \cdot \underset{\sim}{r}} \rangle , \quad \text{(D-15)}$$

where $\underset{\sim}{K}_n = \underset{\sim}{K}_{R_n} = \alpha_n^{-1}(\underset{\sim}{k}+\underset{\sim}{h}_\mu)$ and $\underset{\sim}{K}_{n'} = \alpha_{n'}^{-1}(\underset{\sim}{k}+\underset{\sim}{h}_{\mu'})$. Since $\underset{\sim}{K}_{n'} - \underset{\sim}{K}_n$ is a reciprocal lattice vector and

$$\int_c e^{i \underset{\sim}{h} \cdot \underset{\sim}{r}} \, d\tau = N\Omega \, \delta_{0, \underset{\sim}{h}} \quad \text{(D-16)}$$

if $\underset{\sim}{h}$ is a reciprocal lattice vector [cf. Zim 64, Sec. 1.2], Eq. (D-15) becomes

$$\langle S_m | S_{m'} \rangle = (\Omega_m \Omega_{m'})^{-\frac{1}{2}} \sum_n \sum_{n'} \Gamma_{\gamma\gamma}^{\alpha}(R_n)^* \Gamma_{\gamma\gamma}^{\alpha}(R_{n'}) \, \delta_{\underset{\sim}{K}_n, \underset{\sim}{K}_{n'}} , \quad \text{(D-17)}$$

which is the same as Eq. (IV-40).

To calculate the Hamiltonian matrix element we expand the crystal potential as a Fourier series,

$$V(\underset{\sim}{r}) = \sum_{\underset{\sim}{K}} v(\underset{\sim}{K})\, e^{i \underset{\sim}{K}\cdot\underset{\sim}{r}} \quad , \tag{D-18}$$

where, due to the periodicity of $V(\underset{\sim}{r})$, the sum is restricted to reciprocal lattice vectors [cf. loc. cit.]. We obtain

$$\begin{aligned} \langle S_m | H | S_{m'} \rangle &= \langle S_m | -\nabla^2 + V(\underset{\sim}{r}) | S_{m'} \rangle \\ &= | \underset{\sim}{k} + \underset{\sim}{h}_\mu |^2 \langle S_m | S_{m'} \rangle \\ &+ (N\Omega)^{-1} (\Theta_m \Theta_{m'})^{-\frac{1}{2}} \sum_n \sum_{n'} \Gamma^{\alpha}_{\gamma\gamma}(R_n)^* \Gamma^{\alpha}_{\gamma\gamma}(R_{n'}) \sum_{\underset{\sim}{K}} v(\underset{\sim}{K}) \langle e^{i \underset{\sim}{K}_n \cdot \underset{\sim}{r}} | e^{i \underset{\sim}{K} \cdot \underset{\sim}{r}} | e^{i \underset{\sim}{K}_{n'} \cdot \underset{\sim}{r}} \rangle \, . \end{aligned} \tag{D-19}$$

Use of Eq. (D-16) now yields

$$\begin{aligned} \langle S_m | H | S_{m'} \rangle &= | \underset{\sim}{k} + \underset{\sim}{h}_\mu |^2 \langle S_m | S_{m'} \rangle \\ &+ (\Theta_m \Theta_{m'})^{-\frac{1}{2}} \sum_n \sum_{n'} \Gamma^{\alpha}_{\gamma\gamma}(R_n)^* \Gamma^{\alpha}_{\gamma\gamma}(R_{n'})\, v(\underset{\sim}{K}_n - \underset{\sim}{K}_{n'}) \, , \end{aligned} \tag{D-20}$$

which is the same as Eq. (IV-41).

Matrix element $\langle F_n | V^{NS}(r) | S_m \rangle$: This matrix element, considered in Eqs. (IV-48 and 49), involves the non-spherical terms of the crystal potential, which have been neglected in Eq. (D-14). If we expand $V(\underset{\sim}{r})$ in spherical harmonics (cf. Eq. III-24), $V^{NS}(\underset{\sim}{r})$ contains all the terms with $\ell > 0$:

$$V^{NS}(\underset{\sim}{r}) = \sum_{\ell_1 > 0} \sum_{-\ell_1}^{+\ell_1} {}_{m_1} \, a^{V}_{\ell_1 m_1}(r)\, Y^{m_1}_{\ell_1}(\theta, \phi) \, . \tag{D-21}$$

As in Eq. (D-13), we obtain

$$\langle F_n | V^{NS}(\underset{\sim}{r}) | S_m \rangle = (-i)^{\ell} (\Omega \odot_m)^{-\frac{1}{2}} \sum_R \Gamma^{\kappa}_{\gamma\gamma}(R) e^{i \delta_m \underset{\sim}{K}_R \cdot \underset{\sim}{d}} \langle v_n(\underset{\sim}{r}) | V^{NS}(\underset{\sim}{r}) | e^{i \underset{\sim}{K}_R \cdot \underset{\sim}{r}} \rangle \ . \quad \text{(D-22)}$$

By writing $v_n(\underset{\sim}{r})$ as in Eq. (II-8), and using Eqs. (D-9) and (D-21), the integral at the right hand side of Eq. (D-22) yields

$$\langle v_n(\underset{\sim}{r}) | V^{NS}(\underset{\sim}{r}) | e^{i \underset{\sim}{K}_R \cdot \underset{\sim}{r}} \rangle = 4\pi \sum_{-\ell}^{+\ell} {}_m \, c^{*}_{\ell m} \sum_{\ell_1 > 0} \sum_{-\ell_1}^{+\ell_1} {}_{m_1} \sum_{0}^{\infty} {}_{\ell_2} \sum_{-\ell_2}^{+\ell_2} {}_{m_2} \, i^{\ell_2} \, Y^{m_2 *}_{\ell_2}(\theta, \phi)_{\underset{\sim}{K}_R}$$

$$\times \int_0^{\infty} r \, P_n(r) \, a^{V}_{\ell_1 m_1}(r) \, j_{\ell_2}(Kr) \, dr \int Y^{m *}_{\ell}(\theta,\phi) \, Y^{m_1}_{\ell_1}(\theta,\phi) \, Y^{m_2}_{\ell_2}(\theta,\phi) \, d\Omega \ , \quad \text{(D-23)}$$

where $d\Omega = \sin\theta d\theta d\phi$. The integral involving three spherical harmonics can be expressed in terms of Clebsch-Gordan coefficients as [cf. Ros 57, Eq. 4.34]

$$\int Y^{m *}_{\ell}(\theta,\phi) \, Y^{m_1}_{\ell_1}(\theta,\phi) \, Y^{m_2}_{\ell_2}(\theta,\phi) \, d\Omega = \left[\frac{(2\ell_1+1)(2\ell_2+1)}{4\pi(2\ell+1)} \right]^{\frac{1}{2}} (\ell_1 \ell_2 m_1 m_2 | \ell m)(\ell_1 \ell_2 00 | \ell 0) \quad \text{(D-24)}$$

The indices in the Clebsch-Gordan coefficients are restricted by the following relations [see, e.g., Tin 64, Ch. 5]

$$|\ell_1 - \ell_2| \le \ell \le \ell_1 + \ell_2 \ , \qquad m = m_1 + m_2 \ , \quad \text{(D-25)}$$

which are equivalent to

$$|\ell - \ell_1| \le \ell_2 \le \ell + \ell_1 \ , \qquad m_2 = m - m_1 \ . \quad \text{(D-26)}$$

From Eqs. (D-24) and (D-26), Eq. (D-23) becomes

$$\langle v_n(\underline{r})|V^{NS}(\underline{r})|e^{i\underline{K}_R\cdot\underline{r}}\rangle = 4\pi \sum_{-\ell}^{+\ell}{}_m \sum_{\ell_1>0} \sum_{|\ell-\ell_1|}^{\ell+\ell_1}{}_{\ell_2} \sum_{m-\ell_2}^{m+\ell_2}{}_{m_1} i^{\ell_2} c^*_{\ell m} Y^{m-m_1\,*}_{\ell_2}(\theta,\phi)_{\underline{K}_R}$$

$$\times \left[\frac{(2\ell_1+1)(2\ell_2+1)}{4\pi(2\ell+1)}\right]^{\frac{1}{2}} (\ell_1\ell_2 m_1 m_2|\ell m)(\ell_1\ell_2 00|\ell 0)$$

$$\times \int_0^\infty r P_n(r) a^V_{\ell_1 m_1}(r) j_{\ell_2}(Kr)\,dr \quad . \qquad \text{(D-27)}$$

Substituting Eq. (D-27) into Eq. (D-22) yields Eq. (IV-49).

Appendix E

FOURIER COEFFICIENTS OF THE CRYSTAL POTENTIAL

In Eq. (D-18) the crystal potential is written in Fourier series as

$$V(\underset{\sim}{r}) = \sum_{\underset{\sim}{K}'} v(\underset{\sim}{K}')\, e^{i \underset{\sim}{K}' \cdot \underset{\sim}{r}} , \tag{E-1}$$

where the sum is over reciprocal lattice vectors. If we multiply both sides of Eq. (E-1) by $e^{-i\underset{\sim}{K}\cdot\underset{\sim}{r}}$, integrate over the volume of the crystal, and use Eq. (D-16), we obtain

$$v(\underset{\sim}{K}) = (N\Omega)^{-1} \int_c e^{-i \underset{\sim}{K}\cdot\underset{\sim}{r}} V(\underset{\sim}{r})\, d\tau . \tag{E-2}$$

The crystal potential can be written, as in Eq. (I-40),

$$V(\underset{\sim}{r}) = \sum_{\nu} \left[V_A(\underset{\sim}{r} - \underset{\sim}{R}_\nu) + V_B(\underset{\sim}{r} - \underset{\sim}{R}_\nu - \underset{\sim}{d}) \right] ; \tag{E-3}$$

then, Eq. (E-2) becomes

$$\begin{aligned} v(\underset{\sim}{K}) &= (N\Omega)^{-1} \sum_{\nu} \left[\int_c e^{-i\underset{\sim}{K}\cdot\underset{\sim}{r}} V_A(\underset{\sim}{r} - \underset{\sim}{R}_\nu)\, d\tau + \int_c e^{-i\underset{\sim}{K}\cdot\underset{\sim}{r}} V_B(\underset{\sim}{r} - \underset{\sim}{R}_\nu - \underset{\sim}{d})\, d\tau \right] \\ &= (N\Omega)^{-1} \sum_{\nu} \left[e^{-i\underset{\sim}{K}\cdot\underset{\sim}{R}_\nu} \int_c e^{-i\underset{\sim}{K}\cdot(\underset{\sim}{r}-\underset{\sim}{R}_\nu)} V_A(\underset{\sim}{r} - \underset{\sim}{R}_\nu)\, d\tau + e^{-i\underset{\sim}{K}\cdot(\underset{\sim}{R}_\nu + \underset{\sim}{d})} \int_c e^{-i\underset{\sim}{K}\cdot(\underset{\sim}{r}-\underset{\sim}{R}_\nu-\underset{\sim}{d})} V_B(\underset{\sim}{r} - \underset{\sim}{R}_\nu - \underset{\sim}{d})\, d\tau \right] \\ &= \Omega^{-1} \left[\int_c e^{-i\underset{\sim}{K}\cdot\underset{\sim}{r}} V_A(\underset{\sim}{r})\, d\tau + e^{-i\underset{\sim}{K}\cdot\underset{\sim}{d}} \int_c e^{-i\underset{\sim}{K}\cdot\underset{\sim}{r}} V_B(\underset{\sim}{r})\, d\tau \right] \end{aligned} \tag{E-4}$$

$$= v_A(\underset{\sim}{K}) + e^{-i\underset{\sim}{K}\cdot\underset{\sim}{d}}\, v_B(\underset{\sim}{K}) \quad ,$$

where

$$v_a(\underset{\sim}{K}) = \Omega^{-1} \int_c e^{-i\underset{\sim}{K}\cdot\underset{\sim}{r}}\, V_a(\underset{\sim}{r})\, d\tau \,. \tag{E-5}$$

If we recall that $V_a(\underset{\sim}{r})$ is spherically symmetric around the origin and separate it into its long- and short-range parts (cf. Eqs. I-41, 42), Eq. (E-5) becomes

$$v_a(\underset{\sim}{K}) = -\frac{2e_a}{\Omega}\int_c \frac{1}{r} e^{-i\underset{\sim}{K}\cdot\underset{\sim}{r}}\, d\tau + \frac{1}{\Omega}\int_c e^{-i\underset{\sim}{K}\cdot\underset{\sim}{r}}\, U_a(r)\, d\tau \,. \tag{E-6}$$

We first consider the case $\underset{\sim}{K}\neq 0$. The first integral in Eq. (E-6), if we take the z axis along the direction of $\underset{\sim}{K}$ and use polar coordinates, yields

$$\begin{aligned}\int_c \frac{1}{r} e^{-i\underset{\sim}{K}\cdot\underset{\sim}{r}}\, d\tau &= \iiint \frac{1}{r} e^{-iKr\cos\theta}\, r^2 \sin\theta\, dr\, d\theta\, d\phi \\ &= 2\pi \int_0^{R_c} r\, dr \int_0^{\pi} e^{-iKr\cos\theta} \sin\theta\, d\theta \\ &= 2\pi \int_0^{R_c} r\, dr \left[2\frac{\sin Kr}{Kr}\right] = \frac{4\pi}{K}\int_0^{R_c} \sin Kr\, dr \,.\end{aligned} \tag{E-7}$$

In Eq. (E-7), we have put an upper limit to the radial integral because of the finite size of the crystal. If the crystal had spherical shape, then R_c would be the radius of the sphere. Since by imposing periodic boundary conditions

(cf. Sec. I-2) we assumed that the crystal is a parallelepiped, the radial integral in Eq. (E-7) does not have a well defined upper limit. This integral is generally calculated by introducing a screening factor $e^{-\lambda r}$ in the integrand, where λ is a positive, arbitrarily small number, and letting the upper limit go to infinity. Thus,

$$\int_c \frac{1}{r} e^{-i\underset{\sim}{K}\cdot\underset{\sim}{r}} d\tau \approx \int_\infty \frac{e^{-\lambda r}}{r} e^{-i\underset{\sim}{K}\cdot\underset{\sim}{r}} d\tau = \frac{4\pi}{K} \int_0^\infty e^{-\lambda r} \sin Kr\, dr$$

$$= \frac{4\pi}{K} \left[-\frac{e^{-\lambda r}}{\lambda^2 + K^2} (\lambda \sin Kr + K \cos Kr) \right]_0^\infty$$

$$= \frac{4\pi}{K^2 + \lambda^2} \approx \frac{4\pi}{K^2} \quad . \qquad \text{(E-8)}$$

In the last step of Eq. (E-8) we let $\lambda \to 0$, which implies $\lambda << K$.

The second integral in Eq. (E-6) can be calculated by following the same steps as in Eq. (E-7). Since $U_a(r)$ is a short-range potential, the upper limit in the r-integration can immediately be replaced by ∞. Thus,

$$\int_c e^{-i\underset{\sim}{K}\cdot\underset{\sim}{r}} U_a(r)\, d\tau = \frac{4\pi}{K} \int_0^\infty r\, U_a(r) \sin Kr\, dr \quad . \qquad \text{(E-9)}$$

By introducing Eqs. (E-8) and (E-9) into Eq. (E-6), we obtain the first of Eqs. (IV-45).

We now consider the case $\underset{\sim}{K}=0$. From Eq. (E-2) it is evident that $\upsilon(0)$ is the average of the potential $V(\underset{\sim}{r})$ over

the entire crystal. By using Eqs. (E-4) and (E-5), we obtain

$$\upsilon(0) = \upsilon_A(0) + \upsilon_B(0) = \Omega^{-1} \int_c \left[V_A(r) + V_B(r)\right] d\tau$$
$$= \Omega^{-1} \int_c \left[U_A(r) + U_B(r)\right] d\tau \,, \qquad \text{(E-10)}$$

since the long-range terms cancel each other. Thus, we can redefine $\upsilon_a(\underset{\sim}{K})$ for $\underset{\sim}{K} = 0$ as

$$\upsilon_a(0) = \frac{1}{\Omega} \int_c U_a(r)\, d\tau = \frac{4\pi}{\Omega} \int_0^\infty r^2 U_a(r)\, dr \,. \qquad \text{(E-11)}$$

Eq. (E-11) can also be obtained from Eq. (E-9) by letting $K \to 0$.

Appendix F

MATRIX ELEMENTS OF THE SPIN-ORBIT INTERACTION

A two component Pauli spinor can be written (cf. Eq. II-21)

$$|\psi\rangle = f_\alpha(\underset{\sim}{r})\,|\alpha\rangle + f_\beta(\underset{\sim}{r})\,|\beta\rangle\,, \tag{F-1}$$

where f_α and f_β are scalar functions of position, and $|\alpha\rangle$ and $|\beta\rangle$ are two-component column matrices:

$$|\alpha\rangle = \begin{pmatrix}1\\0\end{pmatrix}, \qquad |\beta\rangle = \begin{pmatrix}0\\1\end{pmatrix}. \tag{F-2}$$

Clearly, $|\alpha\rangle$ and $|\beta\rangle$ satisfy the following relations:

$$\begin{aligned}\langle\alpha|\alpha\rangle &= \langle\beta|\beta\rangle = 1\,,\\ \langle\alpha|\beta\rangle &= \langle\beta|\alpha\rangle = 0\,.\end{aligned} \tag{F-3}$$

The spin-orbit interaction (Eq. I-35) can be written

$$H_{so} = \frac{\hbar}{4m^2c^2}\,\underset{\sim}{\sigma}\cdot\underset{\sim}{\mathcal{L}} = \frac{\hbar}{4m^2c^2}\left(\sigma_x\mathcal{L}_x + \sigma_y\mathcal{L}_y + \sigma_z\mathcal{L}_z\right), \tag{F-4}$$

where $\sigma_x, \sigma_y, \sigma_z$ are the 2x2 Pauli spin matrices [Sch 68, Eq. 41-3],

$$\sigma_x = \begin{pmatrix} 0 & 1 \\ 1 & 0 \end{pmatrix}, \quad \sigma_y = \begin{pmatrix} 0 & -i \\ i & 0 \end{pmatrix}, \quad \sigma_z = \begin{pmatrix} 1 & 0 \\ 0 & -1 \end{pmatrix}, \tag{F-5}$$

and

$$\underset{\sim}{\mathcal{L}} = \underset{\sim}{\nabla} V \times \underset{\sim}{p} = -i\hbar \underset{\sim}{\nabla} V \times \underset{\sim}{\nabla} . \tag{F-6}$$

The Pauli matrices operate on $|\alpha\rangle$ and $|\beta\rangle$ in the following way [loc. cit., Eq. 41-5]:

$$\begin{aligned} &\sigma_x |\alpha\rangle = |\beta\rangle, \quad \sigma_y |\alpha\rangle = i|\beta\rangle, \quad \sigma_z |\alpha\rangle = |\alpha\rangle, \\ &\sigma_x |\beta\rangle = |\alpha\rangle, \quad \sigma_y |\beta\rangle = -i|\alpha\rangle, \quad \sigma_z |\beta\rangle = -|\beta\rangle . \end{aligned} \tag{F-7}$$

By using Eq. (F-7), the following relations are easily proved:

$$\begin{aligned} &\langle f_\alpha \alpha | \underset{\sim}{\sigma} \cdot \underset{\sim}{\mathcal{L}} | g_\alpha \alpha \rangle = \langle f_\alpha | \mathcal{L}_z | g_\alpha \rangle , \\ &\langle f_\beta \beta | \underset{\sim}{\sigma} \cdot \underset{\sim}{\mathcal{L}} | g_\beta \beta \rangle = -\langle f_\beta | \mathcal{L}_z | g_\beta \rangle , \\ &\langle f_\alpha \alpha | \underset{\sim}{\sigma} \cdot \underset{\sim}{\mathcal{L}} | g_\beta \beta \rangle = \langle f_\alpha | \mathcal{L}_x - i \mathcal{L}_y | g_\beta \rangle , \\ &\langle f_\beta \beta | \underset{\sim}{\sigma} \cdot \underset{\sim}{\mathcal{L}} | g_\alpha \alpha \rangle = \langle f_\beta | \mathcal{L}_x + i \mathcal{L}_y | g_\alpha \rangle . \end{aligned} \tag{F-8}$$

Thus, evaluation of matrix elements of the spin-orbit interaction between two functions of the form (F-1) reduces to calculation of the following quantity:

$$\langle f | \underset{\sim}{\mathcal{L}} | g \rangle , \tag{F-9}$$

where $\underset{\sim}{\mathcal{L}}$ is given in Eq. (F-6) and f and g are scalar functions of position.

We now assume that the functions f and g are Bloch sums F (cf. Eq. II-7) or linear combinations of plane waves S (cf. Eq. II-9). We can then have three types of matrix elements of the form (F-9):

$$\begin{aligned} &\text{type 1}: \quad \langle F | \underset{\sim}{\mathcal{L}} | F \rangle , \\ &\text{type 2}: \quad \langle S | \underset{\sim}{\mathcal{L}} | F \rangle , \\ &\text{type 3}: \quad \langle S | \underset{\sim}{\mathcal{L}} | S \rangle . \end{aligned} \tag{F-10}$$

For simplicity, we neglect the normalization factors in F and S, and write them in the following way:

$$F_i = \frac{1}{\sqrt{N}} \sum_{\nu} e^{i \underset{\sim}{k} \cdot \underset{\sim}{R}_{\nu}} v_i (\underset{\sim}{r} - \underset{\sim}{R}^{\delta}_{\nu}) , \tag{F-11}$$

$$S_i = \frac{1}{\sqrt{N\Omega}} \sum_{\mu} d_{i\mu} \; e^{i \underset{\sim}{K}_{\mu} \cdot \underset{\sim}{r}} . \tag{F-12}$$

In Eq. (F-11), $\underset{\sim}{R}^{\delta}_{\nu} = \underset{\sim}{R}_{\nu} + \delta \underset{\sim}{d}$ (cf. Eq. II-7). In Eq. (F-12), $\underset{\sim}{K}_{\mu} = \underset{\sim}{k} + \underset{\sim}{h}_{\mu}$ (cf. Eq. II-9), where $\underset{\sim}{h}_{\mu}$ is a reciprocal lattice vector.

Type 1: We assume that the orbitals v centered on different atomic sites do not overlap. Thus (cf. Eq. IV-21),

$$\langle F_i | \underset{\sim}{\mathcal{L}} | F_j \rangle = \langle v_i (\underset{\sim}{r}) | \underset{\sim}{\mathcal{L}} | v_j (\underset{\sim}{r}) \rangle \delta_{o \gamma_{ij}} , \tag{F-13}$$

where γ_{ij} is defined in Eq. (III-8). Due to the fact that $\underset{\sim}{\nabla} V$ is very large near a nucleus and drops off much faster than V [cf., e.g., Fow 63], Eq. (F-13) can be written

$$\langle F_i | \underset{\sim}{\mathcal{L}} | F_j \rangle = \langle v_i(\underset{\sim}{r}) | \underset{\sim}{\nabla} V_a \times \underset{\sim}{p} | v_j(\underset{\sim}{r}) \rangle \delta_{o\gamma_{ij}} , \tag{F-14}$$

where V_a is the atomic-like potential centered at the origin (cf. Sec. I-5). Remembering that $V_a(\underset{\sim}{r})$ is spherically symmetric about the origin, we obtain

$$\langle F_i | \underset{\sim}{\mathcal{L}} | F_j \rangle = \langle v_i(\underset{\sim}{r}) | \frac{1}{r}\frac{dV_a(r)}{dr} \underset{\sim}{L} | v_j(\underset{\sim}{r}) \rangle \delta_{o\gamma_{ij}} , \tag{F-15}$$

where

$$\underset{\sim}{L} = \underset{\sim}{r} \times \underset{\sim}{p} \tag{F-16}$$

is the angular momentum operator [Sch 68, Secs. 14 and 27]. It is convenient to write the angular part of v_i and v_j in terms of spherical harmonics (cf. Eq. II-8); for example,

$$v_i(\underset{\sim}{r}) = \sum_m c_{im} \frac{P_i(r)}{r} Y_{\ell_i}^m(\theta,\phi) . \tag{F-17}$$

Introducing Eq. (F-17) into Eq. (F-15) yields

$$\langle F_i | \underset{\sim}{\mathcal{L}} | F_j \rangle = \delta_{o\gamma_{ij}} \xi_{ij} \sum_m \sum_{m'} c_{im'}^* c_{jm} \hbar^{-1} \int Y_{\ell_i}^{m'*}(\theta,\phi) \underset{\sim}{L} Y_{\ell_j}^m(\theta,\phi)\, d\Omega , \tag{F-18}$$

where

$$\xi_{ij} = \hbar \int_o^\infty \frac{1}{r}\frac{dV_a}{dr} P_i(r) P_j(r)\, dr . \tag{F-19}$$

We can now make use of the following equations [loc. cit.]:

$$L_z Y_\ell^m(\theta,\phi) = m\hbar\, Y_\ell^m(\theta,\phi) ,$$

$$L_+ Y_\ell^m(\theta,\phi) = \left[\ell(\ell+1) - m(m+1)\right]^{\frac{1}{2}} \hbar\, Y_\ell^{m+1}(\theta,\phi),$$
$$L_- Y_\ell^m(\theta,\phi) = \left[\ell(\ell+1) - m(m-1)\right]^{\frac{1}{2}} \hbar\, Y_\ell^{m-1}(\theta,\phi), \qquad \text{(F-20)}$$

where

$$L_+ = L_x + i L_y ,$$
$$L_- = L_x - i L_y . \qquad \text{(F-21)}$$

From Eqs. (F-18) and (F-20) we obtain

$$\langle F_i | \mathcal{L}_z | F_j \rangle = \delta_{o\gamma_{ij}} \delta_{\ell_i \ell_j} \xi_{ij} \sum_m c^*_{im} c_{jm}\, m ,$$
$$\langle F_i | \mathcal{L}_+ | F_j \rangle = \delta_{o\gamma_{ij}} \delta_{\ell_i \ell_j} \xi_{ij} \sum_m c^*_{i,m+1} c_{jm} \left[\ell_i(\ell_i+1) - m(m+1)\right]^{\frac{1}{2}}, \qquad \text{(F-22)}$$
$$\langle F_i | \mathcal{L}_- | F_j \rangle = \delta_{o\gamma_{ij}} \delta_{\ell_i \ell_j} \xi_{ij} \sum_m c^*_{i,m-1} c_{jm} \left[\ell_i(\ell_i+1) - m(m-1)\right]^{\frac{1}{2}},$$

where, in analogy to Eq. (F-21), we have defined

$$\mathcal{L}_+ = \mathcal{L}_x + i \mathcal{L}_y ,$$
$$\mathcal{L}_- = \mathcal{L}_x - i \mathcal{L}_y . \qquad \text{(F-23)}$$

The integral ξ_{ij}, defined in Eq. (F-19), can be computed numerically [see Fow 63, App. F]. Obviously, due to the δ function $\delta_{\ell_i \ell_j}$ in Eq. (F-22), only those parameters ξ_{ij} are needed, where ℓ_i is equal to ℓ_j.

Type 2. Since the operator $\underset{\sim}{\mathcal{L}}$ has the same translational symmetry as the crystal potential $V(\underset{\sim}{r})$, we obtain (cf. Eq. D-13)

$$\langle S_i | \underset{\sim}{\mathcal{L}} | F_j \rangle = \frac{1}{\sqrt{\Omega}} \sum_\mu d^*_{i\mu} e^{-i \underset{\sim}{K}_\mu \cdot \underset{\sim}{d}} \langle e^{i \underset{\sim}{K}_\mu \cdot \underset{\sim}{r}} | \underset{\sim}{\mathcal{L}} | v_j(\underset{\sim}{r}) \rangle . \qquad \text{(F-24)}$$

By the same argument used in connection with Eqs. (F-14) and (F-15), we can write

$$\langle e^{i \underset{\sim}{K}_\mu \cdot \underset{\sim}{r}} | \underset{\sim}{\mathcal{L}} | v_j(\underset{\sim}{r}) \rangle = \langle e^{i \underset{\sim}{K}_\mu \cdot \underset{\sim}{r}} | \frac{1}{r} \frac{dV_a(r)}{dr} \underset{\sim}{L} | v_j(\underset{\sim}{r}) \rangle . \tag{F-25}$$

Expanding the plane wave in terms of spherical harmonics (cf. Eq. D-9) and using Eq. (F-17) yields

$$\langle e^{i \underset{\sim}{K}_\mu \cdot \underset{\sim}{r}} | \underset{\sim}{\mathcal{L}} | v_j(\underset{\sim}{r}) \rangle = 4\pi \sum_m c_{jm} \sum_{\ell'=0}^{\infty} \sum_{m'=-\ell'}^{+\ell'} (-i)^{\ell'} Y_{\ell'}^{m'}(\theta,\phi)_{\underset{\sim}{K}_\mu} \tag{F-26}$$

$$\times \int_0^\infty j_{\ell'}(K_\mu r) \frac{dV_a}{dr} P_j(r)\, dr \int Y_{\ell'}^{m'*}(\theta,\phi) \underset{\sim}{L} Y_{\ell_j}^{m}(\theta,\phi)\, d\Omega .$$

By making use of Eq. (F-20), we obtain

$$\langle e^{i \underset{\sim}{K}_\mu \cdot \underset{\sim}{r}} | \mathcal{L}_z | v_j(\underset{\sim}{r}) \rangle = J_j^i \sum_m c_{jm}\, m\, Y_\ell^m(\theta,\phi)_{\underset{\sim}{K}_\mu} ,$$

$$\langle e^{i \underset{\sim}{K}_\mu \cdot \underset{\sim}{r}} | \mathcal{L}_+ | v_j(\underset{\sim}{r}) \rangle = J_j^i \sum_m c_{jm} \left[\ell_j(\ell_j+1) - m(m+1)\right]^{\frac{1}{2}} Y_\ell^{m+1}(\theta,\phi)_{\underset{\sim}{K}_\mu} , \tag{F-27}$$

$$\langle e^{i \underset{\sim}{K}_\mu \cdot \underset{\sim}{r}} | \mathcal{L}_- | v_j(\underset{\sim}{r}) \rangle = J_j^i \sum_m c_{jm} \left[\ell_j(\ell_j+1) - m(m-1)\right]^{\frac{1}{2}} Y_\ell^{m-1}(\theta,\phi)_{\underset{\sim}{K}_\mu} ,$$

where we have defined

$$J_j^i = (-i)^{\ell_j} 4\pi\hbar \int_0^\infty j_{\ell_j}(K_\mu r) \frac{dV_a}{dr} P_j(r)\, dr . \tag{F-28}$$

The superscript i in Eq. (F-28) reflects the fact that J_j^i depends only on the magnitude of $\underset{\sim}{K}_\mu$, which is the same for all plane waves in S_i (cf. Sec. II-3).

From Eqs. (F-24) and (F-27), we obtain, for the matrix elements of type 2,

$$\langle S_i | \mathcal{L}_z | F_j \rangle = \frac{1}{\sqrt{\Omega}} J_j^i \sum_\mu d_{i\mu}^* e^{-i\delta} e^{i \underset{\sim}{K}_\mu \cdot \underset{\sim}{d}} \sum_m c_{jm} \, m \, Y_\ell^m(\theta,\phi)_{\underset{\sim}{K}_\mu},$$

$$\langle S_i | \mathcal{L}_+ | F_j \rangle = \frac{1}{\sqrt{\Omega}} J_j^i \sum_\mu d_{i\mu}^* e^{-i\delta} e^{i \underset{\sim}{K}_\mu \cdot \underset{\sim}{d}} \sum_m c_{jm} \left[\ell_j(\ell_j+1) - m(m+1) \right]^{1/2} Y_\ell^{m+1}(\theta,\phi)_{\underset{\sim}{K}_\mu}, \tag{F-29}$$

$$\langle S_i | \mathcal{L}_- | F_j \rangle = \frac{1}{\sqrt{\Omega}} J_j^i \sum_\mu d_{i\mu}^* e^{-i\delta} e^{i \underset{\sim}{K}_\mu \cdot \underset{\sim}{d}} \sum_m c_{jm} \left[\ell_j(\ell_j+1) - m(m-1) \right]^{1/2} Y_\ell^{m-1}(\theta,\phi)_{\underset{\sim}{K}_\mu}.$$

Type 3. From Eq. (F-12) we obtain

$$\langle S_i | \underset{\sim}{\mathcal{L}} | S_j \rangle = \frac{1}{N\Omega} \sum_\mu \sum_{\mu'} d_{i\mu}^* d_{j\mu'} \langle e^{i \underset{\sim}{K}_\mu \cdot \underset{\sim}{r}} | \underset{\sim}{\mathcal{L}} | e^{i \underset{\sim}{K}_{\mu'} \cdot \underset{\sim}{r}} \rangle . \tag{F-30}$$

If we expand the crystal potential in Fourier series, as in Eq. (D-18), the operator $\underset{\sim}{\mathcal{L}}$ becomes

$$\underset{\sim}{\mathcal{L}} = i \sum_{\underset{\sim}{K}} v(\underset{\sim}{K}) \, e^{i \underset{\sim}{K} \cdot \underset{\sim}{r}} \, \underset{\sim}{K} \times \underset{\sim}{p} . \tag{F-31}$$

Recalling that a plane wave of wave vector $\underset{\sim}{K}$ is an eigenfunction of the momentum operator $\underset{\sim}{p}$ with the eigenvalue $\hbar \underset{\sim}{K}$, the result of operating with $\underset{\sim}{\mathcal{L}}$ on $e^{i \underset{\sim}{K}_\mu \cdot \underset{\sim}{r}}$ will be

$$\underset{\sim}{\mathcal{L}} \, | e^{i \underset{\sim}{K}_{\mu'} \cdot \underset{\sim}{r}} > = i \hbar \sum_{\underset{\sim}{K}} v(\underset{\sim}{K}) e^{i \underset{\sim}{K} \cdot \underset{\sim}{r}} (\underset{\sim}{K} \times \underset{\sim}{K}_{\mu'}) \, | e^{i \underset{\sim}{K}_{\mu'} \cdot \underset{\sim}{r}} > . \qquad \text{(F-32)}$$

Then

$$\begin{aligned} & < e^{i \underset{\sim}{K}_{\mu} \cdot \underset{\sim}{r}} | \underset{\sim}{\mathcal{L}} | e^{i \underset{\sim}{K}_{\mu'} \cdot \underset{\sim}{r}} > \\ & = i \hbar \sum_{\underset{\sim}{K}} (\underset{\sim}{K} \times \underset{\sim}{K}_{\mu'}) \, v(\underset{\sim}{K}) < e^{i \underset{\sim}{K}_{\mu} \cdot \underset{\sim}{r}} | e^{i \underset{\sim}{K} \cdot \underset{\sim}{r}} | e^{i \underset{\sim}{K}_{\mu'} \cdot \underset{\sim}{r}} > \\ & = i \hbar \sum_{\underset{\sim}{K}} (\underset{\sim}{K} \times \underset{\sim}{K}_{\mu'}) \, v(\underset{\sim}{K}) \, N\Omega \, \delta_{\underset{\sim}{K}, \underset{\sim}{K}_{\mu} - \underset{\sim}{K}_{\mu'}} \qquad \text{(F-33)} \\ & = i \hbar \, N\Omega \, (\underset{\sim}{k}_{\mu} \times \underset{\sim}{K}_{\mu'}) \, v(\underset{\sim}{K}_{\mu} - \underset{\sim}{K}_{\mu'}) . \end{aligned}$$

In Eq. (F-33) we have used Eq. (D-16). Substituting Eq. (F-33) into Eq. (F-30) yields

$$< S_i | \underset{\sim}{\mathcal{L}} | S_j > = i \hbar \sum_{\mu} \sum_{\mu'} a^*_{i\mu} a_{j\mu'} (\underset{\sim}{K}_{\mu} \times \underset{\sim}{K}_{\mu'}) \, v(\underset{\sim}{K}_{\mu} - \underset{\sim}{K}_{\mu'}) , \qquad \text{(F-34)}$$

or, explicitly,

$$< S_i | \mathcal{L}_z | S_j > = i \hbar \sum_{\mu} \sum_{\mu'} a^*_{i\mu} a_{j\mu'} (K_x^{\mu} K_y^{\mu'} - K_y^{\mu} K_x^{\mu'}) \, v(\underset{\sim}{K}_{\mu} - \underset{\sim}{K}_{\mu'}) ,$$

$$< S_i | \mathcal{L}_+ | S_j > = \hbar \sum_{\mu} \sum_{\mu'} a^*_{i\mu} a_{j\mu'} \left[K_z^{\mu'} (K_x^{\mu} + i K_y^{\mu}) - K_z^{\mu} (K_x^{\mu'} + i K_y^{\mu'}) \right] v(\underset{\sim}{K}_{\mu} - \underset{\sim}{K}_{\mu'}) ,$$

$$< S_i | \mathcal{L}_- | S_j > = \hbar \sum_{\mu} \sum_{\mu'} a^*_{i\mu} a_{j\mu'} \left[K_z^{\mu} (K_x^{\mu'} - i K_y^{\mu'}) - K_z^{\mu'} (K_x^{\mu} - i K_y^{\mu}) \right] v(\underset{\sim}{K}_{\mu} - \underset{\sim}{K}_{\mu'}) .$$

Appendix G

SOME FORTRAN PROGRAMS USED IN CONNECTION WITH THE PRESENT WORK

What follows is a list of some of the programs used in connection with this calculation. We have not listed those short programs that we have written for special purposes, since most of them would not be of much interest to the reader. All programs are written in FORTRAN IV and are available from the author's files.

1. PROGRAM ZNS

This program has been written by the author. It calculates the coordinates and the distance from the origin of the first eight shells of neighbors in the zinc blende structure.

INPUT: Lattice parameter a.

OUTPUT: Coordinates of the lattice sites. Distance from the origin of the two ions in the basis.

2. PROGRAM MAD

This program has been written by the author. It calculates the spherical Madelung potential (cf. Appendix B) numerically for CuCℓ in the 441 point mesh used by Hermann and Skillman [Her 63]. The potential is calculated in either one of the two forms: $M_a(r)$ and $rM_a(r)$, and for both

Cu^+ or $C\ell^-$ at the origin.

INPUT: Atomic number Z. Madelung energy E_M. Radii of first γ shells.

OUTPUT: R mesh. Madelung potential.

3. PROGRAM ATOM

This is essentially the "Hartree-Fock-Slater Self-Consistent Atomic Field Program" used by Hermann and Skillman [Her 63], with a few modifications and with the inclusion of a screened exchange of the form (I-57). Input and output are mostly as described in Hermann and Skillman's book [op. cit., Chap. 7], except that we allow for the inclusion of an external potential.

4. PROGRAM DOUB

This program was originally written by A. Barry Kunz and modified by the author. It calculates two-center integrals of the form of Eq. (III-33) by a direct numerical integration [see Kun 67b, Fig. 1].

INPUT: Atomic numbers Z_A and Z_B. Radial functions and potentials in the form rf(r) and in 441 mesh points. For each integral: function at origin; functions at other center; quantum numbers ℓm for each of these functions; two-center distance.

OUTPUT: Value of the integral.

5. PROGRAM AVERPOT

This program, written by the author, is a variation

of program DOUB. It calculates the contribution of the γth shell of ions to the average short-range sum $\overline{[\Sigma' U]}_o$, as defined in Eq. (III-36).

INPUT: Atomic numbers Z_A and Z_B. Potentials in the form rV(r) and in 441 mesh points. For each shell: kind of ion at the origin; kind of ions on γth shell; radius of shell; number of ions on shell.

OUTPUT: Average short-range potential in the form rV(r) and in 441 mesh points.

6. PROGRAM VALENCE

This program, written by the author, computes the tight-binding matrix elements defined in Eqs. (III-10 and 21).

INPUT: Parameters ε_a, $U_{\alpha\mu}$, and $S_{\alpha\beta\mu}$, and $U_{\alpha\beta\mu}$.

OUTPUT: Matrix elements H_{np} and O_{np}. These usually are not printed, but are transferred to subroutine DIAG (see Appendix H), which solves the secular equation.

7. PROGRAM SINGLE

This program, written by the author, performs the radial integration in one-center integrals.

INPUT: Atomic numbers. Radial functions and potentials in the form rf(r) and in 441 mesh points. For each integral: functions forming the integrand.

OUTPUT: Value of the integral.

8. PROGRAM CONV

This program, written by the author, studies the convergence of the eigenvalues of the MB secular equation by diagonalizing matrices of increasing dimension. It also allows to delete some rows and columns to study the effect of eliminating some functions from the basis set.

INPUT: Number of matrices corresponding to different representations. For each matrix: maximum dimension of matrix; number of Bloch functions in the basis; increment in number of basis functions; row index of the basis functions to be excluded (when it applies); matrix elements.

OUTPUT: The modified matrices are transferred to subroutine DIAG, which gives the eigenvalues (see Appendix H).

9. PROGRAM WFCF

This program has been written by the author. It calculates the coefficients of the wave function by solving Eq. (I-26). The set of linear inhomogeneous equations is solved by using subroutine LEQ (see Appendix H).

INPUT: Dimension of matrix. Numbers of states whose wavefunctions are desired. Matrix elements. Eigenvalues.

OUTPUT: Coefficients of the wavefunctions.

Appendix H

DESCRIPTION AND USE OF THE MIXED-BASIS PROGRAM PAULI

The FORTRAN IV program PAULI performs most of the MB calculation, as mentioned in Sec. IV-4. This program was originally written by A. Barry Kunz in 1969, but the version described here (Revision B: 9/2/1970) reflects several modifications introduced by the author. We give here a list of all the subprograms in the order in which they appear in the deck. The symbol S stands for subroutine, and F for function subprogram.

a	1.	PAULI (Main program)	f	12. DIAG (S)
				13. LOWER (S)
b	2.	ATOM (S)		14. LEQ (S)
	3.	SCHEQ (S)		
	4.	CROSYM (S)	g	15. QREIGEN (S)
				16. QR1 (S)
c	5.	DTCO (S)		17. SUBDIA (S)
				18. DTSHIFT (S)
d	6.	GRAFICO (S)		19. BALANCE (S)
				20. TREGUA (F)
e	7.	BETA (S)		
	8.	CPNN (S)		
	9.	XJL (F)		
	10.	CONN (F)		
	11.	CPPN (S)		

The subprograms listed above can be grouped into seven major sections, which we label a, b, ..., g. We now describe the operations of these sections.

Section a contains the main program, which calls the

subroutines ATOM, DTCO, GRAFICO, and BETA, and computes the Fourier coefficients of the potential.

Section b contains the subprograms 2 to 4 and is essentially the Herman and Skillman program with a few modifications (cf. Appendix G, no. 3).

Section c contains the subroutine DTCO, which forms the cutoff functions $P_{n\ell}^{CO}$ and calculates the cutoff energy parameters $\varepsilon_{n\ell}^{CO}$, as described in Sec. IV-2.

Section d contains the subroutine GRAFICO, which is not an essential part of the program. It just plots the three outermost atomic functions and lists their numerical values.

Section e, which contains the subprograms 7 to 11, computes the MB matrix elements. The group-theory data are read in by the subroutine BETA, which also performs most of the calculations. Function CONN yields the quantity $\Sigma_m c_{nm} Q_\ell^m$ in Eqs. (IV-36 and 37). Subroutine CPPN computes the integral $\int r P_n(r) j_\ell(Kr) dr$ in Eq. (IV-36). Subroutine CPNN computes the equivalent integral involving the potential, as in Eq. (IV-37). Function XJL yields the spherical Bessel functions $j_\ell(Kr)$.

Section f contains the subprograms 12 to 14. It forms the matrix $\underset{\sim}{O}^{-1}\underset{\sim}{H}$, calls the subroutine QREIGEN, and prints the roots of the secular equation. The subroutine LEQ is used to find the inverse of the overlap matrix $\underset{\sim}{O}$.

Section g, which contains the subprograms 15 to 20,

diagonalizes the matrix $\underset{\sim}{A} = \underset{\sim}{O}^{-1}\underset{\sim}{H}$.

For our calculations we used the CDC 6400 computer at Lehigh University and the CDC 6600 at New York University. These computers operate under the SCOPE system [Con 69], and we utilized some of the features of this system in handling the program PAULI. The deck contains approximately 2,400 cards and the field length required for the execution of the program is 233000_8 central memory words, when the largest matrix to diagonalize is of order 70 x 70.

The SCOPE program UPDATE was used to put the MB program PAULI on a tape and to make modifications and corrections, so that we did not have to handle a large number of cards. We list here the control cards for some jobs using UPDATE. For more information on UPDATE and on the SCOPE system we refer to the SCOPE Reference Manual [Con 69] and to some notes recently written by the author [Cal70].

1) To put the program on the tape (with UPDATE), compile, obtain a list of the data, and put the binary on the tape:

```
Job card
UPDATE(N=ECUPDAT)
RUN(S,,,COMPILE,,ECBIN)
COPYSCF(COMPILE,OUTPUT)
REWIND(ECUPDAT,ECBIN)
REQUEST(ECWRITE,HI)    WRITE RING.
REWIND(ECWRITE)
COPYBF(ECUPDAT,ECWRITE)
COPYBF(ECBIN,ECWRITE)
UNLOAD(ECWRITE)
7
8
9
```

```
*DECK PAU
      PROGRAM PAULI (...)
      .
      .
      .
      END
*DECK ATO
      SUBROUTINE ATOM (...)
      .
      .
      .
      END
*DECK DTC
      SUBROUTINE DTCO (...)
      .
      .
      .
      END
*DECK BET
      SUBROUTINE BETA (...)
      .
      .
      .
      END
*DECK CON
      SUBROUTINE CPNN(...)
      .
      .
      .
      END
*DECK DIA
      SUBROUTINE DIAG (...)
      .
      .
      .
      END
*DECK DAT
*CWEOR
      Data
EOF
```

The tape now contains:

File	Mode	Contents
1	Binary	MB program (UPDATE)
2	Binary	MB binary

2) To make modifications, use the binary unmodified decks, execute the program, and obtain a list of the data used:

```
Job card
REQUEST(ECREAD,HI)    NO RING.
REWIND(ECREAD)
COPYBF(ECREAD,ECUPDAT)
COPYBF(ECREAD,ECBIN)
UNLOAD(ECREAD)
REWIND(ECUPDAT,ECBIN)
UPDATE(Q,P=ECUPDAT)
RUN(S,,,COMPILE)
COPYCF(COMPILE,DATA)
REWIND(DATA)
COPYSCF(DATA,OUTPUT)
REWIND(DATA)
LOAD(LGO)
ECBIN(DATA)
7
8
9
*IDENT MODI
     Modifications
*COMPILE ...)
*COMPILE ...)  Decks modified
*COMPILE DAT
EOF
```

INPUT FORMAT FOR PROGRAM PAULI (SCHEMATIC)

1) Heading card (1X,71H)

2) AA,C,BX,BY,BZ,VALM (6F12.6)

AA = a (lattice constant in Bohr units)

C = Ω/a^3 (volume factor)

BX = $\frac{2}{a}d_x$ (x component of basis in units of $\frac{a}{2}$)

BY = $\frac{2}{a}d_y$ (y component of basis in units of $\frac{a}{2}$)

BZ = $\frac{2}{a}d_z$ (z component of basis in units of $\frac{a}{2}$)

VALM = α_a (Madelung constant referred to the lattice parameter a)

3) XK, RNEF, F (6F12.6)

XK = κ (dielectric constant)

RNEF = $\frac{2}{a}|\underset{\sim}{d}|$ (nearest-neighbor distance in units of $\frac{a}{2}$)

F = 1 (screening coefficient)

4) Data for subroutine ATOM [see Her 63, p. 7-3], positive ion.

5) NDTF, RC, RM (I4,2F8.4)

NDTF = No. of positive ion functions to which the cutoff is applied.

RC = r_c (left cutoff parameter in Bohr units)

RM = r_m (right cutoff parameter in Bohr units)

6) Same as No. 4, for negative ion.

7) Same as No. 5, for negative ion.

8) NORUN (I4)

NORUN = No. of points in $\underset{\sim}{k}$ space to be computed.

The rest appears NORUN times.

9) XKPRX, YKPRX, ZKPRX (3F12.6)

XKPRX = $\frac{a}{2\pi} k_x$ (x component of $\underset{\sim}{k}$ vector in units of $\frac{2\pi}{a}$)

YKPRX = $\frac{a}{2\pi} k_y$ (y component of $\underset{\sim}{k}$ vector in units of $\frac{2\pi}{a}$)

ZKPRX = $\frac{a}{2\pi} k_z$ (z component of $\underset{\sim}{k}$ vector in units of $\frac{2\pi}{a}$

10) NOP, NIR (2I4)

NOP = g (No. of operations in the group of $\underset{\sim}{k}$)

NIR = No. of irreducible representations to be used.

11) ZM(J,I); J = 1,9; I=1, NOP (9F4.0)

ZM(J,I)→$\underset{\sim}{\alpha}^{-1}$ (inverse of rotation matrix corresponding to operator R)

J = 1,2,3→first row; J = 4,5,6→second row; J = 7,8,9→third row.

12) INOBAS (I4)

INOBAS = No. of generators of S.C.P.W.'s to be read in.

13) XNN(I,J); J = 1,3; I = 1, NOBAS (3F8.2)

XNN(I,J) $\rightarrow \frac{a}{2\pi} \underset{\sim}{h}_{\mu}$ (generator in units of $\frac{2\pi}{a}$)
J = 1→x component; J = 2→y component; J = 3→ z component.

The rest appears NIR times.

14) ZK(I); I = 1, NOP (12F4.0)

ZK(I) = $\Gamma^{\alpha}_{\gamma\gamma}(R_i)$ (matrix element of irreducible representation)

15) IDENTI(I); I = 1, INOBAS (80I1)

IDENTI = 0, if particular generator not used in this representation; = 1 otherwise.

16) NOX,NOA,NOBAS,NOXO,NOAO,NOTHER (6I4)

NOX = No. of negative ion functions in the basis set.

NOA = No. of positive ion functions in the basis set.

NOBAS = No. of S.C.P.W.'s in the basis set (NOX+NOA+NOBAS = dimension of secular determinant).

NOXO = No. of negative ion functions to be orthogonalized to.

NOAO = No. of positive ion functions to be orthogonalized to.

NOTHER = No. of S.C.P.W.'s requiring alternate generator.

(NOXO=NOAO=NOTHER=0 in our calculation)

No. 17 and 18 appear NOX times.

17) NX1,LLX,AX1,AX2,AX3,AX4 (2I4,4F12.6)

NX1 = ℓ (orbital quantum number)

LLX = n (ordering number of radial function; ex.: n=1→1s, n=2→2s, n=3→2p, ...)

AX1 = c_s (coefficient of normalized cubic harmonic proportional to 1)

AX2 = c_x (coefficient of normalized cubic harmonic proportional to x)

AX3 = c_y (coefficient of normalized cubic harmonic proportional to y)

AX4 = c_z (coefficient of normalized cubic harmonic proportional to z)

18) DX1,DX2,DX3,DX4,DX5 (5F12.6)

DX1 = $c_{3z^2-r^2}$ (coefficient of normalized cubic harmonic proportional to $3z^2-r^2$)

DX2 = $c_{x^2-y^2}$ (coefficient of normalized cubic harmonic proportional to x^2-y^2)

DX3 = c_{xy} (coefficient of normalized cubic harmonic proportional to xy)

DX4 = c_{xz} (coefficient of normalized cubic harmonic proportional to xz)

DX5 = c_{yz} (coefficient of normal cubic harmonic proportional to yz)

No. 19 and 20 appear NOA times.

19) NA1,LLA,AA1,AA2,AA3,AA4 (Same as No. 17, for positive ion)

20) DA1,DA2,DA3,DA4,DA5 (Same as No. 18, for positive ion)

No. 21 appears only if NOTHER > 0

21) ZK(I); I=NOP+1, NOP+NOP (12F4.0)

ZK(I) = $\Gamma^{\alpha}_{\gamma,\gamma\pm1}(R_i)$ (matrix element of irreducible representation)

For normalized cubic harmonic proportional to $3x^2-r^2$ use

DX1 = -0.5, DX2 = 0.866025.

For normalized cubic harmonic proportional to y^2-z^2 use

DX1 = -0.866025, DX2 = -0.5.

BIBLIOGRAPHY

Bal 62: C.J. Ballhausen, *Introduction to Ligand Field Theory* (McGraw-Hill, New York, 1962)

Bas 63: F. Bassani and M. Yoshimine, "Electronic Band Structure of Group IV Elements and of III-V Compounds," Phys. Rev. *130*, 20 (1963)

Bas 65: F. Bassani, R.S. Knox and W. Beall Fowler, "Band Structure and Electronic Properties of AgCl and AgBr," Phys. Rev. *137*, A1217 (1965)

Bas 66: F. Bassani, "Methods of Band Calculations Applicable to III-V Compounds," in *Physics of III-V Compounds*, vol. 1 of *Semiconductors and Semimetals*, edited by Willardson and Beer (Academic Press Inc., New York, 1966)

Bel 54: D. G. Bell, "Group Theory and Crystal Lattices," Rev. Mod. Phys. *26*, 311 (1954)

Blo 28: F. Bloch, "Über die Quantenmechanik der Elektronen in Kristallgittern," Z. Physik *52*, 555 (1928)

Bon 67: C. Bonnelle, "Spectre X de Composés du Cuivre," J. Phys. *28*, C3-65 (1967)

Bor 27: M. Born and J.R. Oppenheimer, "Zur Quantentheorie der Molekeln," Ann. Physik *84*, 457 (1927)

Bou 36: L.P. Bouckaert, R. Smoluchowski, and E. Wigner, "Theory of Brillouin Zones and Symmetry Properties of Wave Functions in Crystals," Phys. Rev. *50*, 58 (1936)

Bri 31: L. Brillouin, *Die Quantenstatistik und ihre Anwendung auf die Elektronentheorie der Metalle* (Springer, Berlin, 1931)

Bri 65: W.F. Brinkman, Ph. D. Thesis, University of Missouri (1965), unpublished.

Bri 66: W. Brinkman and B. Goodman, "Crystal Potential and Correlation for Energy Bands in Valence Semiconductors," Phys. Rev. *149*, 597 (1966)

Bro 58: E. Brown and J.A. Krumhansl, "Energy Band Structure of Lithium by a Modified Plane Wave Method," Phys. Rev. *109*, 30 (1958)

Bro 62: E. Brown, "Role of Orthogonalization in the Determination of Valence States in Crystals," Phys. Rev. *126*, 421 (1962)

Cal 66: Eduardo Calabrese, "Effetti di correlazione nel calcolo di energie di ionizzazione," Thesis for the degree of Dottore in Fisica, University of Messina, Italy (1966), unpublished.

Cal 70: Eduardo Calabrese, "Some sample deck structures for the LU CDC 6400 Computer System," Lehigh University (1970), unpublished.

Cal 55: J. Callaway, "Orthogonalized Plane Wave Method," Phys. Rev. *97*, 933 (1955)

Cal 64: J. Callaway, *Energy Band Theory* (Academic Press, New York, 1964)

Car 63: M. Cardona, "Optical Properties of the Silver and Cuprous Halides," Phys. Rev. *129*, 69 (1963)

Con 64: E.U. Condon and G.H. Shortley, *The Theory of Atomic Spectra* (Cambridge University Press, 1964)

Con 69: Control Data 6000 Series Computer Systems, SCOPE 3 Reference Manual, (Control Data Corporation, 1968, 1969; Rev. I: 7-18-69)

Dee 67: R.A. Deegan and W.D. Twose, "Modifications to the Orthogonalized-Plane-Wave Method for Use in Transition Metals: Electronic Band Structure of Niobium," Phys. Rev. *164*, 993 (1967)

Dir 58: P.A.M. Dirac, *The Principles of Quantum Mechanics* (At the Clarendon Press, Oxford, 4th ed., 1958)

Dre 55: G. Dresselhaus, "Spin-Orbit Coupling Effects in Zinc Blende Structures," Phys. Rev. *100*, 580 (1955)

Fow 63: W. Beall Fowler, "Energy Bands in Solid Krypton," Ph. D. Thesis, University of Rochester (1963), unpublished.

Fow 63a: W. Beall Fowler, "Electronic Band Structure and Wannier Exciton States in Solid Krypton," Phys. Rev. *132*, 1591 (1963)

Har 57: D. R. Hartree, *The Calculation of Atomic Structures* (John Wiley & Sons, New York, 1957)

Har 58: D. R. Hartree, "Representation of the Exchange Terms in Fock's Equations by a Quasi-Potential," Phys. Rev. *109*, 840 (1958)

Her 63: F. Herman and S. Skillman, *Atomic Structure Calculations* (Prentice-Hall, Inc., Englewood Cliffs, New Jersey, 1963)

Hyl 30: E.Q. Hylleraas and B. Undheim, "Numerische Berechnung der 2S-Terme von Ortho- und Par-Helium," Z. Physik *65*, 759 (1930)

Int 52: *International Tables for X-ray Crystallography*, published for the International Union of Crystallography by the Kynoch Press, Birmingham, England, 1952

Kit 66: C. Kittel, *Introduction to Solid State Physics*, 3rd ed. (John Wiley & Sons, Inc., New York, 1966)

Kno 64: R.S. Knox and A. Gold, *Symmetry in the Solid State* (W.A. Benjamin, Inc., New York, 1964)

Koo 33: T.A. Koopmans, "Über die Zuordnung von Wellenfunktionen und Eigenwerten zu den einzelnen Elektronen eines Atoms," Physica *1*, 104 (1933)

Kos 57: G.F. Koster, "Space groups and their representations," *Solid State Physics*, edited by F. Seitz and D. Turnbull, vol. 5 (Academic Press Inc., New York, 1957)

Kos 63: G.F. Koster, J.O. Dimmock, R.G. Wheeler and H. Statz, *Properties of the Thirty-two Point Groups* (M.I.T. Press, Cambridge, 1963; second printing: 1966)

Kun 66: A. Barry Kunz, "A Study of the Valence Bands in Sodium Iodide," Ph. D. Thesis, Lehigh University (1966), unpublished.

Kun 67a: A. Barry Kunz, "Calculation of the Spin-Orbit Parameters for the Valence Bands of the fcc Alkali Chlorides, Alkali Bromides, and Alkali-Iodides," Phys. Rev. *159*, 738 (1967)

Kun 67b: A. Barry Kunz, "Three-Center Corrections to the NaCl Valence Band," Phys. Rev. *162*, 789 (1967)

Kun 68: A. Barry Kunz, "Application of the Orthogonalized-Plane-Wave Method to Lithium Chloride, Sodium Chloride, and Potassium Chloride," Phys. Rev. *175*, 1147 (1968)

Kun 69: A. Barry Kunz, "Combined Plane-Wave Tight-Binding Method for Energy-Band Calculations with Application to Sodium Iodide and Lithium Iodide," Phys. Rev. *180*, 934 (1969)

Lat 55: R. Latter, "Atomic Energy Levels for the Thomas-Fermi and Thomas-Fermi-Dirac Potential," Phys. Rev. *99*, 510 (1955)

Lev 70: Ira N. Levine, *Quantum Chemistry*, vol. 1 (Allyn and Bacon, 1970)

Lip 70: Nunzio O. Lipari, "Effects of Electronic Correlation on the Energy Bands of Insulating Crystals: Application to Argon," Ph. D. Thesis, Lehigh University (1970), unpublished.

Liu 62: L. Liu, "Effects of Spin-Orbit Coupling in Si and Ge," Phys. Rev. *126*, 1317 (1962)

Mac 33: J.K.L. MacDonald, "Successive Approximations by the Rayleigh-Ritz Variation Method," Phys. Rev. *43*, 830 (1933)

Mes 68: A. Messiah, *Quantum Mechanics*, vol. I (North-Holland Publishing Company, Amsterdam; John Wiley & Sons, Inc., New York, 1968)

Nik 62: S. Nikitine, "Exciton Spectra in Semiconductors and Ionic Compounds," *Progress in Semiconductors*, vol. 6 (John Wiley & Sons, Inc., 1962)

Par 55: R.H. Parmenter, "Symmetry Properties of the Energy Bands of the Zinc Blende Structure," Phys. Rev. *100*, 573 (1955)

Per 39: E. Persico, *Fondamenti della Meccanica Atomica* (Zanichelli, Bologna, 1939)

Pil 68: F.L. Pilar, *Elementary Quantum Chemistry* (McGraw-Hill, New York, 1968)

Rei 55: J.R. Reitz, "Methods of the One-Electron Theory of Solids," *Solid State Physics*, edited by F. Seitz and D. Turnbull, vol. 1 (Academic Press Inc., New York, 1955)

Rob 62: J.E. Robinson, F. Bassani, R.S. Knox and J.R. Schrieffer, "Screening correction to the Slater exchange potential," Phys. Rev. Letters *9*, 215 (1962)

Ros 57: M.E. Rose, *Elementary Theory of Angular Momentum* (John Wiley & Sons, Inc., New York, 1957)

Sch 68: L.I. Schiff, *Quantum Mechanics* (McGraw-Hill, New York; 3rd ed., 1968)

Sei 40: F. Seitz, *The Modern Theory of Solids* (McGraw-Hill, Inc., New York, 1940)

Sla 51: J.C. Slater, "A simplification of the Hartree-Fock method," Phys. Rev. *81*, 385 (1951)

Sla 54: J.C. Slater and G.F. Koster, "Simplified LCAO Method for the Periodic Potential Problem," Phys. Rev. *94*, 1498 (1954)

Sla 60: J.C. Slater, *Quantum Theory of Atomic Structure* (McGraw-Hill, New York, 1960)

Sla 63: J.C. Slater, *Quantum Theory of Molecules and Solids*, vol. 1 (McGraw-Hill, Inc., New York, 1963)

Sla 65: J.C. Slater, *Quantum Theory of Molecules and Solids*, vol. 2 (McGraw-Hill, Inc., New York, 1965)

Son 67: K.S. Song, "Structure de bandes des halogénures de cuivre; Application aux spectres excitoniques," Thèses, Université de Strasbourg (1967), unpublished.

Son 67a: K.S. Song, "Structure de Bandes d'Energie du Chlorure Cuivreux," J. Phys. *28*, 195 (1967)

Tay 69: B.N. Taylor, W.H. Parker, and D.N. Langenberg, "Fundamental Physical Constants," Rev. Mod. Phys. *41*, 375 (1969)

Tin 64: M. Tinkham, *Group Theory and Quantum Mechanics* (McGraw-Hill, New York, 1964)

Tos 64: M. Tosi, "Cohesion of Ionic Solids in the Born Model," *Solid State Physics*, edited by F. Seitz and D. Turnbull, vol. 16 (Academic Press Inc., New York, 1964)

VdL 47: F.C. Von der Lagl and H.A. Bethe, "A Method for Obtaining Electronic Eigenfunctions and Eigenvalues in Solids with Application to Sodium," Phys. Rev. *71*, 612 (1947)

Wig 59: E.P. Wigner, *Group Theory and its Application to the Quantum Mechanics of Atomic Spectra* (Academic Press, New York, 1959; fourth printing: 1964)

Woo 57: T.O. Woodruff, "The Orthogonalized Plane-Wave Method," *Solid State Physics*, edited by F. Seitz and D. Turnbull, vol. 4 (Academic Press Inc., New York, 1957)

Wyc 48: R.W.G. Wyckoff, *Crystal Structures* (Interscience Publishers, Inc., New York, 1948 and later; 2nd ed., 1963)

Zim 64: J.M. Ziman, *Principles of the Theory of Solids* (Cambridge University Press, 1964)

VITA

Eduardo Calabrese was born in Messina, Italy, on January 1, 1943, to Tiberio and Filadelfia Calabrese. He received his elementary and high school education in Messina. In 1960 he graduated from the "Liceo Classico Maurolico" and entered the University of Messina as a Physics major. During his years there, he was recipient of an annual scholarship from the "Istituto Regionale di Energia Nucleare." In June 1966 he graduated, magna cum laude, with the degree of "Dottore in Fisica."

On September 1966 he came to the United States to begin his graduate work at the Physics Department of Lehigh University under the direction of Professor W. Beall Fowler. He worked as a research assistant from 1966 to 1969, as a teaching assistant during the academic year 1969-70, and again as a research assistant until the completion of his thesis.

He is a member of "Societá Italiana di Fisica" (Italian Physical Society).